2016

Fugro Seacore: airlift pump modelling proposal

Hobson, M.

Hobson, M. (2016) 'Fugro Seacore: airlift pump modelling proposal', The Plymouth Student Scientist, 9(2), p. 95-122.
http://hdl.handle.net/10026.1/14130

The Plymouth Student Scientist
University of Plymouth

Appendix Section

This section contains the entire Appendix list with brief descriptions. The documents then appear in alphabetical order with the appendix letter shown in the footer of each page.

APPENDIX A – The Interim Report
This Appendix contains the totally unchanged interim report from the data of submission. Note; no Appendix note appears in the footer as the document is unchanged from that submitted for the interim report.

APPENDIX B – Domain Drawings
This Appendix contains full CFD domain drawings and a brief explanation as to why domains have been revised including geometry boundary setup.

APPENDIX C – CFD Work Record (In Screen Shots)
This document shows all CFD work undertaken in chronological order with screen shots explaining the findings and reasoning of each step taken.

APPENDIX D – Mathematical Modelling
This Appendix shows the mathematical model created.

APPENDIX E – Project Gantt Charts
This document shows all 9 revisions of project Gannt charts discussing project time management in detail including reasons for deviation from the original project program.

APPENDIX F – Validation Data
This shows and analysis the method for collecting all data required for model validation.

APPENDIX G – Details of CFD Runs
This table records all of the CFD runs undertaken over the course of the project. It is a clear and concise way of displaying the settings for each CFD run.

APPENDIX H – Mathematical Modelling Manual
This document gives a detailed account of the design and implementation of the conventional mathematical model including recommendations of further work which could be implemented.

APPENDIX I – Project Poster
This Appendix shows the project poster printed on A4 paper.

Final Year Project Interim Report

Fugro Seacore Airlift Proposal: Behavior over tidal cycles

Matthew Hobson

This Interim report shows the initial area of research for the project defined by aims and objectives. The main aim is to allow the prediction to be made for airlift pumps at varying submergence ratios. Preliminary and more detailed research is conducted by reviewing relevant literature. Due to the complexity of the proposed project within the time scale, it is decided to adopt a method of Computational Fluid Dynamics (CFD) modeling validated by formulae extracted from academic papers only if required. Due to the elimination of physical testing, the project plan is re-organized to account for a newly defined set of aims and objectives. Finally all other progress achieved during the first part of this project is presented and briefly evaluated.

1. PROJECT DEFINITION

This section will fully explain the proposed project area and the reason behind this research by relating the objectives and aims of the project to its industrial application.

1.1 Airlift Pumps – Basic Knowledge

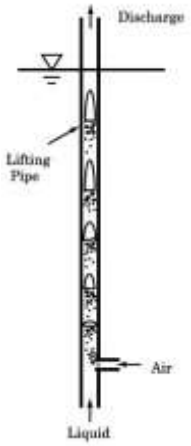

"Figure 1; Basic Airlift Pump - Reproduced from (Fujimoto et al., 2004; Pougatch & Salcudean, 2008)."

Airlift pumps lift particles within water or other liquid. Compressed air is injected into the bottom of the riser or pipe forming bubbles. These bubbles rise up the pipe carrying water with them due to the interfacial friction (Pougatch & Salcudean, 2008). As more air travels up the pipe, the pressure becomes less than at the bottom of the pipe. This pressure difference allows particles to be sucked into and then lifted up the pipe (Reinemann et al., 1990) (Pougatch & Salcudean, 2008). Airlift pumps are used for applications where characteristics such as reliability, low maintenance and the ability to pump particles in water are required (Kassaba et al., 2009). In 1968 Stenning and Martin stated that airlift pumps could be used for underwater exploration, raising coarse particles to the surface (Tighzert et al., 2013). Figure 1 is a diagram of a basic airlift pump reproduced from (Tighzert et al., 2013).

1.2 Fugro GeoServices – Industrial Application

Seacore, now Fugro GeoServices, were originally a geotechnical Survey Company specializing in overwater drilling and marine construction, established over 35 years ago (Fugro, 2015b). In 2007 Seacore were acquired by Fugro specializing in geotechnical, survey, subsea and, geosciences services (Fugro, 2015a). Fugro GeoServices conduct a large amount of this work from jack-up barges.

These vessels are the most popular type of drilling platform in the world (Rigzone.com, 2015). The barge floats onto location before jacking itself up to the point that the hull is fully out of the water and the legs are supporting all of the barges weight (Rigzone.com, 2015); the barge is effectively stood on the sea floor. This allows drilling operations to be performed without the barge being affected by the tide or weather conditions (Crowley Maritime Corporation, 2015).

1.3 Use of Airlift Pumps

In some areas that Fugro Geoservices undertake drilling operations, environmental regulations mean that drill cuttings cannot be left on the seabed. Cuttings left on the seabed can cause contamination which is discussed by (PennWell Corporation, 1999). This means that the cuttings must be brought to the surface for disposal off site. Airlift pumps are used to lift the cuttings from the seabed to the jack-up barge, as a conventional pump would sustain damage from the solid particles. A simpel form of this arrangment is shown in Figure 2. Note: This diagram only shows the locaton of the riser with respect to the barge. Figure 3 shows actual flow at the base of the riser.

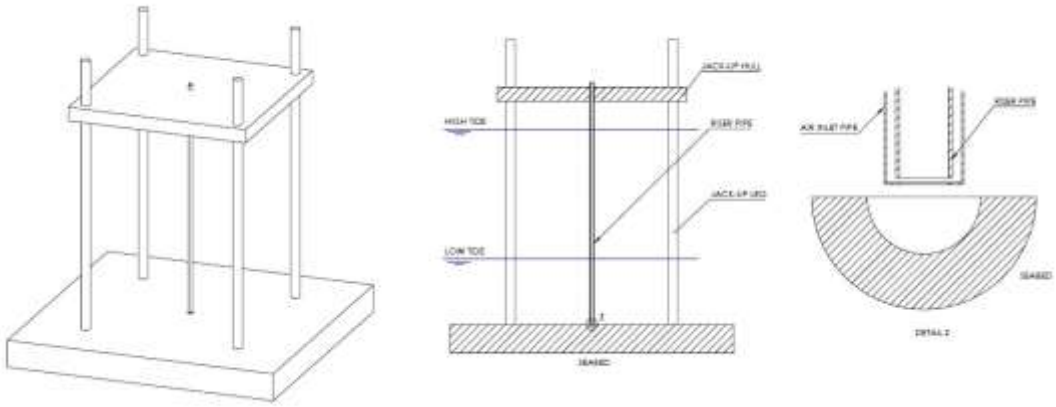

Figure 2; The Jack-Up Arrangement with Riser Pipe

The drilling is conducted from Jack-up Barges which stand on the sea floor, this means they do not move up or down during the tide cycle (Crowley Maritime Corporation, 2015). While the water pressure on the seabed changes during a tide cycle, the vertical distance to pump remains constant (Crowley Maritime Corporation, 2015). Fugro have found that pumping during low tide is more difficult and sometimes not possible. Fugro would like to know how to better predict the time during a tide cycle the airlift system will be operational for.

1.4 Project Aims and Objectives

The primary aim of this project is to understand how changing tide heights affect the ability of the pumping operation, to achieve this aim; the following objectives have been set; the creation and testing of a physical scale model and a virtual computational fluid dynamic model of the airlift pump. Results from these will be compared with results from mathematical models in literature to validate any findings. It is expected that these objectives will develop throughout the project to ensure that they are achievable and allow research to be conducted in a relatively unknown area. For this reason the use of physical or theoretical modeling may or may not be required depended on the strength of literature found.

2. REVIEW OF LITERATURE

The first step of this project is to conduct a review of relevant literature. This should help to; identify areas of current knowledge, locate mathematical models of airlift pumps and to further understand airlift pumps in general. This will form the basis of the project by providing information on the position of current research and areas, which have been overlooked within the type of operation this project is interested in.

2.1 Simple Airlift Pumps

Airlift pumps lift mixtures of solids or liquids through vertical risers by pumping compressed air into the bottom of the pipe (Tighzert et al., 2013). The airlift pumping method is popular due to its simplicity; reducing maintenance, and an ability to pump solids (Kassaba et al., 2009). These properties ensure that airlift pumps are present in a wide variety of areas; volcanoes, upwelling ocean water (Fan et al., 2013), sewage plants, oil extraction, and dredging (Wahba et al., 2014).

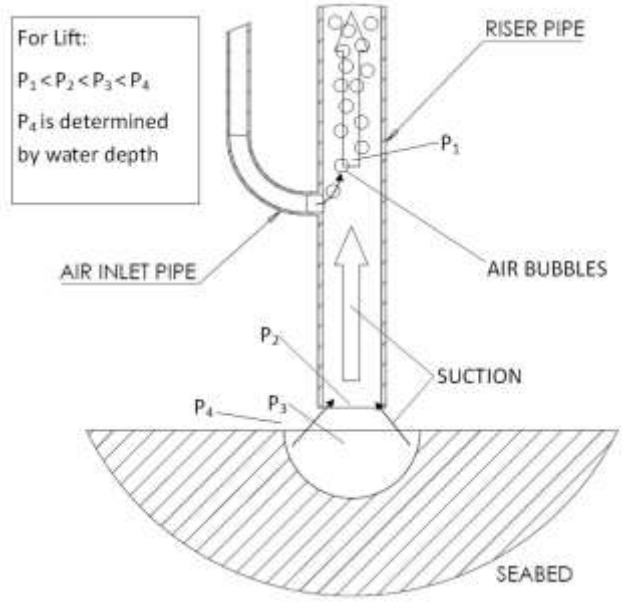

Figure 3; Basic Pressure Requirements for Airlift Pumping

Most simply considered, the air injected at the base of the riser travels up the pipe as it is less dense than the liquid in the rise. This lowers the density of the water and air now in the tube. When the pressure conditions in Figure 3 are met suction is generated at the tubes lower entrance due to the pressure difference. This allows solid particles to be lifted into and then up the pipe known as the riser (Reinemann et al., 1990). The effect of pressure difference caused by a less dense object creating uplift is discussed by (Kinsky, 1982) this theory was used when producing Figure 3.

2.2 More Complex Two-Phase Models

To accurately model two-phase flow; flow comprising of water and air, in the airlift pumps, the factors related to the sizes of the pressures shown above must be understood. This allows theoretical models to be produced of the pump. The first models used the buoyancy force of the injected air as the driving factor taking into account riser pipe diameter, the ratio of air to water and the submergence ratio of the riser (Wahba et al., 2014).

Due to the relative simplicity of these models it is proposed to use an analytical model to validate experimental and computational fluid dynamic results during the calibration phase of testing. It is proposed to use Stenning and Martin's model.

This one dimensional model was developed in 1968 form the results of physical tests (Stenning & Martin, 1968). The experiment used a riser with a height of 168 inches and diameter of 1 inch (Stenning & Martin, 1968). Starting with Bernoulli's equation to calculate pressures, the equation in Figure 4, was derived from the results (Stenning & Martin, 1968):

$$\frac{H}{L} - \frac{1}{\left[1 + \frac{Q_g}{sQ_f}\right]} = \frac{V_1^2}{2gL}\left[(K+1) + (K+2)\frac{Q_g}{Q_f}\right] \quad (17)$$

where $K = \frac{4fL}{D}$, and D is the hydraulic diameter of the pipe.

"Figure 4; Two Phase Airlift Pump Equation reproduced from (Stenning & Martin, 1968)"

Where: H/L is riser submergence ratio (L is riser height), A is the riser pipe cross-sectional area, Q_g is the gas volume flow rate, Q_f is the liquid volume flow rate, V_1 is Q_f divided by A^2, L is the length of riser pipe, D is the riser pipe diameter, S is the slip factor and F is the friction ratio (Stenning & Martin, 1968).

Due to the fact that this formula is present in over three peer-reviewed journals and has been used as the basis for the research of others such as; Kassab et al (Wahba et al., 2014) it is felt that this model will be of reasonable accuracy for use during the validation of testing models.

As models evolved to become more accurate they were developed for specific scenarios. For example Reinemann et al takes into account surface tension effects, which are the governing factor for pumps with small diameter risers (Wahba et al., 2014). This research tested risers with diameters of 3 to 25 mm finding that in risers with a diameter of less than 20 mm the bubble rises more slowly due to surface tension (Reinemann et al., 1990). This will have to be taken into account when deciding upon the size of any experimental models. The findings of Rieinemann et al show that when conducting research experiments or simulations it is important to be aware of other parameters, which if changed, could affect results.

Other parameters to be assessed in detail by two-phase flow models include research on the air injection into the bottom of the riser. This work shows that the pipe diameter and air inlet shape are key to efficiency which increases with pipe diameter due to reduced wall friction for the volume being transported (Fan et al., 2013). Although these two parameters will be kept constant in this research it is important that any tests use dimensions, which have been correctly scaled with regards to dimensionless numbers such as the Reynolds number. Despite this issues such a smaller riser diameter causing reduced wall friction (Fan et al., 2013) and slower bubble speeds (Reinemann et al., 1990) should still be considered during testing design if these are significantly different.

The parameter of interest for this project is the riser submergence ratio, which has already been identified as changing during the tide cycle. For two-phase pumping this

has been investigated using physical tests by (Kassaba et al., 2009), who improved the Stenning and Martin Model to allow for a more accurate slip ratio (Wahba et al., 2014).

The Efficiency of airlift pumping is known to increase up to a submergence ratio of 75% (Tighzert et al., 2013). This research was conducted by experimental testing using a 3.1 m riser with 33 mm inner diameter. This article also looks at the effects of void fraction, the fraction of air in the riser, in relation to efficiency. The void fraction determines if the slugging of air bubbles occur (Tighzert et al., 2013) due to its findings this paper goes some way to corroborating Rienemann et al's work.

2.3 Three-Phase Modelling

Despite a large amount of proven research being available for two-phase airlift pumps, a further dimension is added to the problem when three-phase flow is considered. Three-phase flow represents solids being lifted up the riser (Fujimoto et al., 2004), in Fugro's case; drill cuttings.

Fujimoto et al investigates the effects of bends in the riser pipe situated before and after air is injected. Different sized aluminium balls are lifted making the experiment 3-phase (Yoshinaga & Sato, 1996). It is found that when the air in injected into the riser after the bend, the bend has little effect on the pumping operation. The only effect being; increased wall frication due to increased wall length despite the height lifted being the same as the straight riser (Fujimoto et al., 2004). This paper also describes the flow as almost entirely turbid.

Due to the nature of this project, research where the flow is modelled is ultimately of more use than studies, which purely determine if a factor does or doesn't affect airlift pumps. T.Yoshinaga and Y.Sato conducted this type of research when studying the potential of airlift pumps for extracting manganese from deep-sea mines (Yoshinaga & Sato, 1996). These experiments tested both spherical uniform and uninform partials while systematically changing the submergence ratio (Yoshinaga & Sato, 1996). Results from these experiments show strong relations between flow rated, the size of particles discharged and the amount of air supplied.

Lung Cheng et al have also conducted similar research using risers of varying diameter with a height of 250 cm where the submergence ratio was also changed (Cheng et al., 1997). Whilst this research is very specialized with regards to three-phase internal loop reactors, it does show that theoretical formulas can be used to good effect to determine the characteristics of an airlift pumping operation.

It has also been found that pumping rates are affected by the size and form of partials (Mahrous, 2012). Mahrous investigated the findings of many other research papers to come to the conclusion that larger diameter partials have a detrimental effect on pump performance. In this work, the possibility of treating two and three phase pumps as a homogenous mixture similar to Boës et al is also mentioned (Mahrous, 2012). Yoshinaga et al's work is also analyzed showing a reduction in the speed of gas and liquid phases as the submergence ratio is decreased.

Whist this research is useful it also provides the stimulus for questions, which could be problematic to answer when it is considered that drilling creates a large variety of solid partial shapes and sizes, which will all, require different parameter magnitudes to lift them efficiently.

3. TESTING OPTIONS

Having gained further understanding of the complexity of three-phase airlift pumps, it is now felt that completing both physical and Computational models of the process to a suitable standard for data from them to be trusted will not be achievable within the projects time constraints. This section will look into the situation, which it is planed to investigate in more detail. Having done this, the merits of progressing with either physical or computational models will be discussed.

3.1 Fugro GeoServices Application

As proven in the initial and more detailed research phases, many factors affect the airlift system. For this reason it is essential that any test or simulations are designed to relate as closely as possible to the problem in hand.

Fugro GeoServices have been contacted and asked to provide drawings featuring the set-up of a real airlift project. Using engineering drawings ensures that the airlift equipment was set up correctly; thus ensuring the validity of this information.

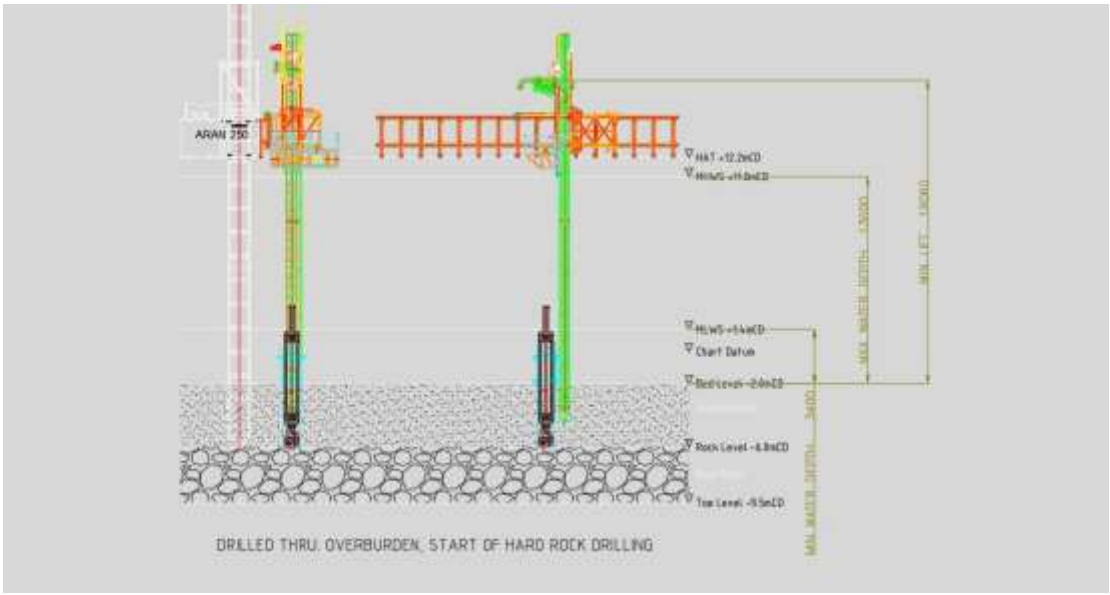

"Figure 5; A Diagram of Fugro's Jersey Project Setup from (Hackwell, 2015)"

Figure 5 form (Hackwell, 2015) shows an example of a project where airlift pumping was be used. This example contains a tidal range of around 9.6 m. during work on this project Fugro experienced difficulties with pumping at low tide (Hackwell, 2015). It should be noted that as the depth drilled increases the submergence ratio of the riser would become more favourable. While this has little significance on shallow drilled holes, this requires consideration if the holes drilled depth is considerably larger than the tidal range. This is shown by Graph 1, which has been generated based on the water depths and tidal heights supplied by Fugro. In Graph 1 the maximum depth of the hole has been increased to highlight the submergence ratio improving as the hole is drilled deeper.

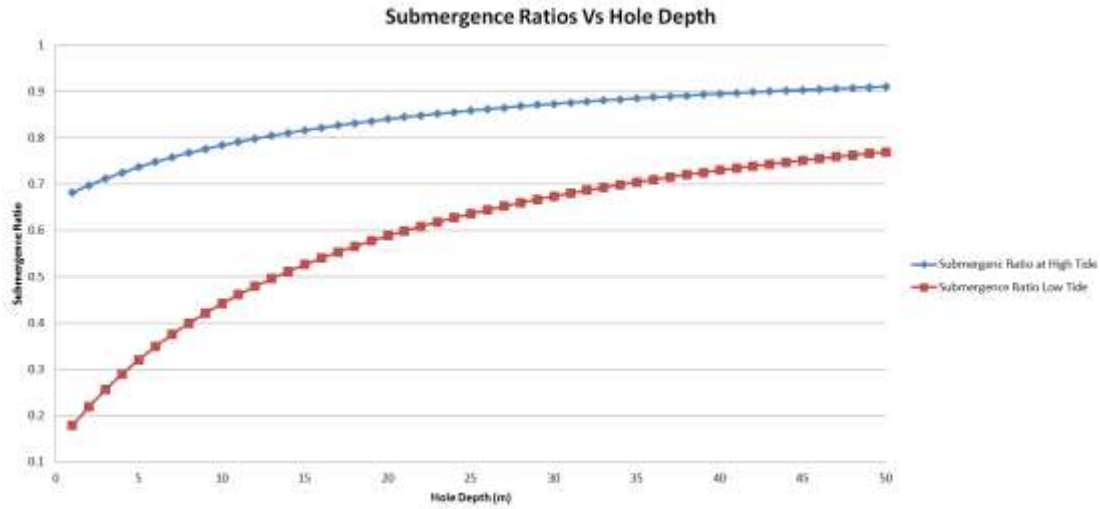

Graph 1; Submergence Ratio Vs Hole Depth calculated from (Hackwell, 2015)'s data

This case, which has been provided by Fugro, is to act as a base case for all testing or simulation modelling. There is little point in experimenting with submergence ratios higher or lower than this as it is know that the airlift operation stopped working between these two points.

By taking 0 m drilled to contain the worst submergence ratio a graph of the water depth during the tide cycle, a submergence ratio against time graph can be formed using Reeds Nautical Almanac; (Towle & Fishwick, 2015), which provides information on tide cycles used by the seagoing community for navigation of tidal regions.

The relationship of water depth to tide height can be generally given by the 12ths rule whereby during the six hours between high a low tide, the tides height will decrease by 1/12 during the first hour; 2/12 in the second hour, 3/12 in the third hour, 3/12 in the fourth hour, 2/12 in the fifth hour and 1/12 in the sixth hour (Towle & Fishwick, 2015). This information is plotted for a 24 hour time cycle in Graph 2, which uses information of high and low water heights taken from Figure 5. The 12^{ths} rule is appropriate for Jersey harbour however it may require adjustment if working in large estuaries or areas such as the Isle of Wight where different models should be adopted due to the shape of the coastline (Towle & Fishwick, 2015).

Graph 2; Submergence Ratio Vs Tide Heights calculated using data from (Hackwell, 2015) and (Towle & Fishwick, 2015).

When considering the dimensions of this test case, the parameters, which may be changed to aid the completion of testing, have been identified. It has been decided that

due to a potential change in the characteristics of air flow; from bubbles to slug flow, when reducing the pipe diameter (Reinemann et al., 1990), it should be attempted to keep this the same. Changing this diameter would also result in the need to change the size of the solid drill partials. Instead, it has been decided that the height of the testing could be changed, as long as the submergence ratio remains the same. If this scaling method is adopted it may be necessary to derive a drag coefficient to be added to results as the reduced surface area of a shorter riser height will reduce the wall drag created as stated by (Fujimoto et al., 2004).

It is important to be aware that changing sizes will cause results of any test to differ from reality. This will also need to be considered when comparing the data generated from tests with any figures predicted by a theoretical mathematical model. Figure 6 compares the geometric dimensions used in tests when collecting data to form various mathematical models used with the dimensions of Fugro's case study. It should be remembered that the purpose of this comparison is to be aware of the reason for differences in results and not to select a particular mathematical model to use.

			Two Phase Modelling				Three Phase Modelling		
Case	Units	Fugro - Jersey	Reimann et al	Stenning et al	Kassab et al	Tighzert et al	LungCheng et al	Fujimoto et al	Yoshinaga et al
Riser Diameter	mm	194	19.1	101.6	25.4	33	140	18	26
Riser Cross-sectional Area	mm^2	59118.49	573.04	16214.64	1013.41	1710.60	30787.61	508.94	1061.86
Riser Diameter	mm	194	3.18	101.6	25.4	33	90	18	26
Riser Cross-sectional Area	mm^2	59118.49	15.88	16214.64	1013.41	1710.60	12723.45	508.94	1061.86
Riser Hieght	mm	26215	1800	11760	3750	3100	2500	3200	7860
Riser Submergance	mm	13000	1620	8820	2812.5	2325	1500	2433.00	6288
Submergance Ratio	N/A	0.50	0.90	0.75	0.75	0.75	0.60	0.76	0.80
Riser Hieght	mm	26215	1800	11760	3750	3100	2500	3200	7860
Riser Submergance	mm	3400	1080.00	8820	750	775	700	1925	6288
Submergance Ratio	N/A	0.13	0.60	0.75	0.2	0.25	0.28	0.60	0.80
Riser height/Diameter Ratio	N/A	135.13	94.24	115.75	147.64	93.94	17.86	177.78	302.31

Figure 6; A Comparison of Airlift Dimensions Using Data from; (Hackwell, 2015), (Reinemann et al., 1990), (Stenning & Martin, 1968), (Kassaba et al., 2009), (Tighzert et al., 2013), (Cheng et al., 1997), (Fujimoto et al., 2004) and (Yoshinaga & Sato, 1996).

From Figure 6 it is clear that the literature available and Fugro's cases possess reasonably similar dimensions. This table also strengthens the case for using Stenning and Martin's work as the base for a two-phase study as it is a dimensionally similar model when taking into account key ratios and comparing actual dimension sizes.
It is also important that non-dimensional numbers such as the Reynolds number are similar. This is as it is capable of comparing geometric, kinematic and dynamic parameters simultaneously (NASA, 2014). All of these parameters affect areas of interest in modelling such the size of lamina flow boundaries.

Having determined the dimensions of the test case, it is now important to understand the capabilities of the compressor that was used to supply the air, because without the air supply there would be no airlift. The theoretical models also show that larger compressors allow for a greater range of operation during reduced submergence ratios as more air is injected allowing greater reductions in density inside the riser to be achieved. This information has been obtained from an operating manual for the pump used by Fugro in Jersey provided by (Hackwell, 2015). It is stated that the actual free air delivery is 14.9 m^3 min^-1 operating at a pressure of 12.7 bar (Doosan Trading Limited, 2009).

3.2 Computational Fluid Dynamics

Following the analysis of two-phase mathematical models, Wahba et al continues with a discussion on three-phase pumps. This is achieved by balancing formulas taken form the fundamental laws of physics, such as the conservation of mass, for each section or element of the riser tube (Wahba et al., 2014). It is also of interest that for this particular simulation the states of the two phase pump are combined to form a homogenous mixture similar to that formed by Boës et al which is mentioned in (Mahrous, 2012). By combining the different phases interactions at phase boundaries are removed which simplifies the analysis and therefore the amount of elements required. This is something, which will have to be considered if computational Fluid Dynamics (CFD) is chosen as the modeling constituent of this research.

For this research the main advantage of CFD is that it has no limits of input parameters that a physical model may have. For example; air flow rates can be adjusted without the fear of the testing apparatus limits being reached. As the testing is computer biased it also means that parameters can be measured from any part of the experiment and the dimensions can be adjusted quickly should it be found that they are having unforeseen effects on the results.

Should CFD be chosen as the modeling component the university already provides the facilities needed therefore this research can be conducted without having to invest in, design or construct physical testing equipment. Despite these advantages CFD is notoriously complex and can be very hard to execute due to the number of variables, which require changing. For this reason it should be approached with caution and only used if it is thought that the results produced are lightly to help meet the aims of the research.

3.3 Physical Scale Model Testing

To carry out physical testing of the study case, a test rig would require manufacture. The equipment available in within the university will dictate the maximum size, which this test can be. It is anticipated most of this could be acquired relatively easily apart from the compressed air supply. Without a large enough compressed air supply, the maximum possible diameter of the riser is reduced, this could be problematic given the size of the compressed air supply used Fugro's jersey operation.

This would also require the design and manufacture of testing equipment. Then due to the large amounts of parameters effecting airlift systems it could be difficult to obtain reliable results form any tests. Furthermore accurately measuring any results with the equipment available would inherently lead to uncertainty without extremely rigorous experiment design. For these reasons physical experiments will not be considered as a method of validating theory.

4. DECISION ON PROJECT PATH

Following the discussion above it has been decided to use CFD analysis if required and abandon any physical experiments. This has lead to the need to reconsider the project aims and objectives and the project plan to be adjusted to account for this and the information, which has been uncovered during work up to this point in the project.

4.1 Refined Project Aims and Objectives

The primary aim of this project remains to understand how changing tide heights affect the ability of the pumping operation. However, due to the findings of preliminary research it is now necessary to adjust the objectives required to fulfil this aim.

Time constraints and the strength of current literature on the topic, mean that it has now been decided to conduct CFD analysis only if required. This will be determined by the start of February 2016. It is also now an aim to create a working mathematical model which will determine if pumping is possible given the submergence ratio and other parameters which should be known during the planning stages of any given project. Current mathematical models show this should be possible. To achieve this aim, further research into the parameters required to start airlift pumping will be required.

4.2 Revised Gannt Chart

Due to the evolution of the project, the following changes have been made to the project gannt chart. Figure 7 shows the gannt chart revision number and the reason for these revisions, Gannt chart REV01 is in Figure 8, REV04 is shown in Figure 9.

Revisions Directory	Date	Reson for Revision
REV01	30/09/2015	First revison
REV02	07/10/2015	Improved to account for interm report date (04/12/15)
REV03	14/10/2015	Improved to account for a university trip to Alabama
REV04	26/11/2015	Improved to account for the removal of pyhsical Testing and adjusted with knowlegde of work from the first 9 weeks
ALL	26/11/2015	Revision numbers added to ALL gannt charts for ease of identification

Figure 7; Gannt Chart Revisions Directory

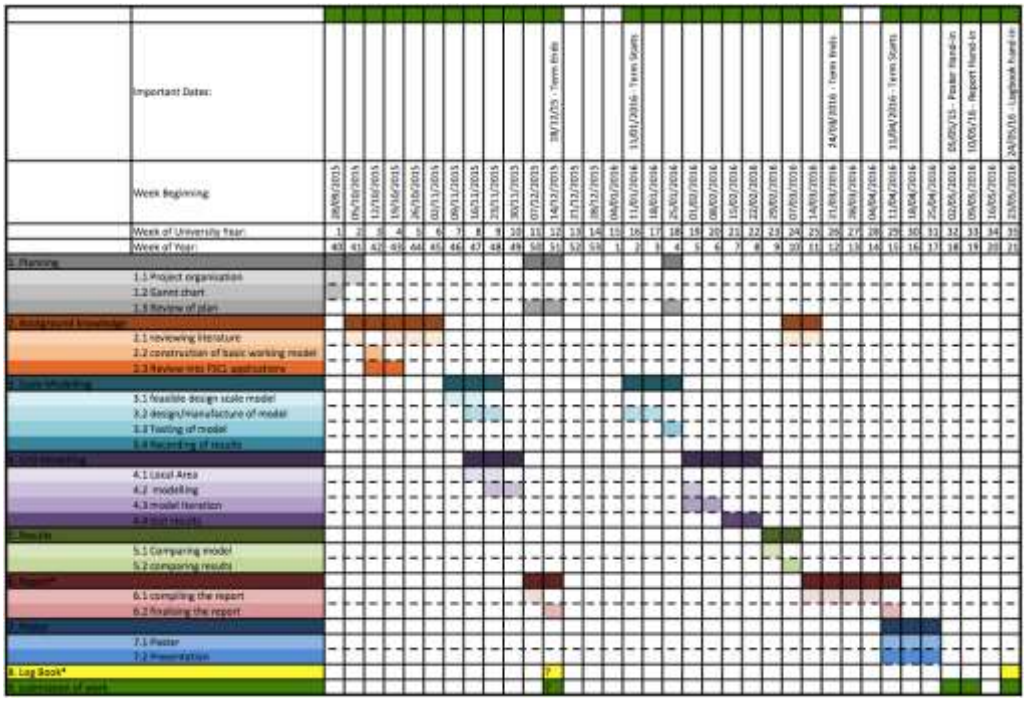

Figure 8; Gannt Chart REV01 (30/09/15)

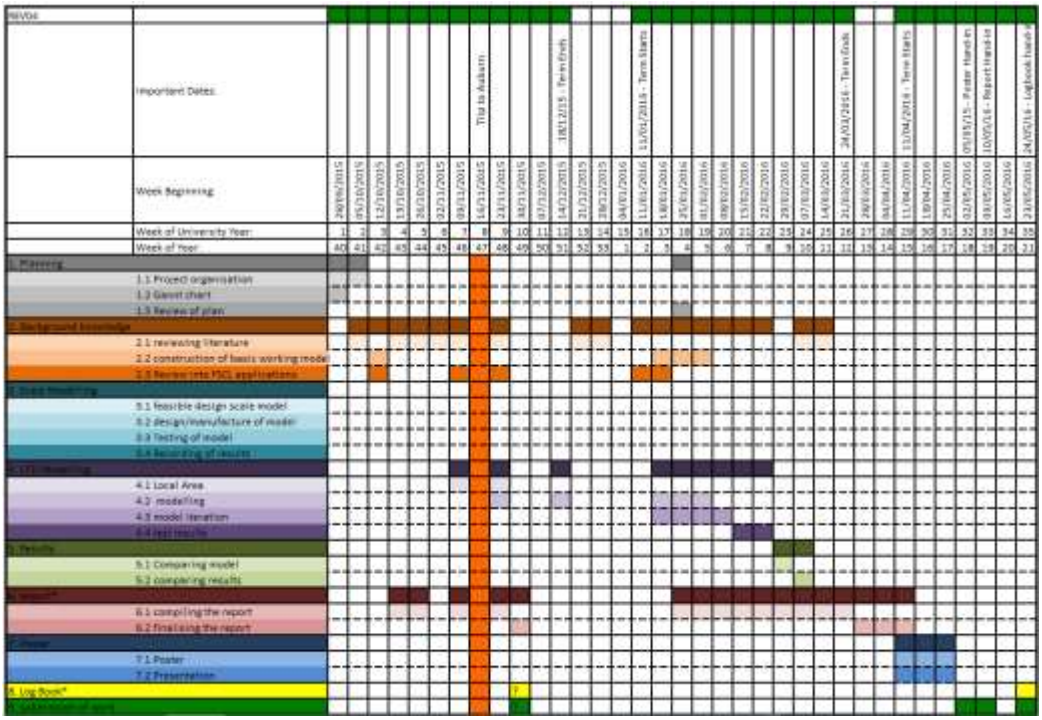

Figure 9; Gannt Chart REV04 (Updated 26/11/15)

When creating REV04 of the Gannt chart the change in project objectives and progress until this point were considered. To see how the project has unfolded this term, the first step was to update the chart to show which tasks had actually been attempted each week. This shows that no scale model work has been done as it was decided not to pursue this objective. It also shows that construction of the interim report began far earlier than anticipated because of the trip to Auburn and the way it was used to identify areas of research to undertake. For this reason the plan for the remaining time shows that the report writing is to be conducted in parallel with the other tasks on a weekly basis. CFD modelling is currently still expected to take up a large amount of time if required however this section is potentially the most lightly to change going into next year with the decision to be made on it by early February from the research which is to be conducted in January.

5. PROJECT WORK COMPLETED

This section is limited as much of the project progress achieved can be classed as scholarly learning because understanding of airlift pumps has had to be developed outside of taught modules at the university.

Following the decision to use formulae from the work of others potentially validated by computational fluid dynamics (CFD) to further this project, the first step was to construct a principle domain for all CFD work.

Using Furgo's Jersey project as a basis for this investigation, this domain was constructed using the dimensions supplied by Fugro's drawing (Figure 5). Note that this is the initial domain (Figure 10) therefor the dimensions are as close to reality as possible. As discussed in section 4.1, the height of the domain may need to be changed to allow for the analysis to be run using the computational resources available. This is possible provided that the submergence ratio remains the same and a drag coefficient is

added. Further to this the implementation of a homogenous liquid to reduce computational resources is to be considered as mentioned in Boës et al taken from (Mahrous, 2012).

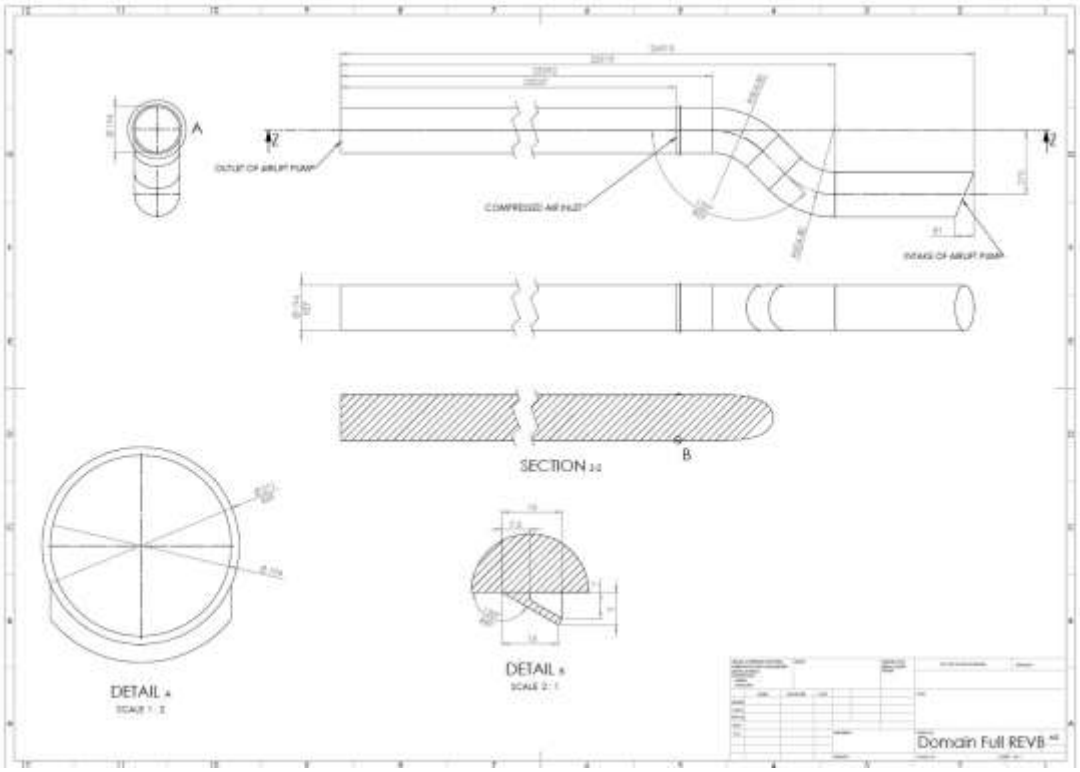

Figure 10; The Initial Domain Created Using Dimensions From (Hackwell, 2015) Whilst

constructing the CFD domain, the parameters taken form Fugro's case study was also input into Stenning and Martin's two-phase mathematical model. This was achieved by the creation of a parametric spreadsheet. The estimated variation in water depth during a tide cycle has also been input. This is shown in Figure 11.

Hour of Tide cycle	T	Hours	0	1	2	3	4	5	6
submergance Depth	H	m	3.40	4.20	5.80	8.20	10.60	12.20	13.00
Riser Hieght	L	m	26.22	26.22	26.22	26.22	26.22	26.22	26.22
Riser Cross-sectional Area	A	m^2	0.06	0.06	0.06	0.06	0.06	0.06	0.06
Gas Volume Flow Rate	Qg	m^3 s^-1	0.24	0.24	0.24	0.24	0.24	0.24	0.24
Liquid Volume Flow Rate	Qf	m^3 s^-1	0.0017	0.0021	0.0029	0.0041	0.0052	0.0060	0.0064
Riser Diameter	D	m	0.19	0.19	0.19	0.19	0.19	0.19	0.19
Slip Factor	S	N/A	1.00	1.00	1.00	1.00	1.00	1.00	1.00
Friction Ratio	F	N/A	1.00	1.00	1.00	1.00	1.00	1.00	1.00
K = (4FL) / D	K	N/A	540.52	540.52	540.52	540.52	540.52	540.52	540.52
Gravity	g	m s^-2	9.81	9.81	9.81	9.81	9.81	9.81	9.81
Flow Speed Out of Pipe - Vout = Qf/A	Vout	m s^-1	0.03	0.04	0.05	0.07	0.09	0.10	0.11
Left Hand Side	LHS	N/A	0.12	0.15	0.21	0.30	0.38	0.44	0.47
Right Hand Side	RHS	N/A	0.12	0.15	0.21	0.30	0.38	0.44	0.47
Total (Should = 0)	LHS-RHS	N/A	0.00	0.00	0.00	0.00	0.00	0.00	0.00
density of Sea water	ρ	kg m^-3	1029.00	1029.00	1029.00	1029.00	1029.00	1029.00	1029.00
Presure at Sea Bed - P4 = ρHg	P4	Pa	34321.27	42396.86	58548.04	82774.82	107001.59	123152.78	131228.37

"Figure 11; Fugro's Set-Up Applied To Stenning et al's Model (equation in figure 4), Data From; (Stenning & Martin, 1968), (Doosan Trading Limited, 2009) and (Hackwell, 2015)"

In this table Qf has been calculated using the goal seek function whilst trying to set the values in the Total row to zero. The Total row can be set to zero as the left hand side (LHS) and right had side (RHS) of Stenning and Martin's equation should equal each other (Total = LHS – RHS). Both F and S have been set at one, as they are currently

unknown factors. From this work it is possible to clearly define the questions that remain to be answered to complete this phase of research, and these are as follows:

- How should Friction (F) and Slip (S) be calculated?
    - These can be calculated from pre-existing data such as the Moody table however more research will be required.
- At what point is the flow rate too low for particles to be lifted or sucked into the riser?
- What is the size of the effect of lifting, denser, solid particles?

The points above should be the first three areas to be addressed when continuing with work.

6. Summary

The first phase of research has now been completed (Shown in sections 1.1, 1.2, and 2.1). This allowed the construction of a strong understanding of airlift systems and their uses. This was also used to identify important information such as parameters to be aware of whilst designing experimental or CFD models or comparing different theoretical models. More targeted research, in sections 2.2 and 2.3, then uncovered a variety of both two and three phase theoretical models, which have been produced from the analysis of physical experiments. This phase of the project is also mentioned in section 5 as scholarly learning because understanding of airlift pumps has had to be created outside of taught modules.

The importance of this project has been shown by both literature and its links to the commercial drilling operations of Fugro and similar companies (shown in sections 1.2, 1.3 and 3.1). Due to the complexity of airlift pumps uncovered by the research, it was decided to use a suitable test case as a basis for the research. The Furgo Jersey project has been identified as such a project in section 3.1. This will be used to reduce the number of variable parameters during the research. It will also be used to justify the selection of parameters such as riser diameter and air injection rate. Analysis of dimensional similarities between this and the experiments used to derive the theoretical models has also been undertaken. The creation of Figure 10, in section 5, aided this.

Despite the location of a suitable test case, the size of the project was also found to be too demanding for the time scale. In reaction to this the aims and objectives in section 1.4 have been reconsidered with physical experiments being removed due to the discussion in sections 3.2 and 3.3 with the need for CFD analysis being unlikely because of the strength of current literature already found on the topic and problems with obtaining trustable results.

In section 5, the test case parameters have been input into Stenning and Martin's theoretical model for two-phase pumping. This allowed the identification of further questions, which require more investigation to complete the research.

Taking into account the findings from the first ten weeks the Gannt chart for tasks to be completed over the rest of the project has been revised, in section 4.2, to allow for a workable timetable, which should be capable of fulfilling section 4.1; the refined project aims and objectives.

Bibliography

Cheng, L., Shyh, J. & Hwang, Y., 1997. Gas holdup and liquid velocity in three-phase internal-loop airlift reactors. *Chemical Engineering Science*, 52, pp.3949-960.

Crowley Maritime Corporation, 2015. *Marine Solutions*. [Online] Available at: http://www.crowley.com/What-We-Do/Marine-Solutions/Vessel-Specifications/Barges/Jack-Up-Barges [Accessed 04 November 2015].

Doosan Trading Limited, 2009. *12/50 Operation and Maintenance Manual*.

Energy 365, 2015. *Fugro to provide marine drill coring system to JOGMEC for Methane Hydrate investigations*. [Online] Available at: http://www.energy-pedia.com/news/general/fugro-to-provide-marine-drill-coring-system-to-jogmec-for-methane-hydrate-investigations [Accessed 13 June 2015].

Fan, W. et al., 2013. Experimental study on the performance of an air-lift pump for artificial upwelling. *Ocean Engineering*, 59, p.47–57.

Fugro, 2015a. *About Us*. [Online] Available at: http://www.fugro.com/about-fugro [Accessed 13 June 2015].

Fugro, 2015b. *about-us*. [Online] Available at: http://www.seacore.com [Accessed 13 June 2015].

Fujimoto, H., Murakami, S., Omura, A. & Takuda, H., 2004. Effect of local pipe bends on pump performance of a small air-lift system in transporting solid particles. *International Journal of Heat and Fluid Flow*, pp.996-1005.

Furgo, 2015c. *Cone Penertration Testing (CPT)*. [Online] Available at: http://www.fes.co.uk/services/CPT/ [Accessed 15 June 2015].

Furgo, 2015d. *about-us*. [Online] Available at: http://www.fes.co.uk/about-us/ [Accessed 13 June 2015].

Furgo, 2015e. *fugro at a glance*. [Online] Available at: http://www.fugro.com/about-fugro/group-overview/fugro-at-a-glance [Accessed 13 June 2015].

Hackwell, 2015 Private Communications with Fugro GeoSevices, Project Design Engineer.

Kassaba, S.Z., Kandila, H.A., Wardaa, H.A. & Ahmedb, W.H., 2009. Air-lift pumps characteristics under two-phase flow conditions. *International Journal of Heat and Fluid Flow*, 30(1), p.88–98.

Kinsky, R., 1982. *Applied Fluid Dynamics*. 1st ed. Sydney: McGraw-Hill Book Company.

Mahrous, A.F., 2012. Numerical Study of Solid Particles-Based Airlift Pump Performance. *WSEAS Transactions on Applied and Theoretical Mechanics*, 7(3).

NASA, 2014. *Reynold Number*. [Online] Available at: https://www.grc.nasa.gov/www/BGH/reynolds.html [Accessed 03 December 2015].

PennWell Corporation, 1999. *Research focusing on degree of contamination from cuttings piles*. [Online] Available at: http://www.offshore-mag.com/articles/print/volume-59/issue-8/departments/international-focus/research-focusing-on-degree-of-contamination-from-cuttings-piles.html [Accessed 04 November 2015].

Pougatch, K. & Salcudean, M., 2008. Numerical modelling of deep sea air-lift. *Ocean Engineering*, 35(11-12), p.1173–1182.

Ragner, C.L., 2008. *The Northen Sea Route*. [Online] norden Available at: http://norden.se [Accessed 15 June 2015].
Reinemann, D.J., Parlange, J.Y. & B, T.M., 1990. Theory of Small-Diameter Airlift Pumps. *International Journal for Multiphase Flow*, 16, pp.113-22.
Rigzone.com, 2015. *How Do Jackups Work?* [Online] Available at: http://www.rigzone.com/training/insight.asp?insight_id=339&c_id=24 [Accessed 04 November 2015].
Stenning, A.H. & Martin, C.B., 1968. An Analytical and Experimental Study of Air-Lift Pumpo Performance. *A Journal of Engineering for Power*, pp.106 - 110.
subseaworldnews, 2015. *fugro completes hornsea project one geotechnical campaign*. [Online] Available at: http://subseaworldnews.com/2015/04/23/fugro-completes-hornsea-project-one-geotechnical-campaign/ [Accessed 16 June 2015].
Tighzert, H., Brahimi, M., Kechroud, N. & Benabbas, F., 2013. Effect of submergence ratio on the liquid phase velocity, efficiency and void fraction in an air-lift pump. *Journal of Petroleum Science and Engineering*, 110(1), p.155–161.
Towle, P. & Fishwick, M., 2015. *Reeds Nautical Almanac 2016 (Reed's Almanac)*. Aberdeen: Harold Brunton-Reed.
Wahba, E.M. et al., 2014. On the Performance of Air-Lift Pumps: From Analytical Models to Large Eddy Simulation. *Journal of Fluids Engineering*, pp.on-line.
Yoshinaga, T. & Sato, Y., 1996. PERFORMANCE OF AN AIR-LIFT PUMP FOR CONVEYING COARSE P ARTICLES. *PInt. J. Multiphase Flow Vol. 22, No. 2, pp. 223-238, 1996*, 22(2), pp.223-38.

Domain Drawings

This document contains all of the domain drawings constructed from dimensions of experimental equipment and information from Fugro's Jersey Project. All drawings have been printed A3 size to allow them to be easily displayed in the log book. The drawings are displayed in sections relating to the literature from which they have been taken.

No revisions triangles are shown as nothing was manufactured therefore they are not needed for changes to manufactured products. Instead the whole new geometry is holistically re-imported into Ansys.

Table of Contents

Construction of the Geometry

To construct the geometry the following steps were followed:

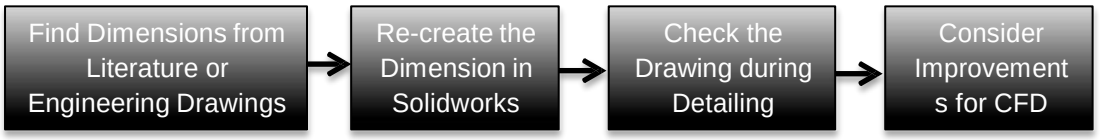

Models Constructed

Table 1 shows a list of all of the geometry made for testing. The literature used was selected by:

- Information being available,
- A range of data being available (for model validation),
- To ensure that a range of models with different dimensions are studied.

The literature used in Table 1 is named by the code LitXXXX. In the code the X locations are populated with numbers. Each number represents a piece of reference material. This is used throughout the project as a fast way of sighting reference material for editing and in the logbook. This was all controlled by an information directory spread sheet. Full dimension given are shown in Appendix F.

The literature codes in Table 1 are as follows;

- Lit0005 - (Kassaba, Kandila, Wardaa, & Ahmedb, 2009)
- Lit0007 - (Tighzert, Brahimi, Kechroud, & Benabbas, 2013)
- Lit0020 - (Stenning & Martin, 1968)

Test type	Literature		Size	Rev	Description
Two Phase					
	Lit0005				
		Domain	FULL	A	Full Length with standard inlet holes
	Lit0007				
		Domain	FULL	A	Full Length with standard inlet holes
	Lit0020				
		Domain	FULL	A	Full Length with standard inlet holes
		Domain	FULL	A1	Full Length with standard inlet holes (merge removed)
		Domain	1/8	A	1/8 domain for meshing after meeting with AK
		Domain	1/8	B	1/8 domain with base added
		Domain	1/8	C	1/8 domain with base and top added
		Domain	1/8	D	1/8 domain with top and extended base
Three Phase					
	Seacore - Jersey				
		Domain	FULL	A	Full Length with bend and estimated holes for air inlet
		Domain	FULL	B	Full Length with bend and real air inlet sizes

		Domain	FULL	C	Full Length with No bend and real air inlet sizes

Table 1 – The Geometry Created

Changes to Lit0020 Domain Geometry

Due to time constraints CFD modelling was only undertaken on Lit0020 geometries. During this the geometry was developed to allow for more efficient meshing and improved results. For this reason Lit0020 has by far the most revisions. The description column in Table 1 briefly explains the component geometry of each revision.

Due to the complex nature of Lit0020 Domain 1/8 the complete geometry is an assembly of several parts. For this section the full assemblies and then sub-assemblies are shown with a drawing hierarchy (Table 2).

All changes to Lit0020 geometry are discussed in Appendix C. Lengthening the domain below the air inlet will increase drag from the walls however this is thought to be negligible as only 48 mm is added. This accounts for a 1.2% increase in the overall length of the domain.

Changes to Fugro Jersey Domain Geometry

Unlike the geometry for literature, the Fugro Jersey Domain has been created from an engineering drawing (Figure 1) supplied by (Hackwell, 2015). Using engineering drawings ensures that the dimensions are an accurate representation of the Airlift pump on site.

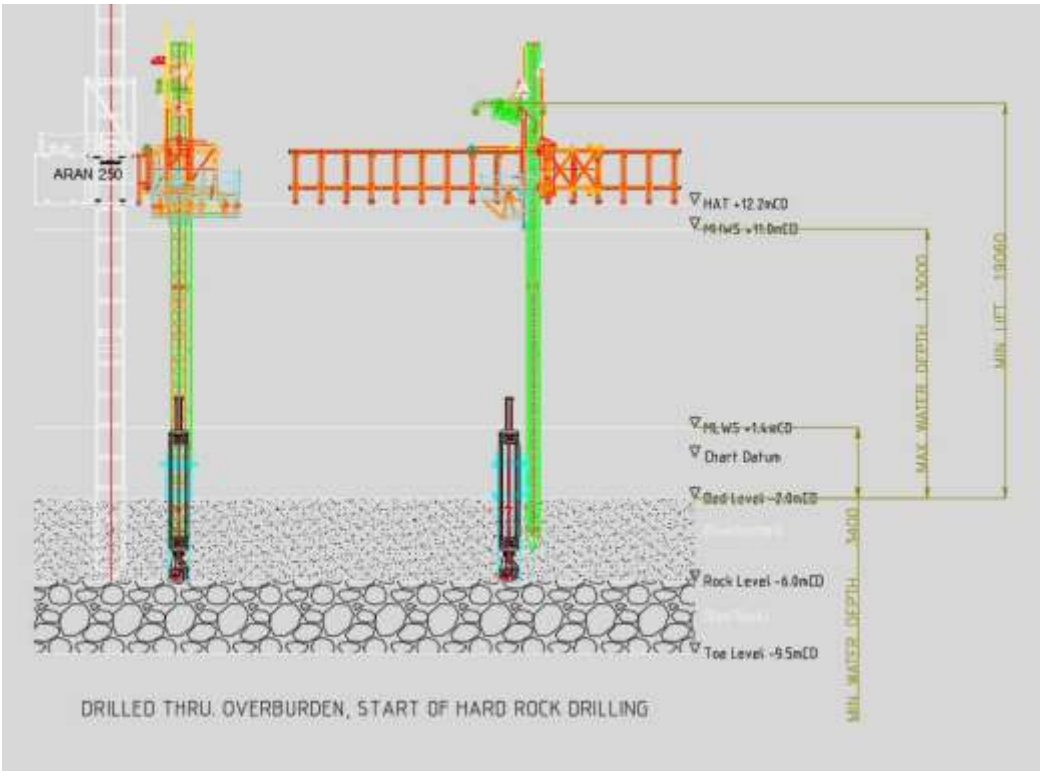

"Figure 1 - A Diagram of Fugro's Jersey Project Setup from (Hackwell, 2015)"

Figure 1 from (Hackwell, 2015) shows the Jersey project where Airlift pumping was used with a tidal range of around 9.6 m. During work on this project Fugro

experienced difficulties with pumping at low tide (Hackwell, 2015). As the depth drilled increases the submergence ratio of the riser becomes greater increasing the pumps performance.

From Figure 1, the riser can be drawn. This has a bend before the air is injected so that the intake is able to follow the cutting face of the drill head as the drill head rotates. This is shown in Figure 2.

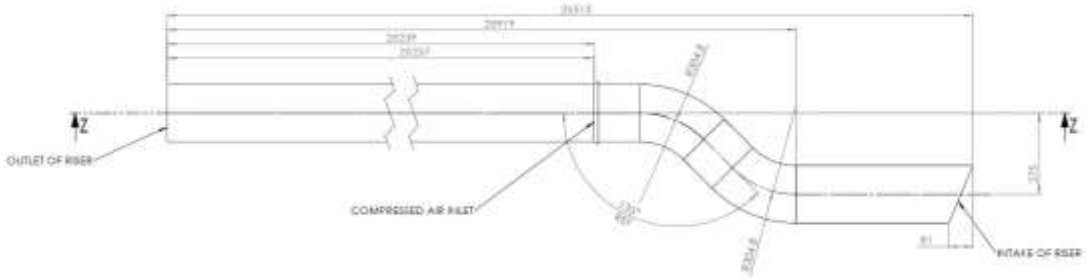

Figure 2 -The Riser Drawn With Dimensions from Figure XX (Hackwell, 2015)

The riser shape and therefore the CFD domain shape can be simplified by straightening the domain as shown in Figure 2. This is acceptable because the only effect of the bend is more surface area increasing the amount of friction stated by (Fujimoto, Murakami, Omura, & Takuda, 2004) because the bend is before the air inlet.

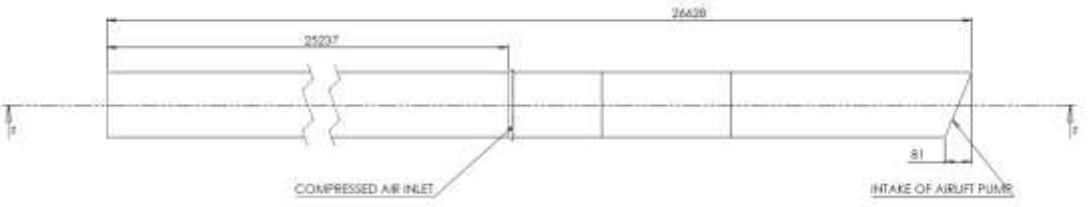

Figure 3 - The Riser Drawn With Dimensions from Figure XX (Hackwell, 2015) Simplified

Figures 2 and 3 are shown in full in of pages 20 and 21 respectivly.

Drawings

This section shows all drawings printed on A3 paper so they can be easily displayed in this document.

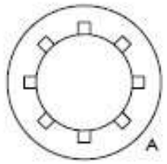

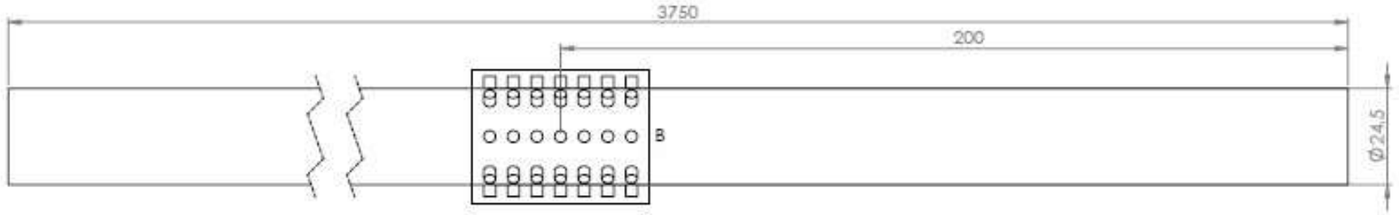

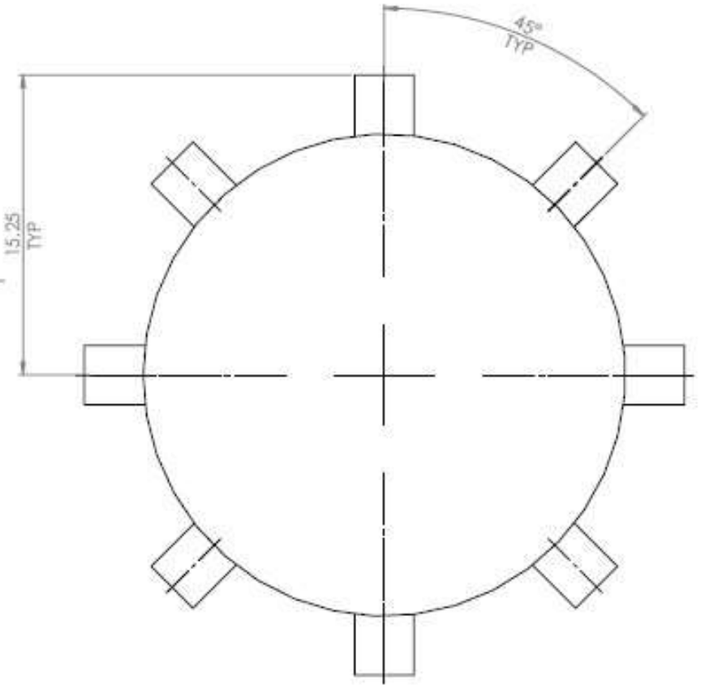

DETAIL A
SCALE 5 : 1

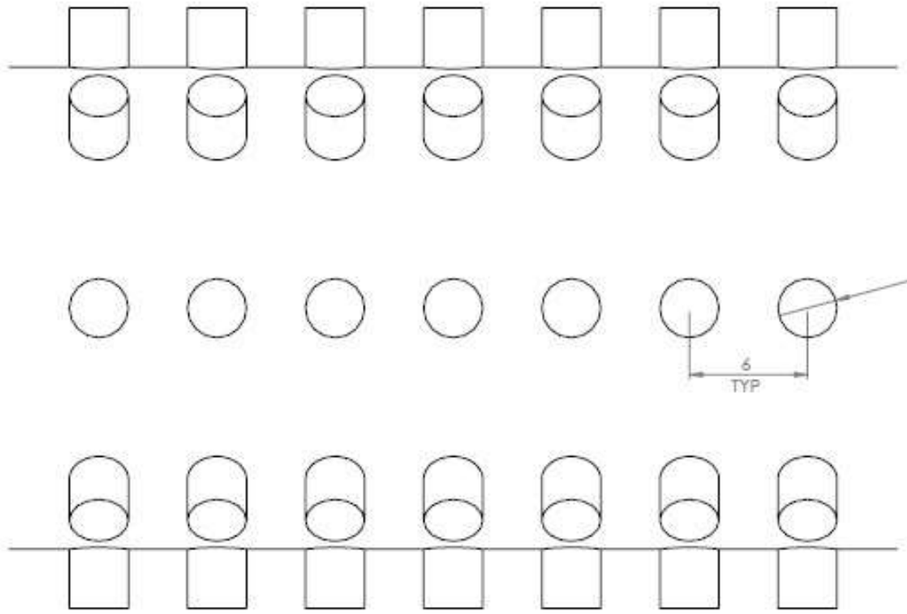

DETAIL B
SCALE 5 : 1

LIT0005 Domain FULL REV A

BSI Standards
All Dimensions in mm
Drawn by MH
3rd Person Orthographic

NOT TO SCALE

Appendix B

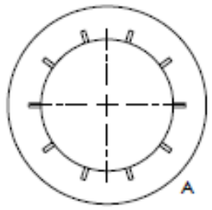

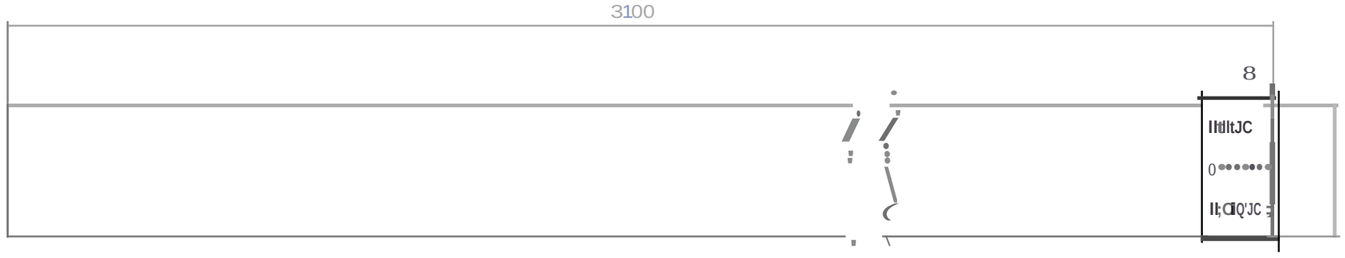

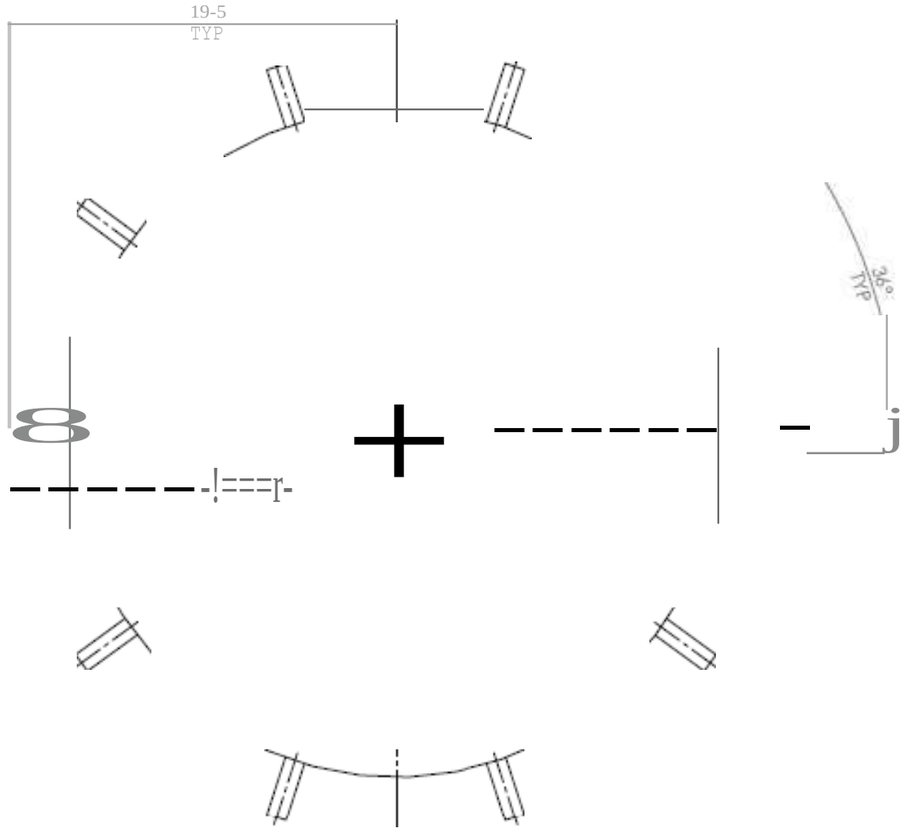

DETAIL A
SCALE 5 : 1

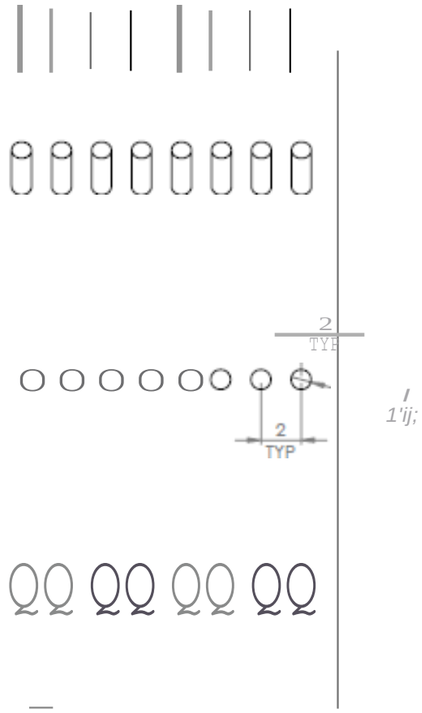

DETAIL S
SCALE 5 : 1

NOT TO SCALE

LIT0007 Domain FULL REV A	
BSI Stand.,ds	
ALL **Dimensions in mm**	
DraWI by MH	
3" Person Orthographic	

Appendix B

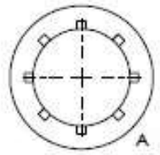

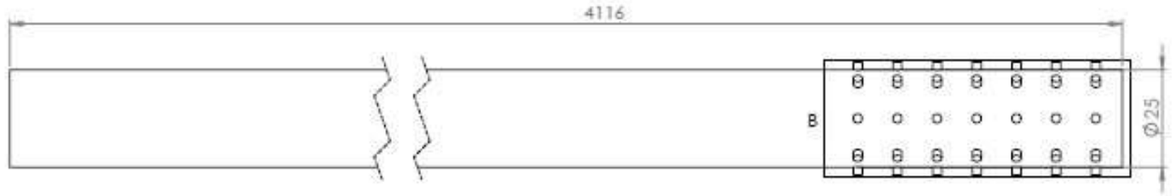

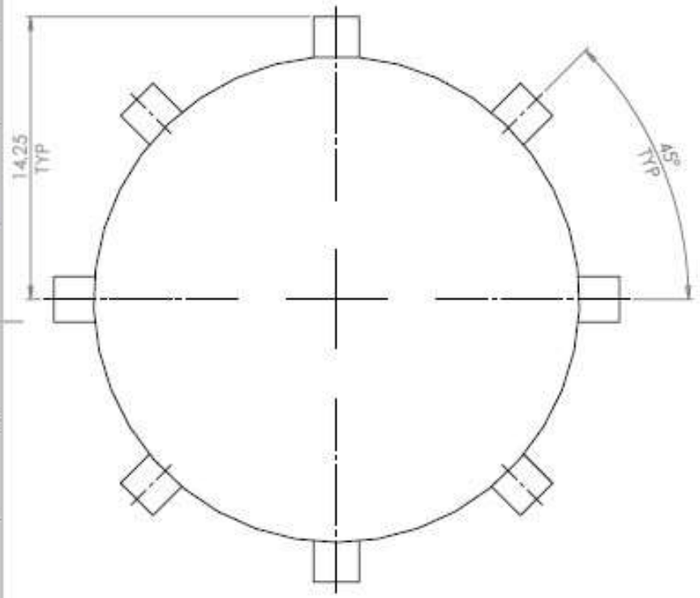

DETAIL A
SCALE 5 : 1

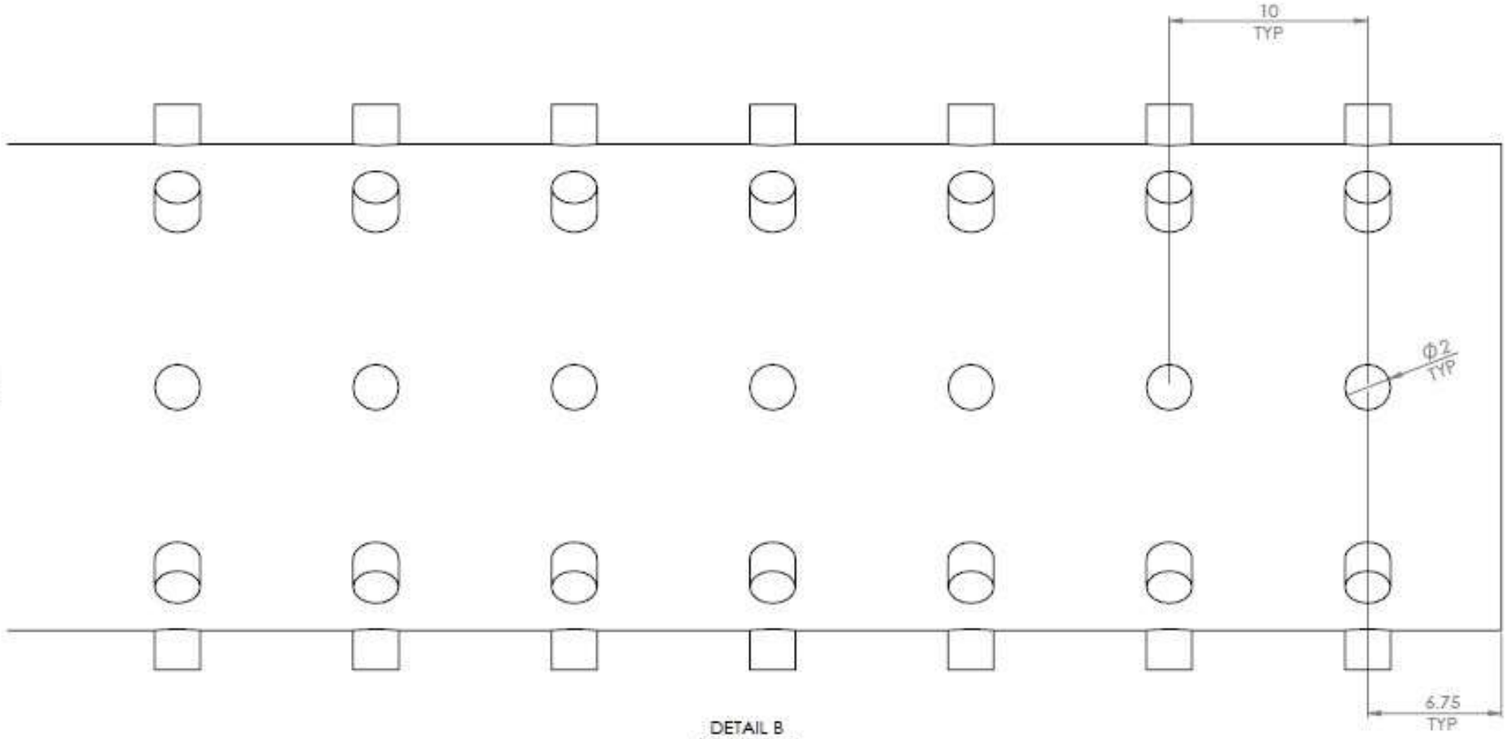

DETAIL B
SCALE 5 : 1

NOT TO SCALE

LIT0020 Domain FULL REV A

BSI Standards
All Dimensions in mm
Drawn by MH
3rd Person Orthographic

Appendix B

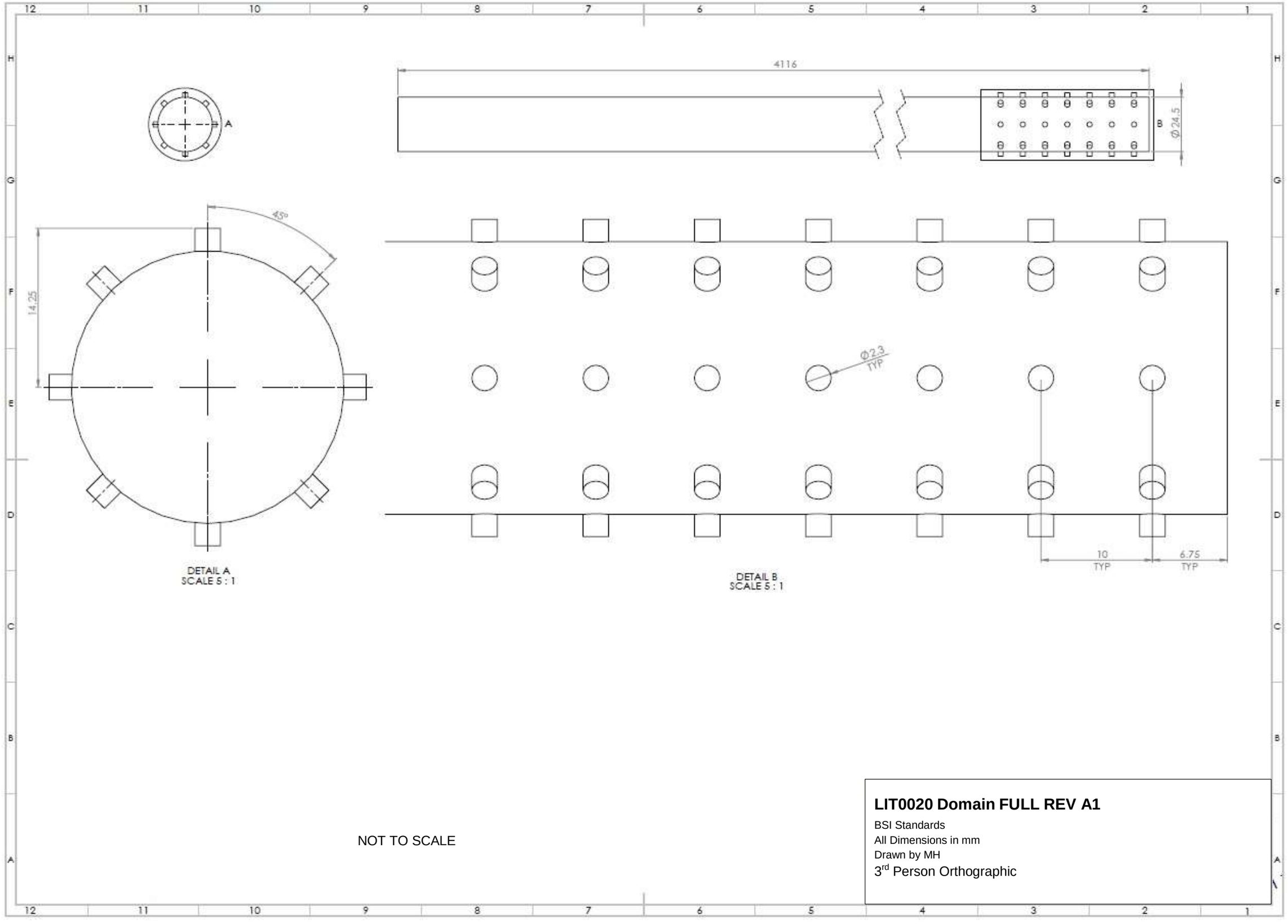
4116
A
B
Φ24.5
45°
14.25
Φ2.3
TYP
10
TYP
6.75
TYP
DETAIL A
SCALE 5 : 1
DETAIL B
SCALE 5 : 1
NOT TO SCALE
LIT0020 Domain FULL REV A1
BSI Standards
All Dimensions in mm
Drawn by MH
3rd Person Orthographic

Appendix B

Lit0020 Domain 1/8 Hierarchy

This was the model developed for the CFD modelling. As such the reasons for these revisions are mentioned in Appendix C. Each change was made following CFD modelling needs. The first of these being the creation of the 1/8th model from the full riser to reduce the mesh count and therefore computing times.

Other changes were also made. For Lit0020 Domain 1/8 all of the assemblies are shown, then the different revisions of every component is shown before Top Assembly REV B is shown as an example of the full domain when all 1/8^{ths} are combined forming the complete the geometry.

Lit0020 Domain Drawing Hierarchy											
Rank			Description			File Name			Revision	Reason For Level	
	2			1/8			ASSEMBLY		A	1/8th of Domain	
		3			Component			n/a	B	Component Weldment Only	
		3			Component			(top)	A		
1			Top			TOP ASSEMBLY			B	Shows Full Domain Assembly	
	2			1/8			ASSEMBLY		B	1/8th of Domain Assembly	
		3			Component			n/a	B	Component Weldment Only	
		3			Component			(top)	A		
		3			Component			Base	A		
	2			1/8			ASSEMBLY		C	1/8th of Domain Assembly	
		3			Component			n/a	B	Component Weldment Only	
		3			Component			(top)	A		
		3			Component			Base	A		
		3			Component			Outlet	A		
	2			1/8			ASSEMBLY		D	1/8th of Domain Assembly	
		3			Component			n/a	B	Component Weldment Only	
		3			Component			(top)	A		
		3			Component			Base	B		
		3			Component			Outlet	A		

Table 2 – Lit0020 Hierarchy

All Drawings listed in Table 2 are displayed in the following sections. To avoid duplication the drawings are organised in rank, height they first appear in and revision taken from Table 2.

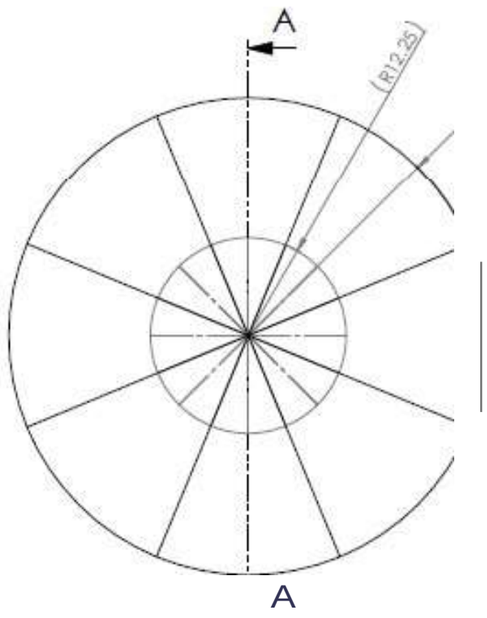

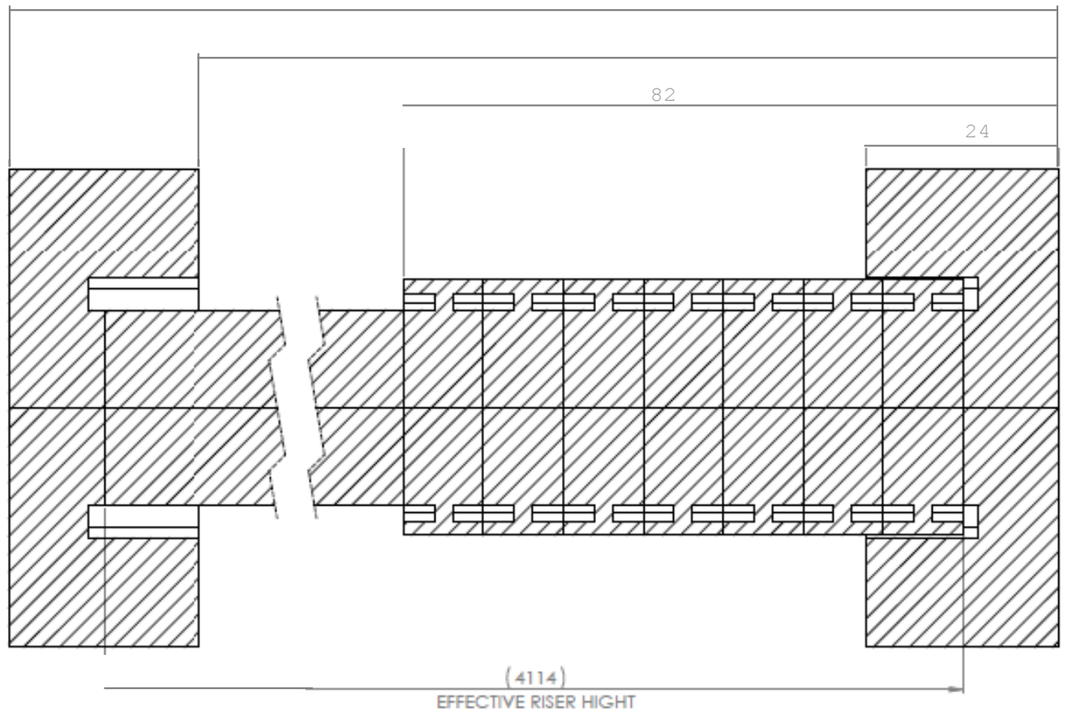

SECTION A-A

NOT TO SCALE

LIT0020 Domain Top Assembly REV B

BSI Standards
All Dimensions in mm
Drawn by MH
3rd Person Orthographic

ITEM NO.	PART NUMBER	QTY.
	tmJ020 Domain 118 REVS	7
2	Ui0020 Domain 118 (opp) REVA	

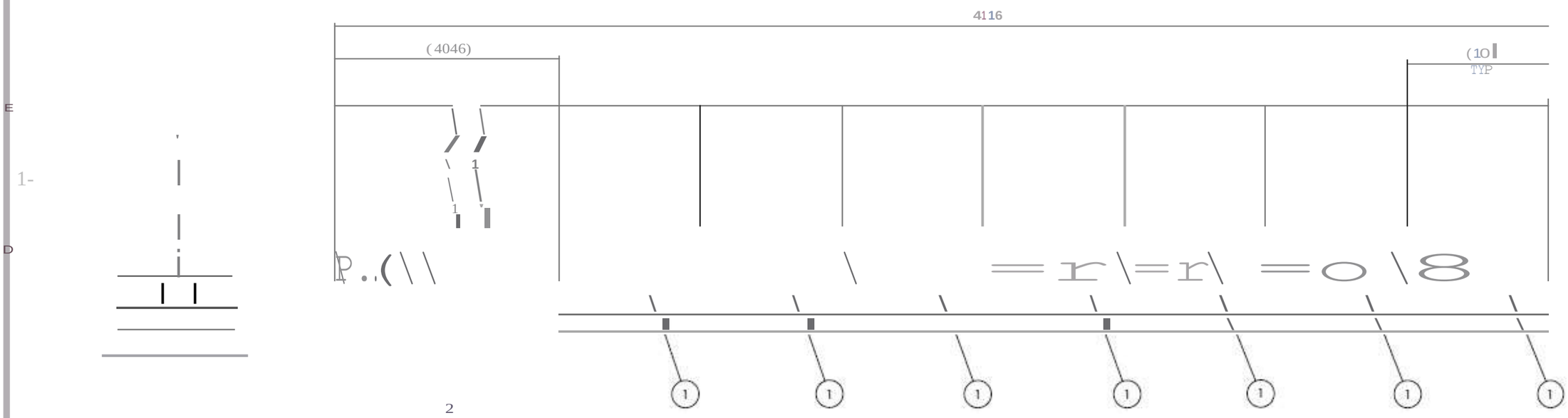

NOT TO SC.AJ...E

LIT0020 Domain 118 Assembly REV A

BSIStandards
.AJI**Dimensions in mm**
DrOWI by MH
3 • Person Orthographic

Appendix 8

ITEM NO.	PART NUMBER	QTY.
1	LIT0020 Domain 1 8th REVB	7
2	LIT0020 Domain 1 8th (top) REVA	1
3	LIT0020 Domain 1 8th Base REVA	1

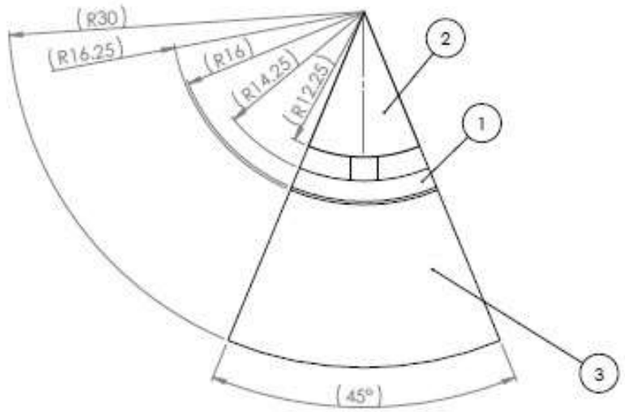

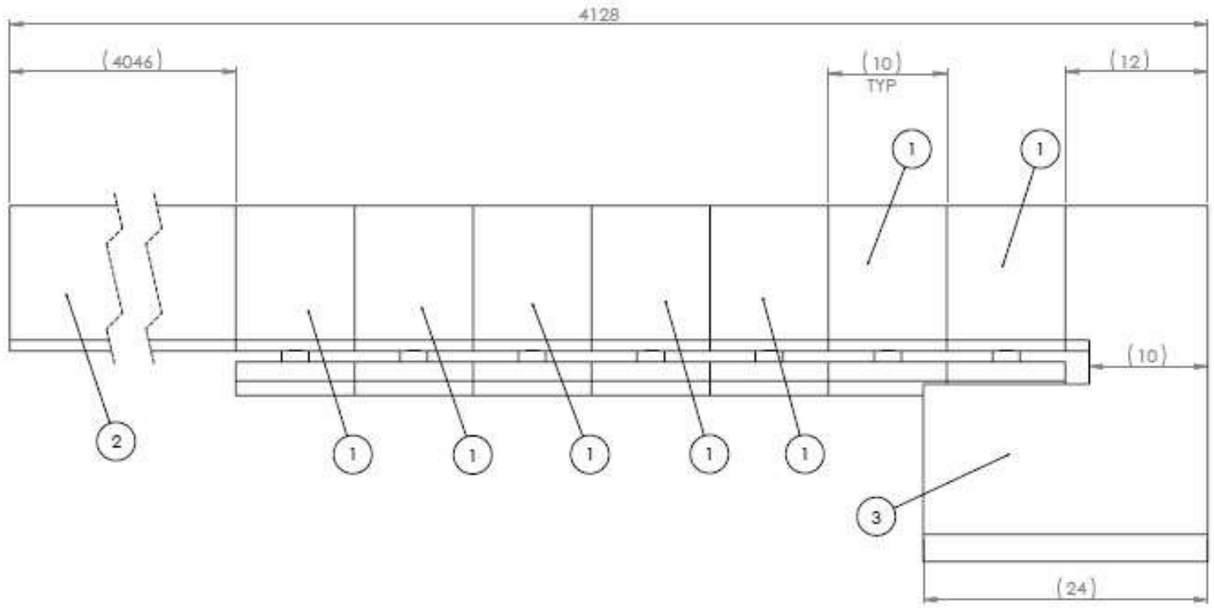

NOT TO SCALE

LIT0020 Domain 1/8 Assembly REV B

BSI Standards
All Dimensions in mm
Drawn by MH
3rd Person Orthographic

ITEM NO.	PART NUMBER	QTY.
1	LIT0020 Domain 1 8th REVB	7
2	LIT0020 Domain 1 8th (top) REVA	1
3	LIT0020 Domain 1 8th Base REVA	1
4	LIT0020 Domain 1 8th Outlet REVA	1

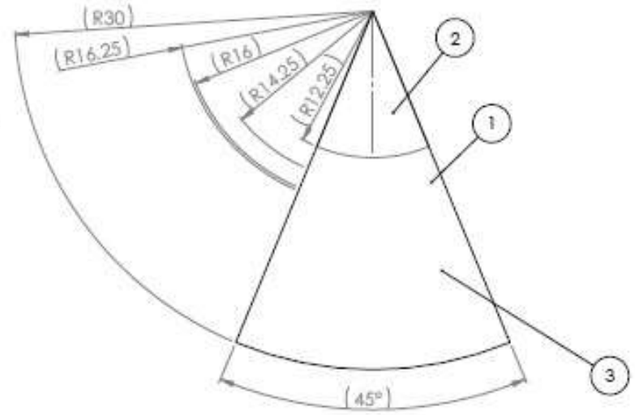

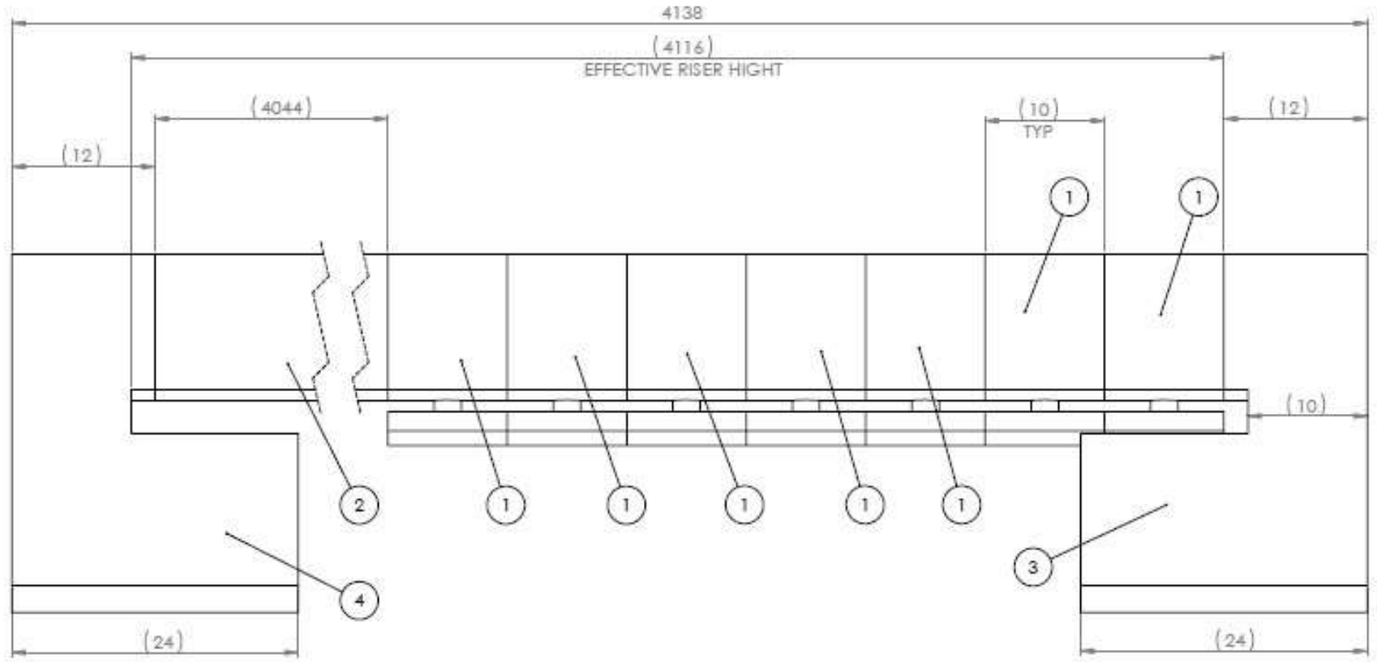

NOT TO SCALE

LIT0020 Domain 1/8 Assembly REV C

BSI Standards
All Dimensions in mm
Drawn by MH
3rd Person Orthographic

Appendix B

ITEM NO.	PART NUMBER	QTY.
1	LIT0020 Domain 1 8th REVB	7
2	LIT0020 Domain 1 8th (top) REVA	1
3	LIT0020 Domain 1 8th Base REVB	1
4	LIT0020 Domain 1 8th Outlet REVA	1

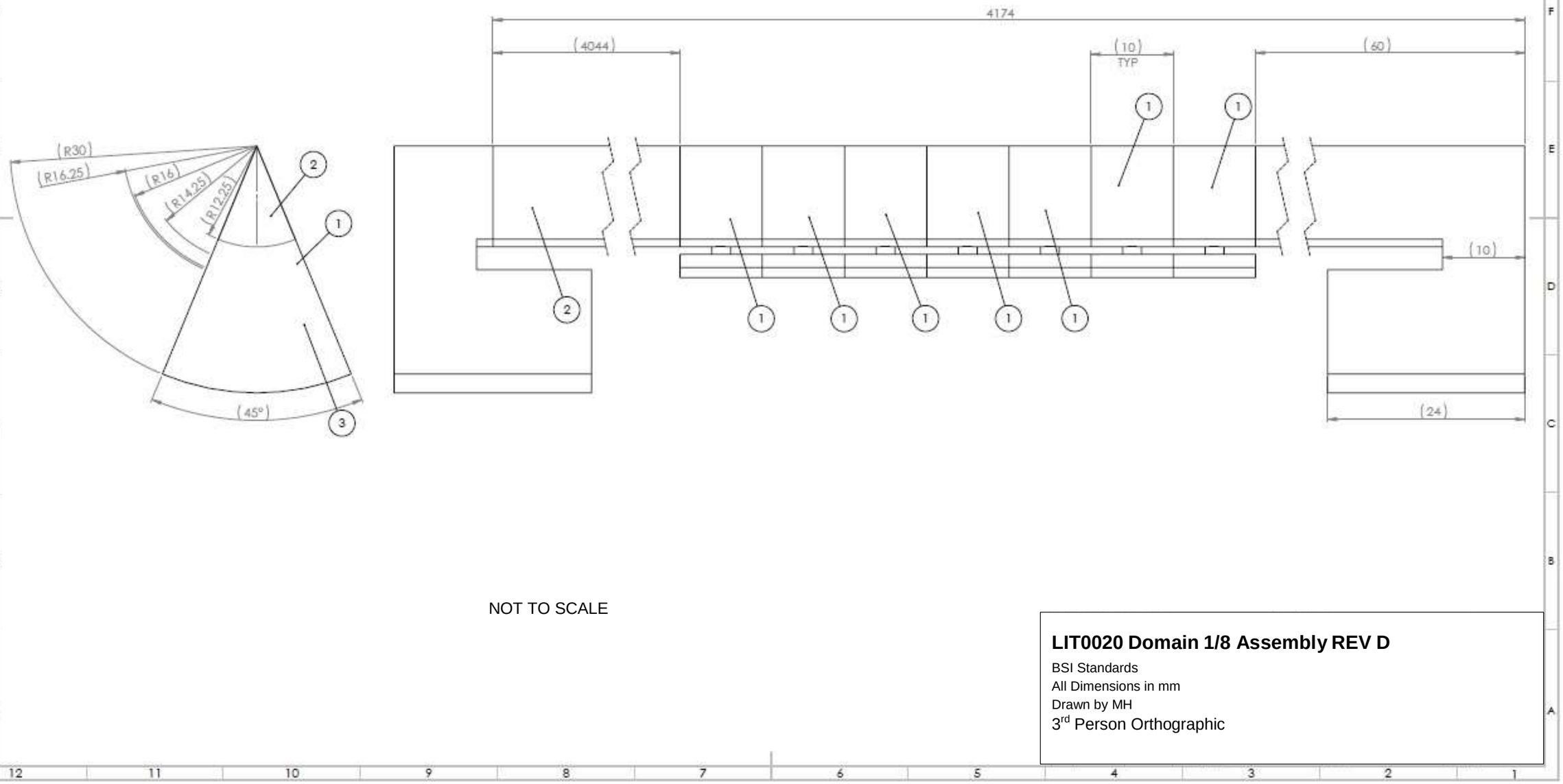

NOT TO SCALE

LIT0020 Domain 1/8 Assembly REV D

BSI Standards
All Dimensions in mm
Drawn by MH
3rd Person Orthographic

Appendix B

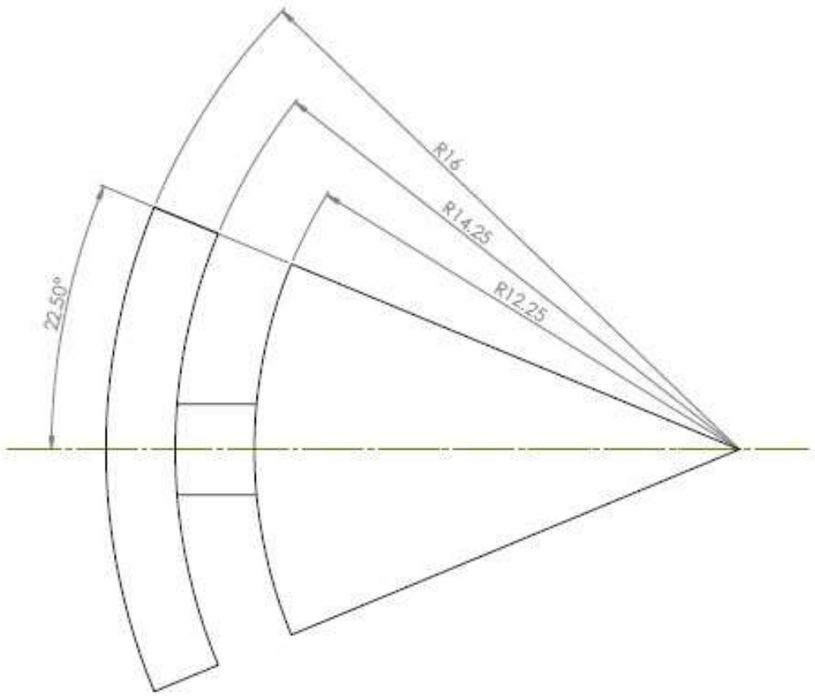

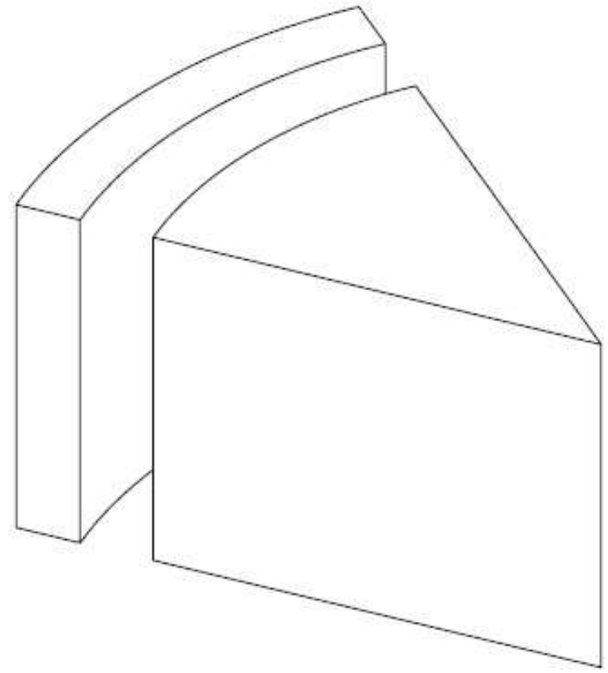

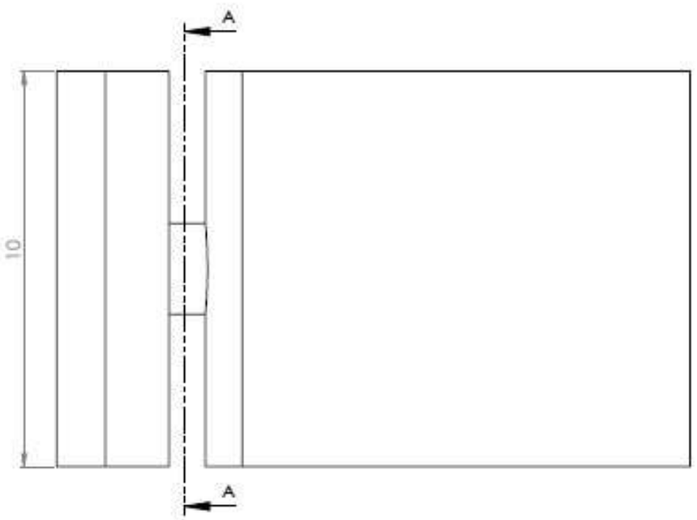

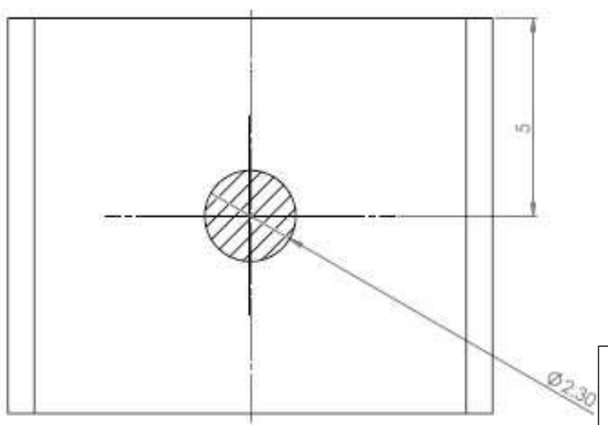

SECTION A-A

NOT TO SCALE

LIT0020 Domain 1/8 REV B

BSI Standards
All Dimensions in mm
Drawn by MH
3rd Person Orthographic

Appendix B

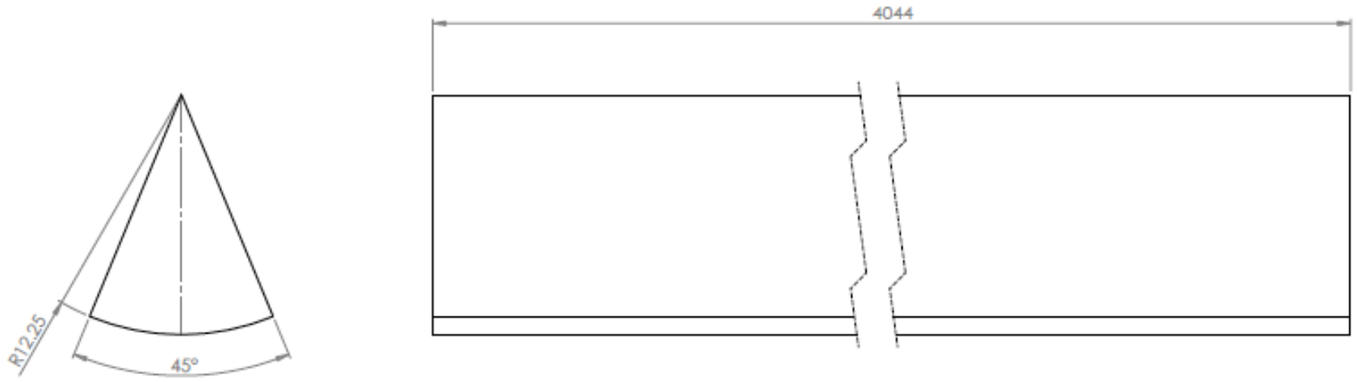

NOT TO SCALE

LIT0020 Domain 1/8 (top) REV A

BSI Standards
All Dimensions in mm
Drawn by MH
3rd Person Orthographic

Appendix B

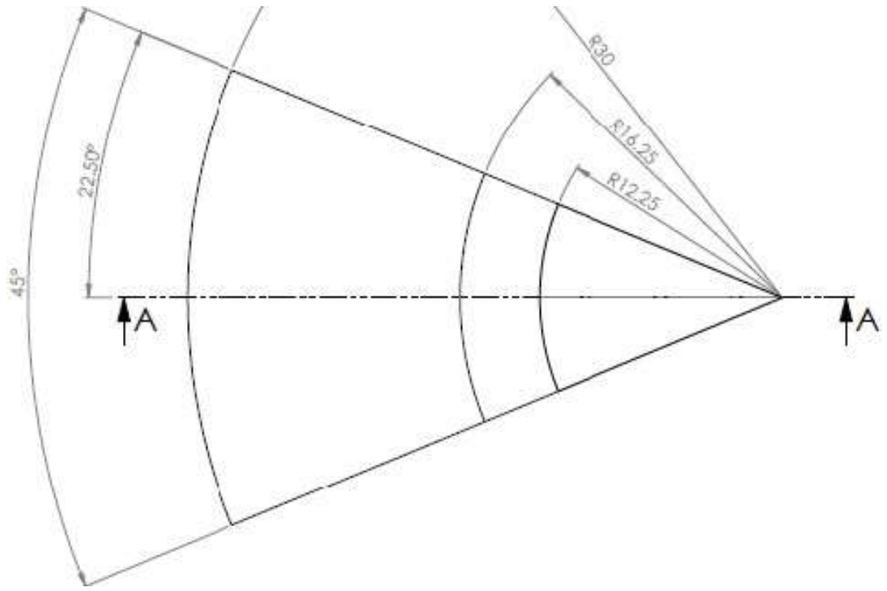

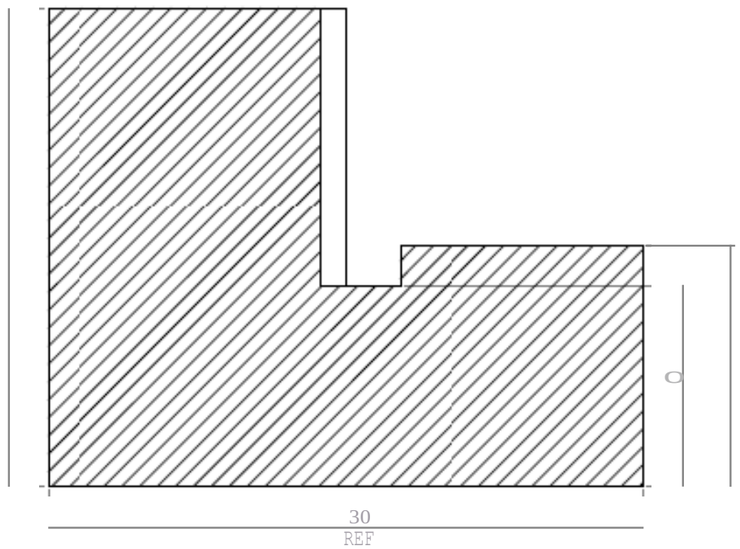

SECTION A-A
NOTTO SCALE

LIT0020 Domain 118 Base REV A
BSI Standards
.AJl Dimensions in mm
Dra'l\fl by MH
3''Person Orthographie

Appendix 8

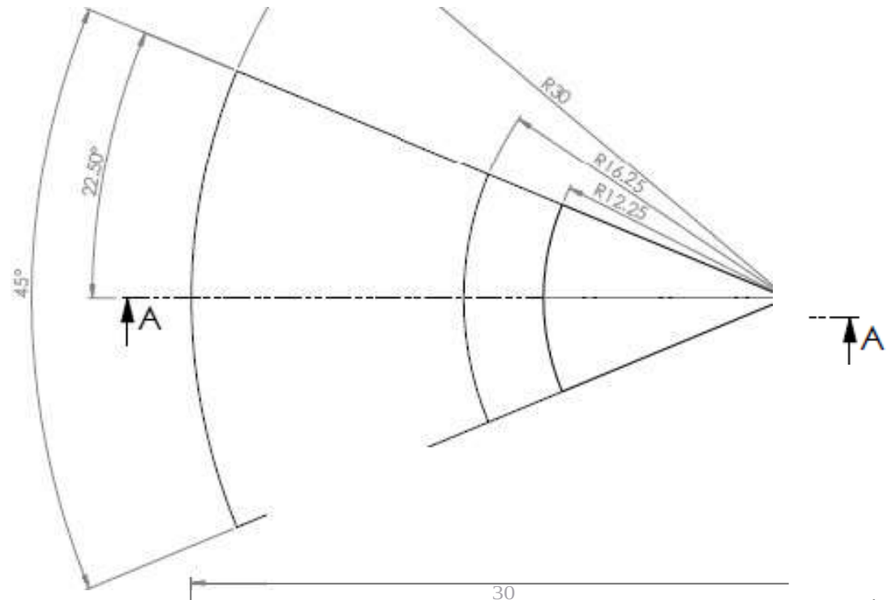

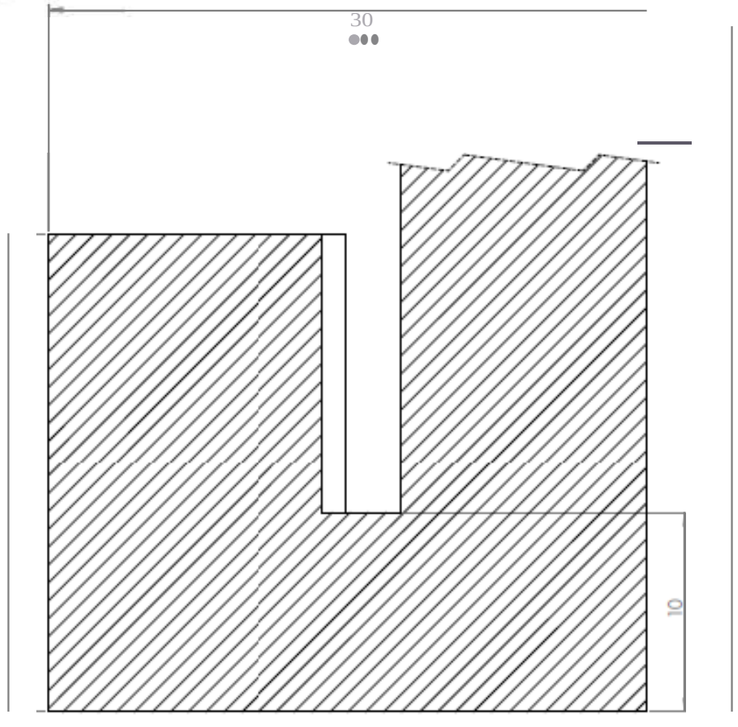

NOT TO SC.AJ...E

SECTION A-A

LIT0020 Domain 118 Base REV B
BSI Standards
.AJI Dimensions in mm
Dra'I\0 by MH
3" Person Orthographic

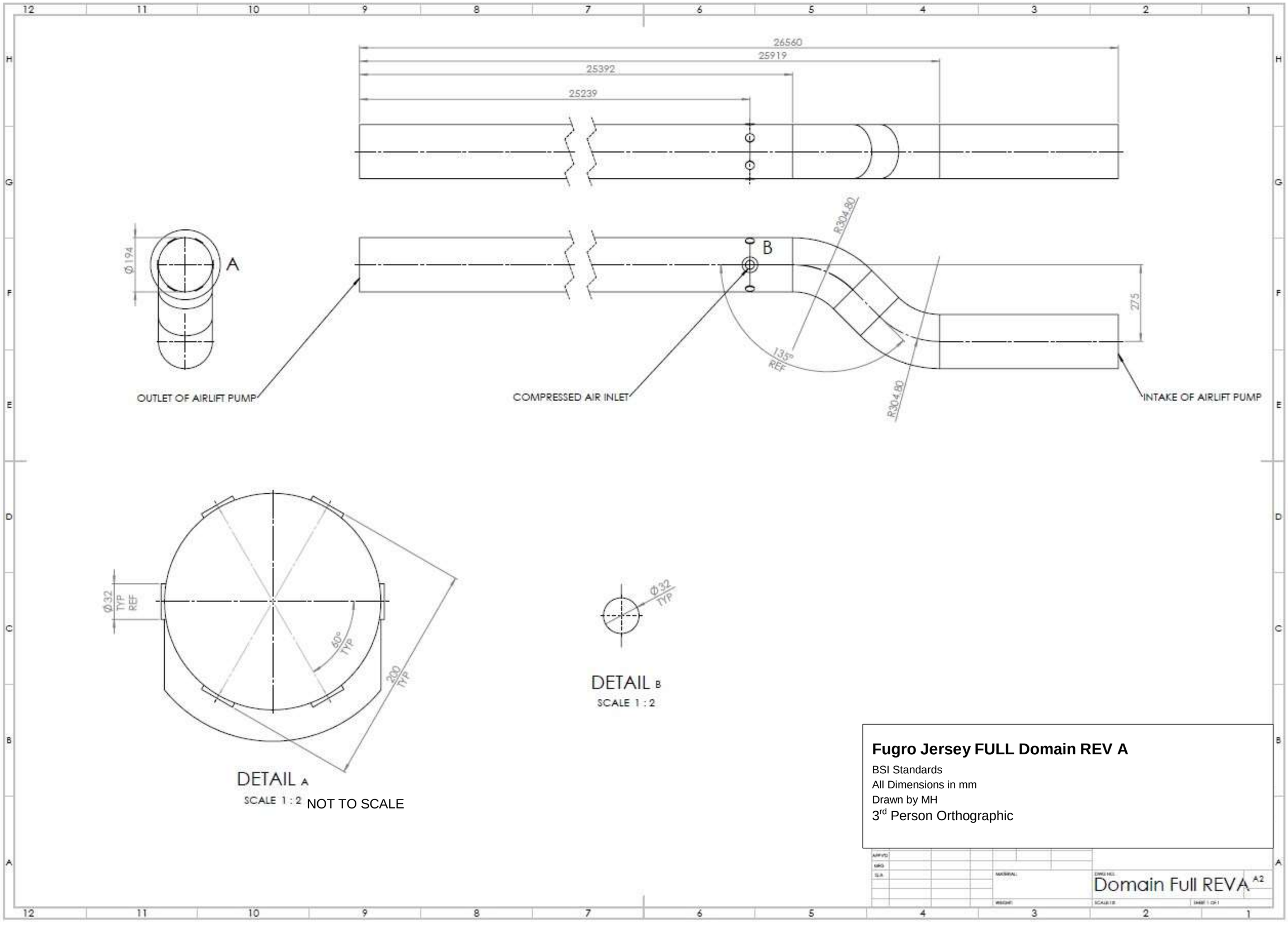
26560
25919
25392
25239
Ø194
A
B
R304.80
275
135°
REF
R304.80
OUTLET OF AIRLIFT PUMP
COMPRESSED AIR INLET
INTAKE OF AIRLIFT PUMP
Ø32
TYP
REF
60°
TYP
200
TYP
DETAIL A
SCALE 1 : 2 NOT TO SCALE
Ø32
TYP
DETAIL B
SCALE 1 : 2
Fugro Jersey FULL Domain REV A
BSI Standards
All Dimensions in mm
Drawn by MH
3rd Person Orthographic
Domain Full REVA
A2

Appendix B

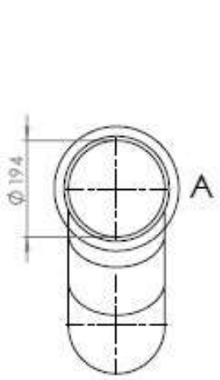

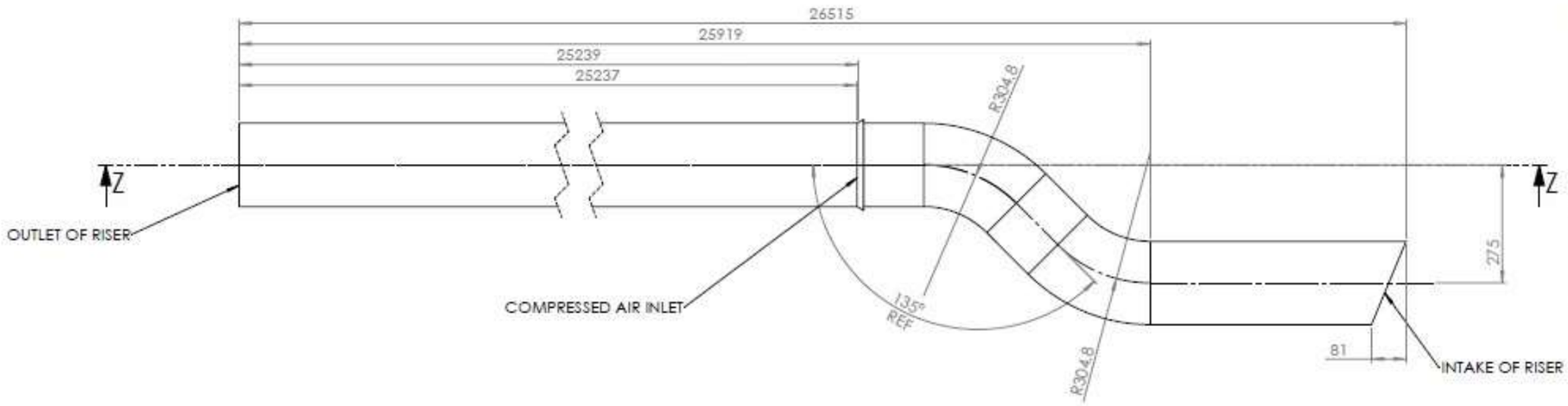

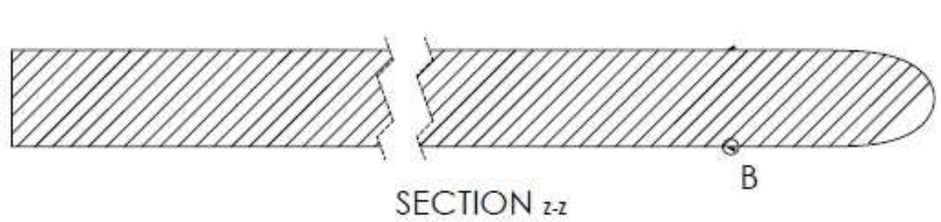

SECTION Z-Z

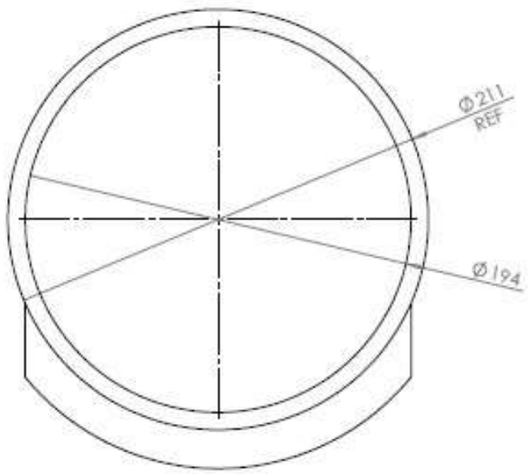

DETAIL A
SCALE 1 : 2

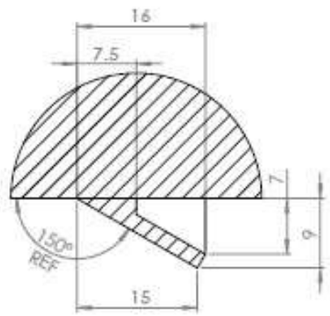

DETAIL B
SCALE 2 : 1

NOT TO SCALE

Fugro Jersey FULL Domain REV B

BSI Standards
All Dimensions in mm
Drawn by MH
3rd Person Orthographic

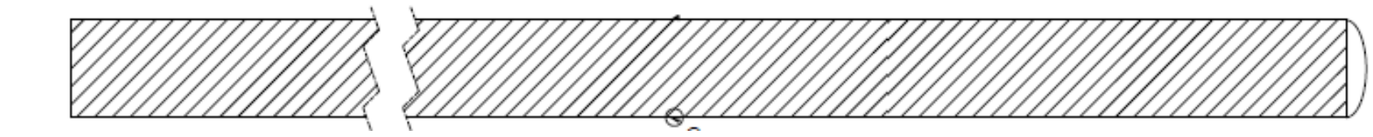

SECTION 7-7

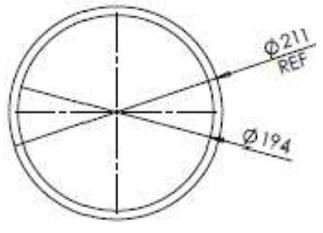

DETAIL A
SCALE 1 : 4

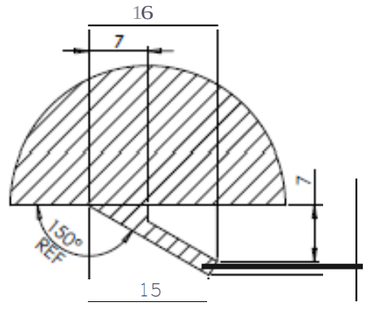

DETAIL C
SCALE 2 : 1

NOTTO SCALE

Fugro Jersey FULL Domain REV C

BSI Stancbrds
Dimensions in mm
DraWI byMH
3'' Person Orthographic

Lit0020 Geometry Boundary Setup

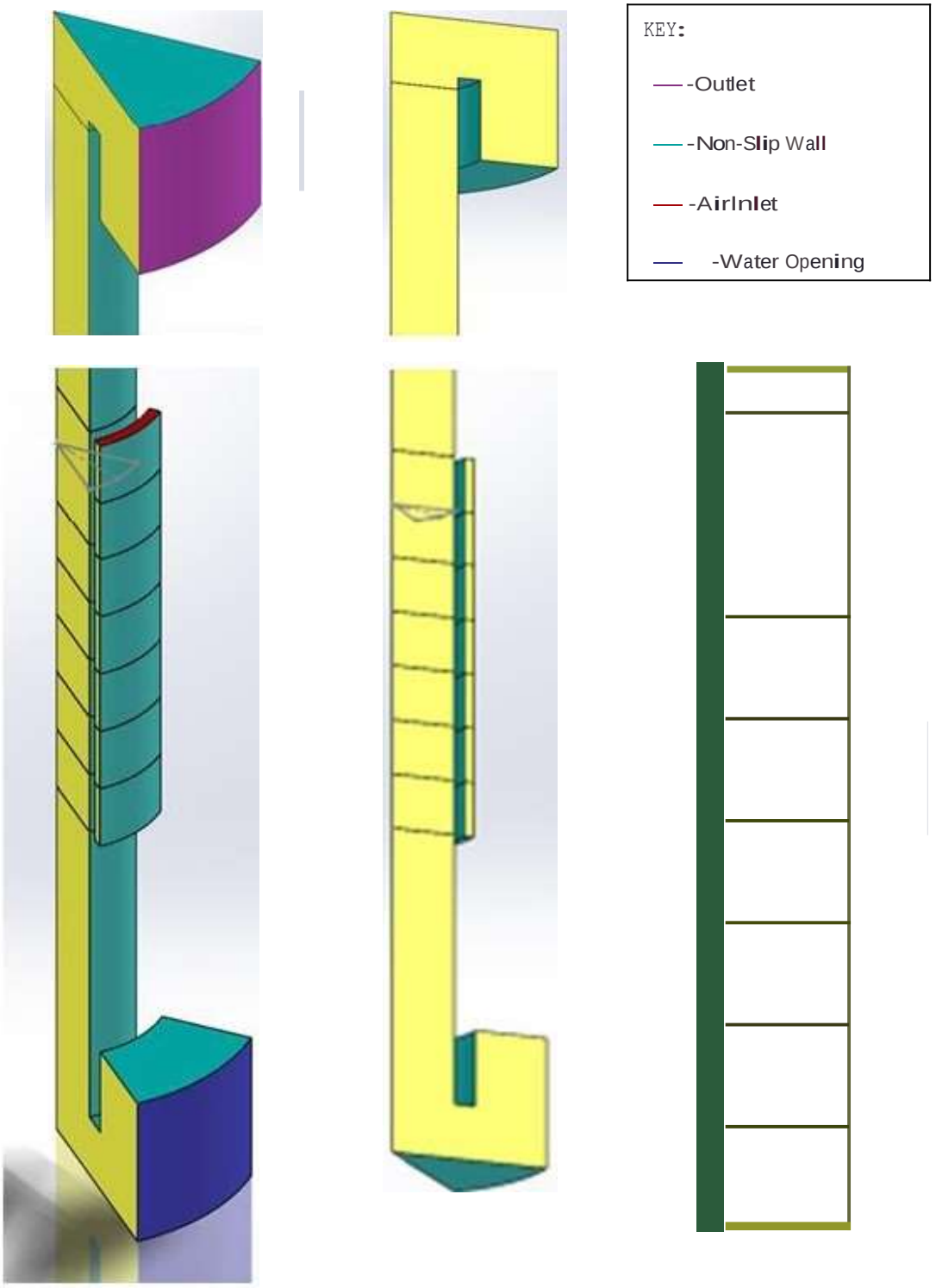

Figure 3- The Standard Boundary Setup for Lito020 Domains

Bibliography

Fujimoto, H., Murakami, S., Omura, A., & Takuda, H. (2004). Effect of local pipe bends on pump performance of a small air-lift system in transporting solid particles. *International Journal of Heat and Fluid Flow*, 996-1005.

Hackwell, 2015 Private Communications with Fugro GeoSevices, Project Design Engineer.

Kassaba, S. Z., Kandila, H. A., Wardaa, H. A., & Ahmedb, W. H. (2009, 02). Air-lift pumps characteristics under two-phase flow conditions. *International Journal of Heat and Fluid Flow, 30*(1), 88–98.

Stenning, A. H., & Martin, C. B. (1968). An Analytical and Experimental Study of Air-Lift Pumpo Performance. *A Journal of Engineering for Power*, 106 - 110.

subseaworldnews. (2015). *fugro completes hornsea project one geotechnical campaign.* Retrieved 06 16, 2015, from http://subseaworldnews.com: http://subseaworldnews.com/2015/04/23/fugro-completes-hornsea-project-one-geotechnical-campaign/

Tighzert, H., Brahimi, M., Kechroud, N., & Benabbas, F. (2013, 10). Effect of submergence ratio on the liquid phase velocity, efficiency and void fraction in an air-lift pump. *Journal of Petroleum Science and Engineering, 110*(1), 155–161.

CFD Work Record (In Screen Shots)

This document details all of the CFD work Undertaken in Chronological ordered after the geometry has been imported from Solid works. The runs are structured so that one follows on from the last; the run being shown is named in the sub-sections titles.

The document is not dated as this project was a steep learning curve; therefore parts had to be added retrospectively once their importance was known. This meant the document could not be produced in date order as it would be very difficult to follow.

As this is used as a fast way of recording CFD work with screen shots the figures are not numbered but are simply captioned by the text immediately below them.

Due to the project time and excessive run times often two or more factors are changed between each run. This is acceptable at the start of projects as it is obvious that some things are not physically accurate.

Table of Contents

Assumption 0 – The CFD must be 3D, this makes it a more accurate description to what is going on

Meshing geometry in ICEM:

All domain dimensions are available in appendix B

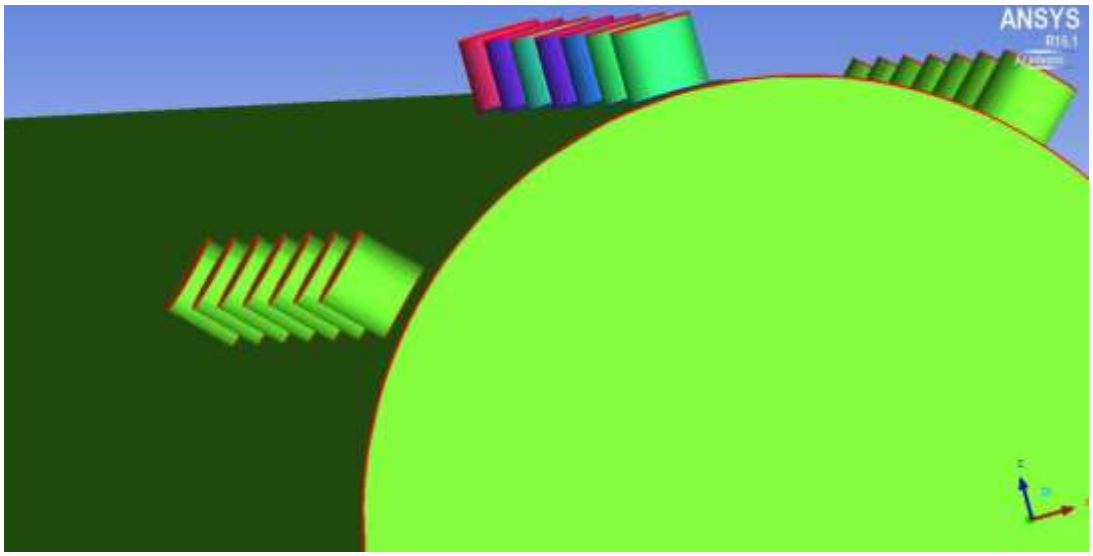

Image of LIT0020 Domain FULL REVA in ICEM note red curve lines showing 2 faces meeting and blue lines showing 3 faces meeting. The base of the air inlet tubes should not be red.

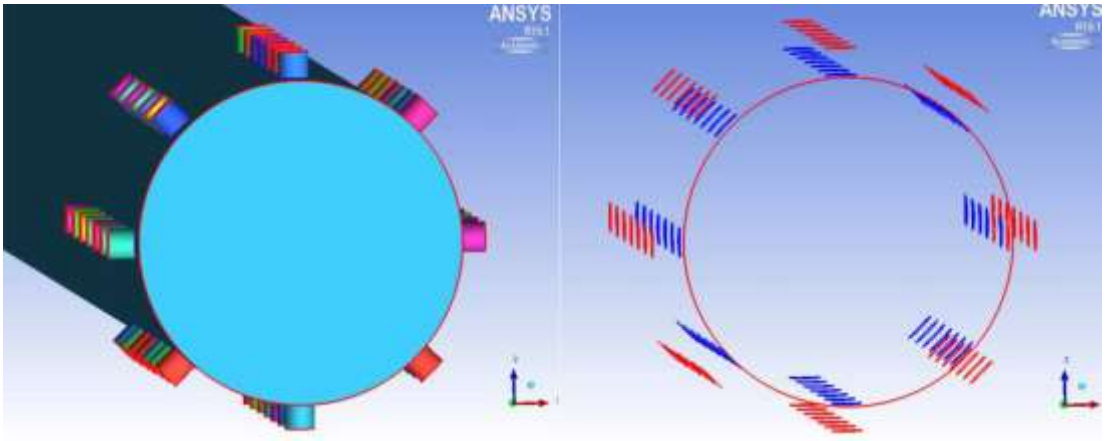

Image of LIT0020 Domain FULL REVA1 in ISEM note red curve lines showing 2 faces meeting and blue lines showing 3 faces meeting. The base of the air inlet tubes are now blue showing three faces are meeting at this point.

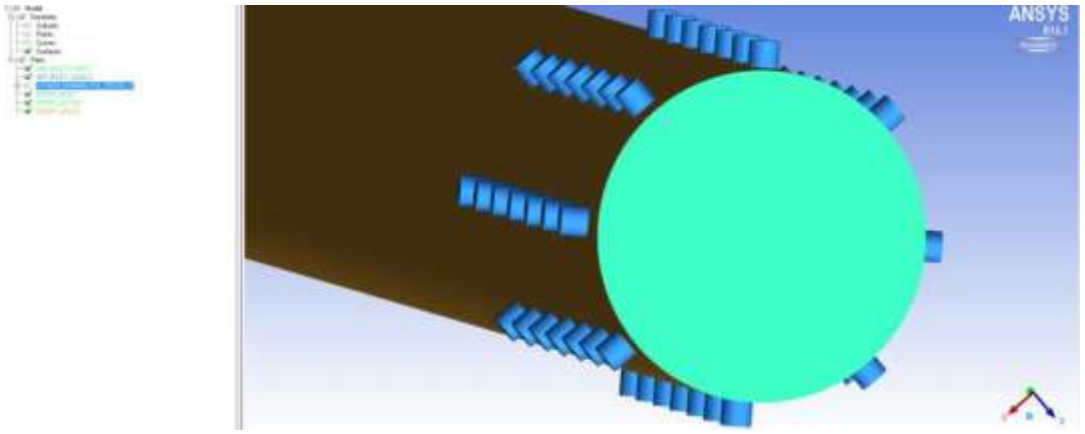

LIT0020 REVA1 showing the grouping of parts in the parts tree before meshing.

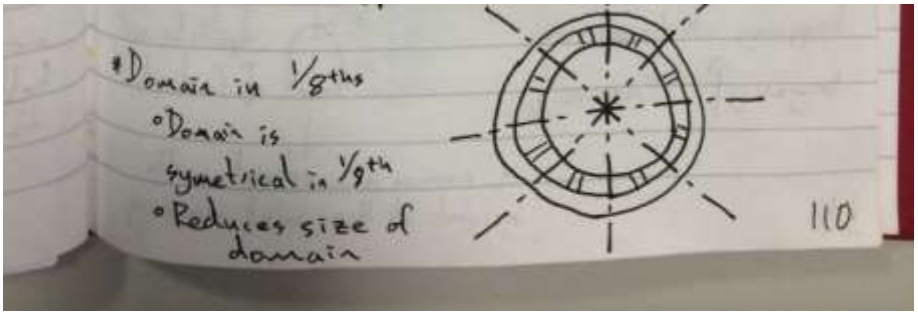

This shows the symmetry in the geometry, it can be cut into 8ths to reduce the number of elements in the mesh decreasing run times.

Run A

Assumption 1 – How the air enters the domain is of interest

While this may be different geometry to Fugro's case, it must be modelled to allow any results to be compared to the experimental data.

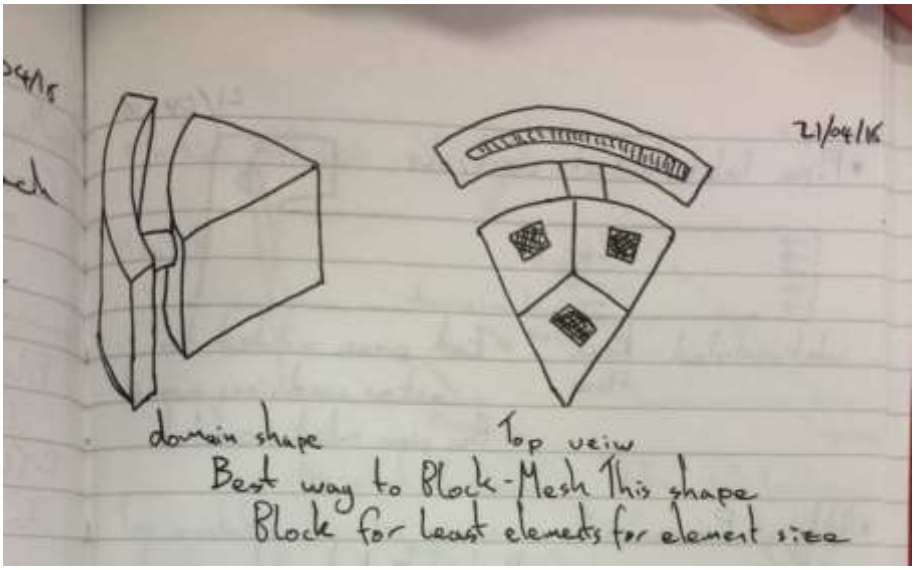

This shows how the efficiently mesh the geometry into blocks. This is the most element efficient from of meshing. Unfortunately due to the complexity of the geometry this can only be achieved though ICEM.

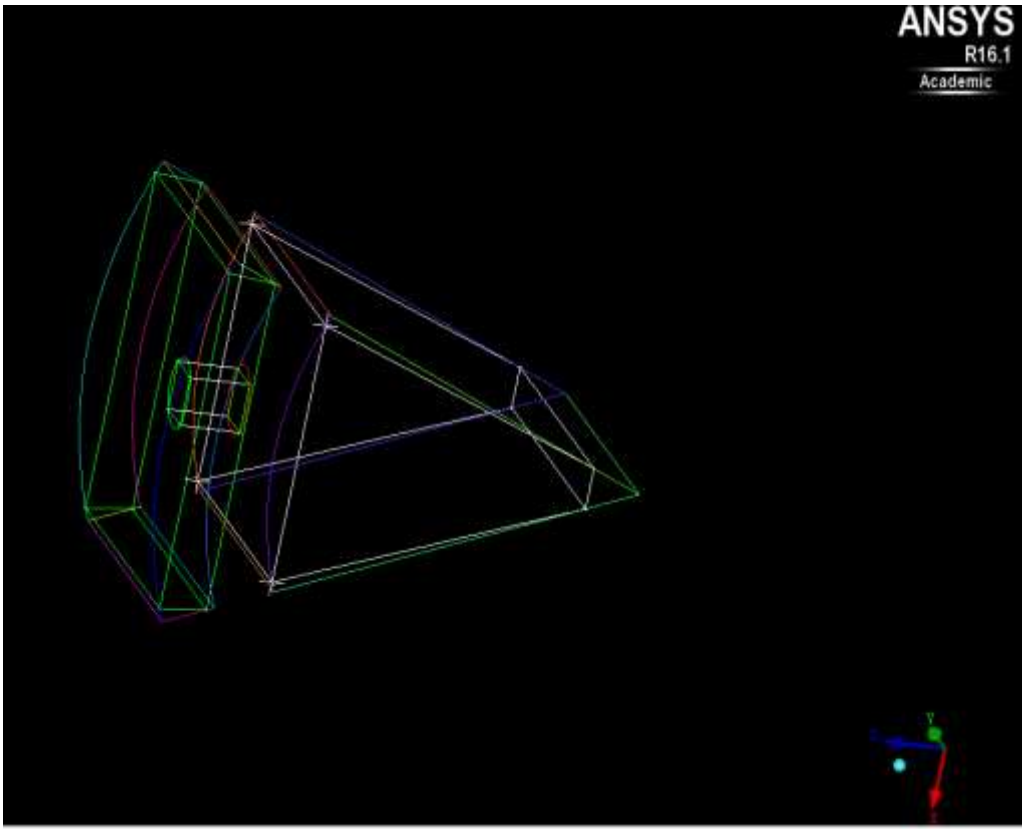

LIT0020 1/8 REVA showing initial blocks associated to curves.

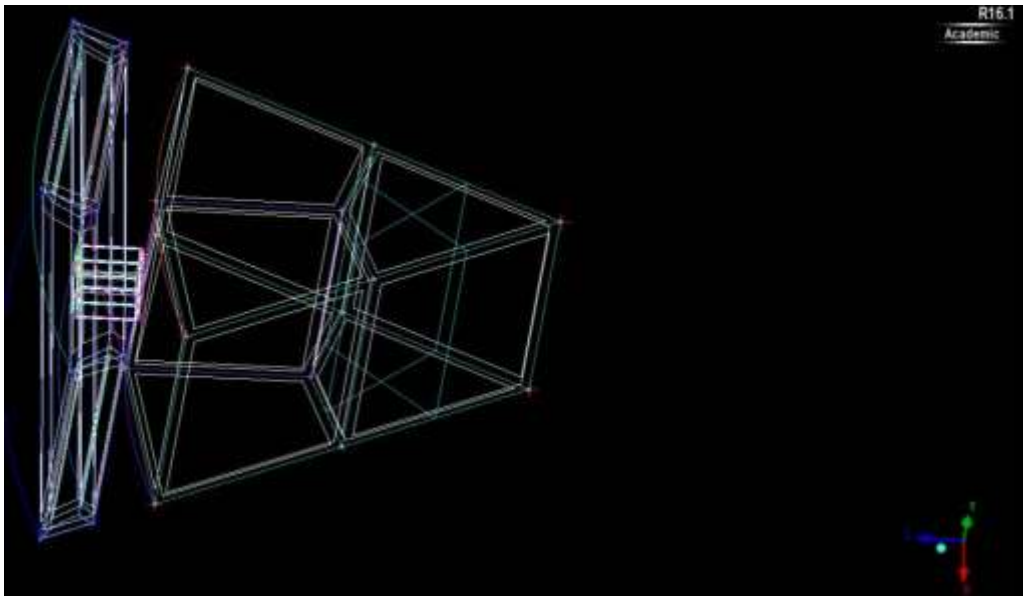

LIT0020 1/8 REVA showing initial blocks associated to curves with triangle split into 3 four sided shapes, this is convenient for blocking

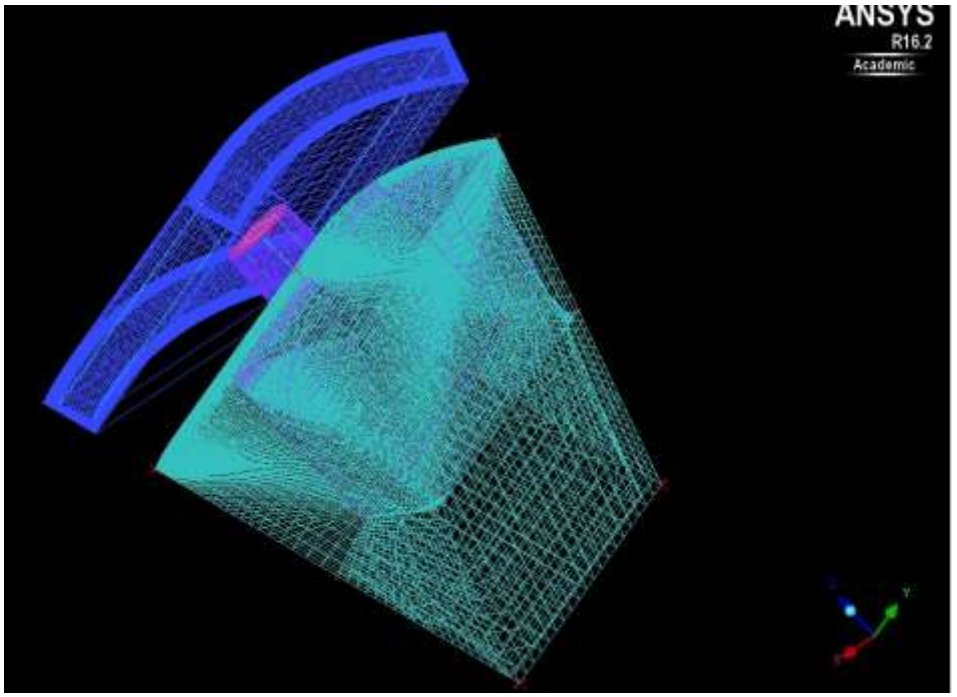

LIT0020 1/8 REVA (ANSYS B) First pre mesh note geometry is very bad.

ICEM Abandoned – ANSYS Meshing Will Be Used

Run C

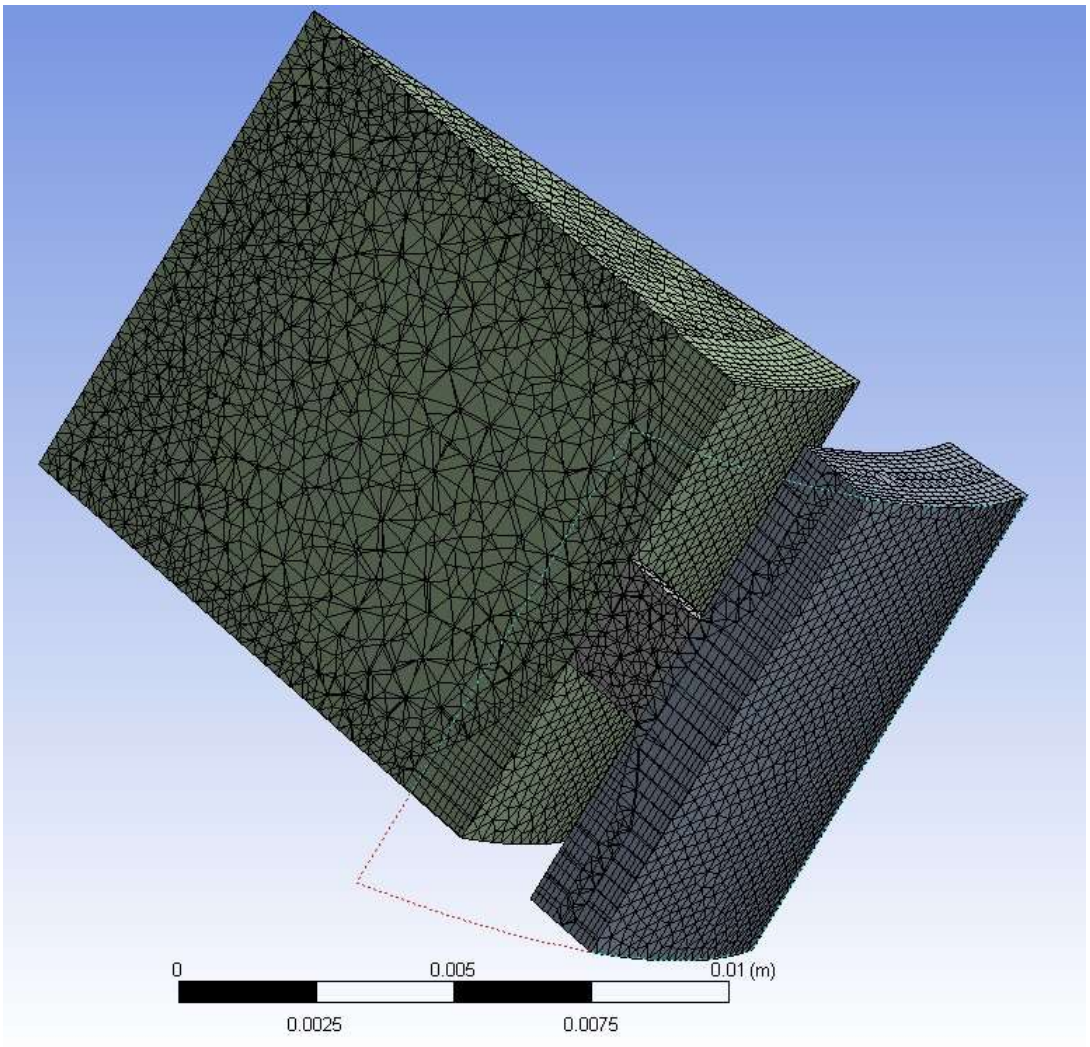

LIT0020 1/8 REVA (ANSYS A) mesh in Ansys note Inflation doesn't follow all faces

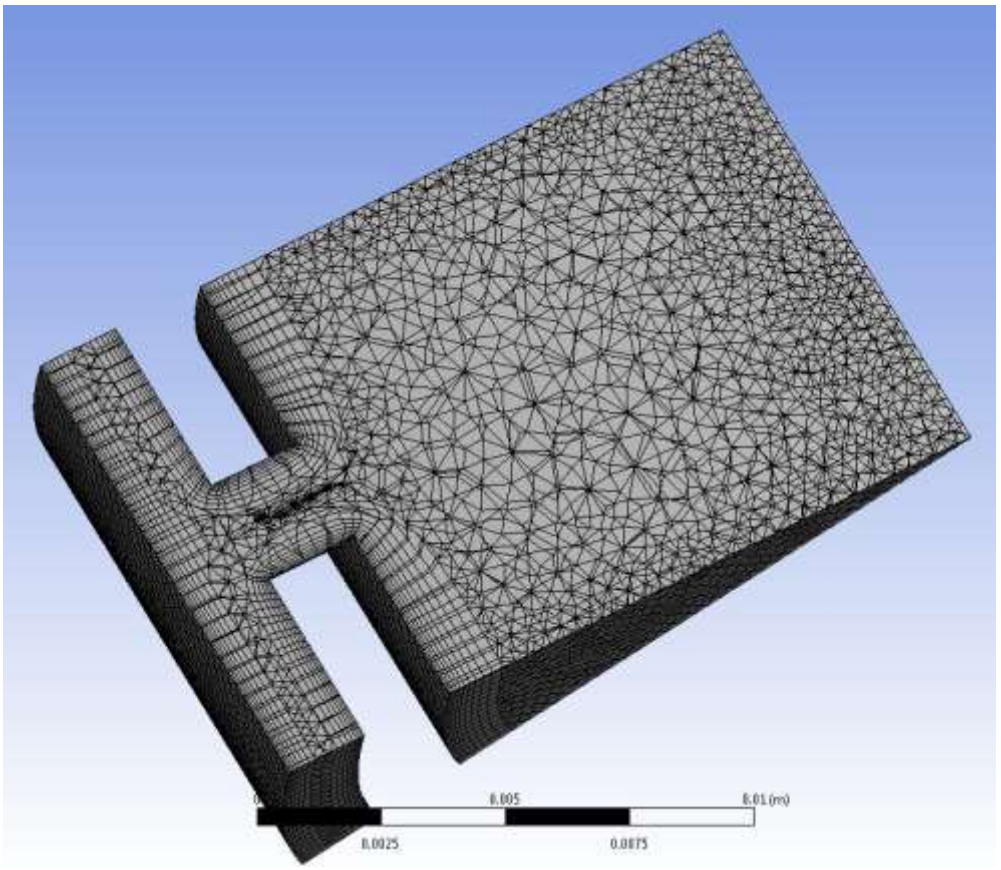

LIT0020 1/8 REVA (ANSYS A) mesh in Ansys note Inflation follows all faces
Single body is used

Building the Geometry by Mirroring It

Run E

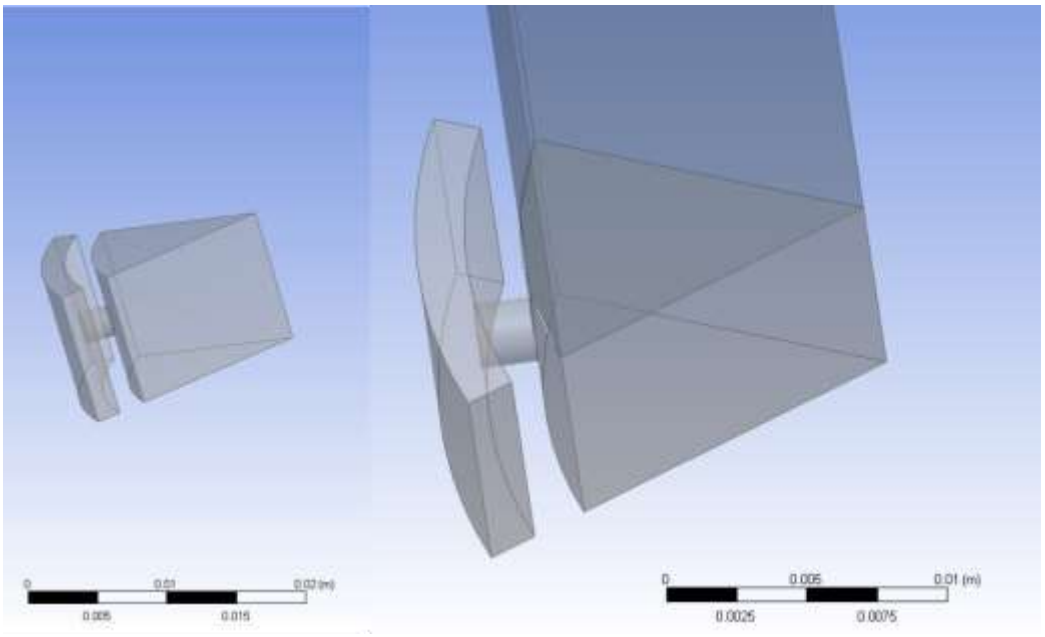

LIT0020 1/8 REVA (ANSYS A) mesh in Ansys With top section added

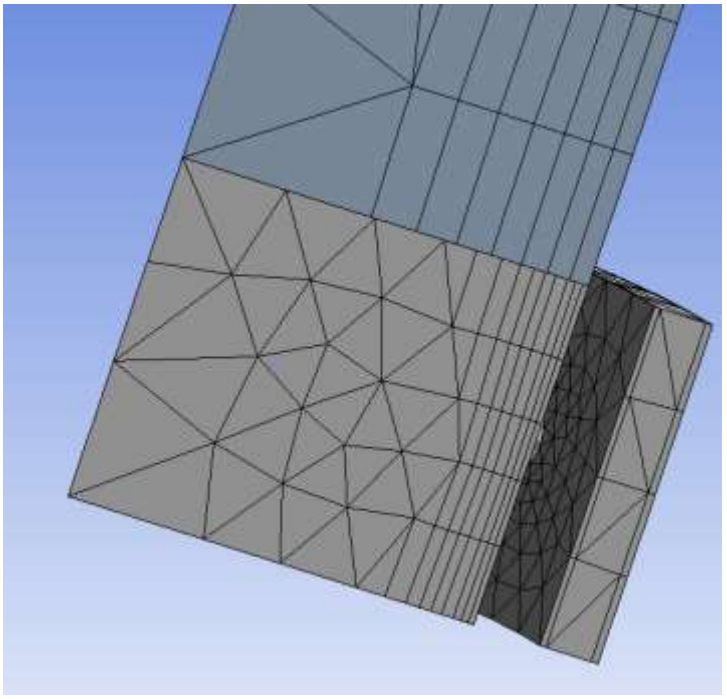

LIT0020 1/8 REVA (ANSYS A) mesh in Ansys without the mesh balanced

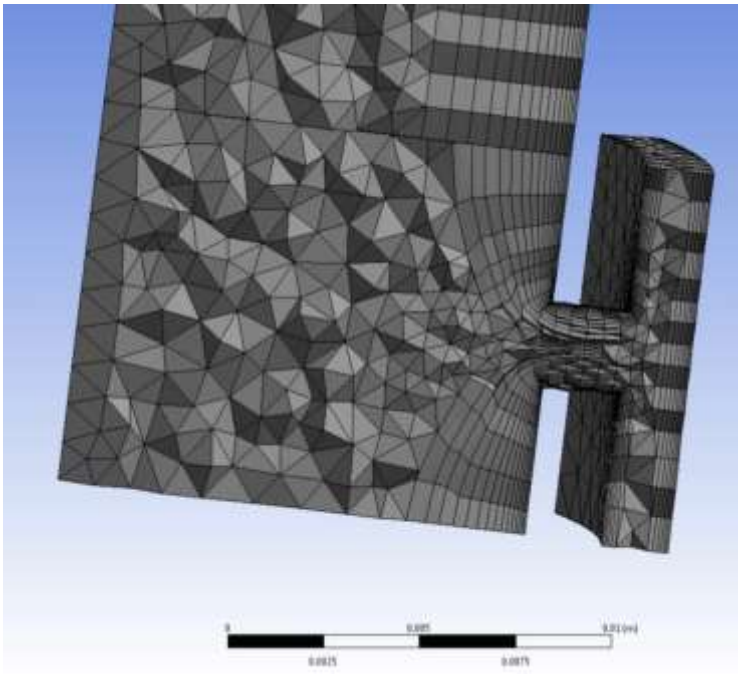

LIT0020 1/8 REVA (ANSYS A) mesh in Ansys mesh first attempt. Interfaces will be used at the required boundaries.

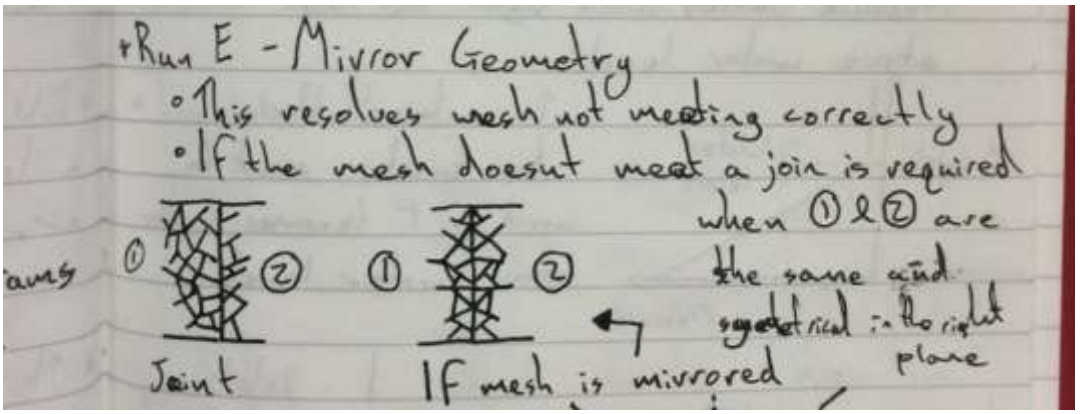

Mirroring geometry means all of the mesh elements meet at the end of the domains so interpolation of data to meet the new mesh location is not required. This makes the model more stable but is only achievable when the geometry is repeated that is symmetrical about the mirror line.

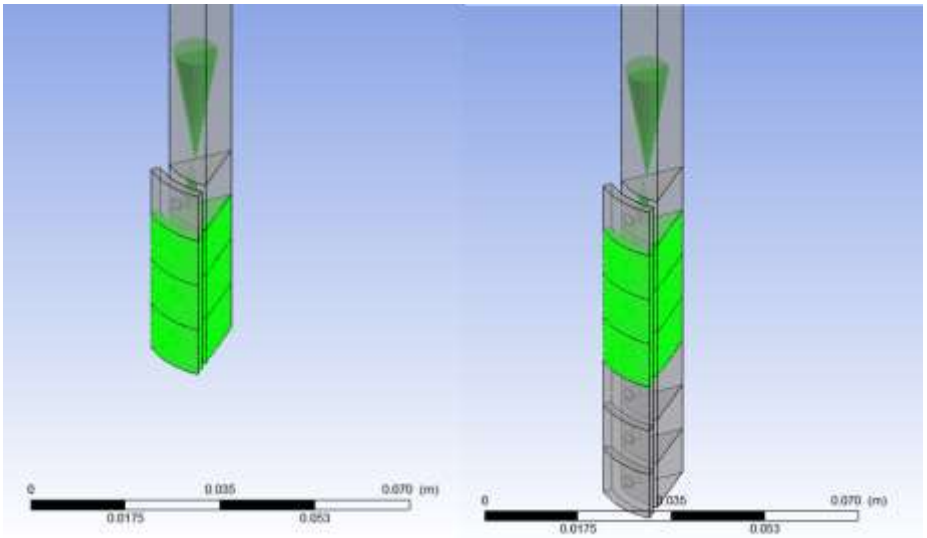

Shows LIT0020 1/8 REVA (ANSYS A) mesh being mirrored to form the full 1/8th of the domain. Mirroring is used so that the mesh meets at component faces.

Naming Boundaries

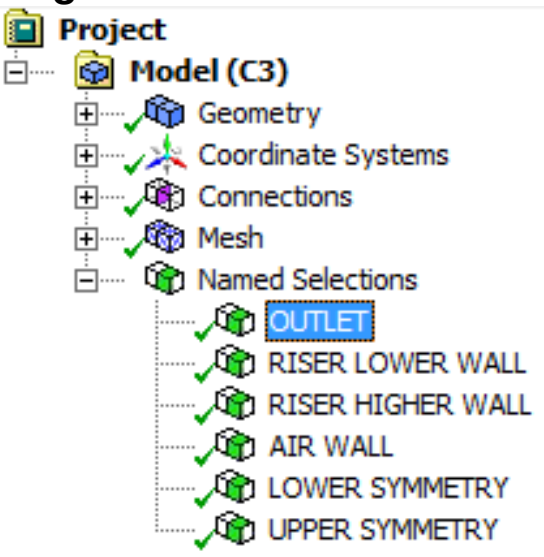

Shows LIT0020 1/8 REVA (ANSYS A) Naming key faces

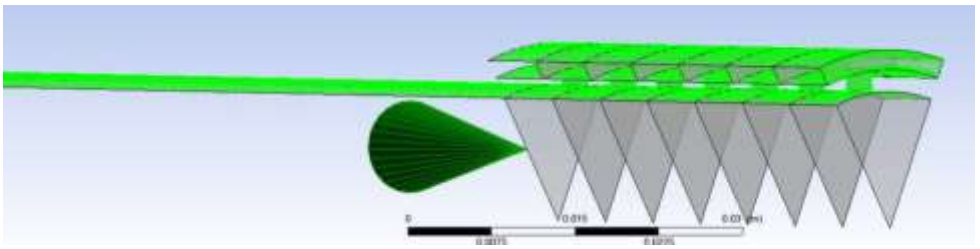

Shows LIT0020 1/8 REVA (ANSYS A) Boundary walls

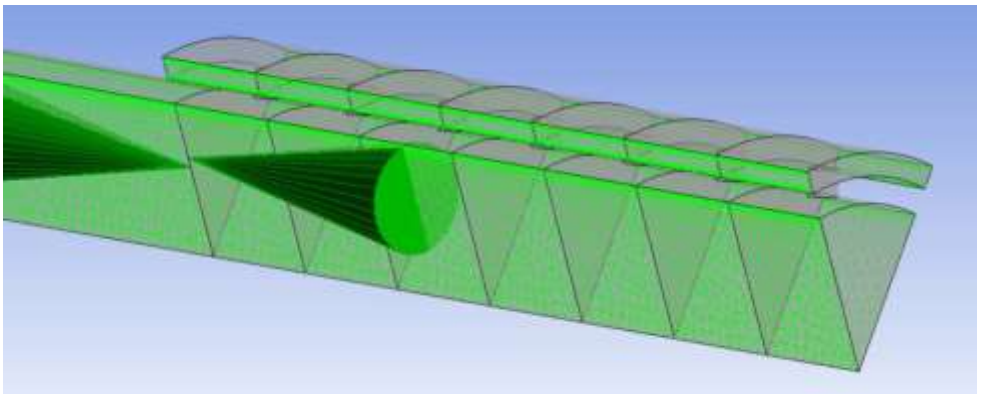

Shows LIT0020 1/8 REVA (ANSYS A) Boundary Symmetry

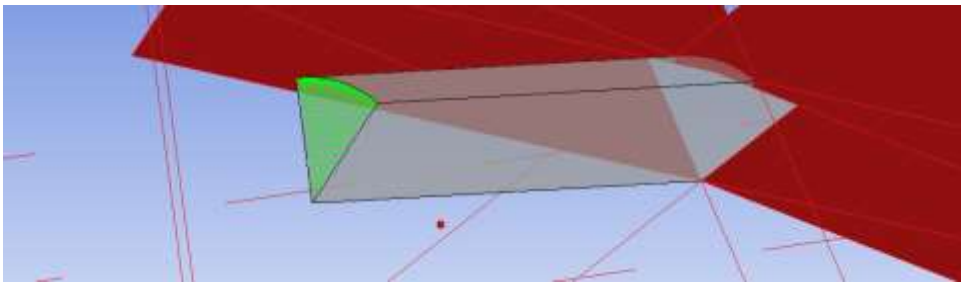

Shows LIT0020 1/8 REVA (ANSYS A) Boundary Outlet

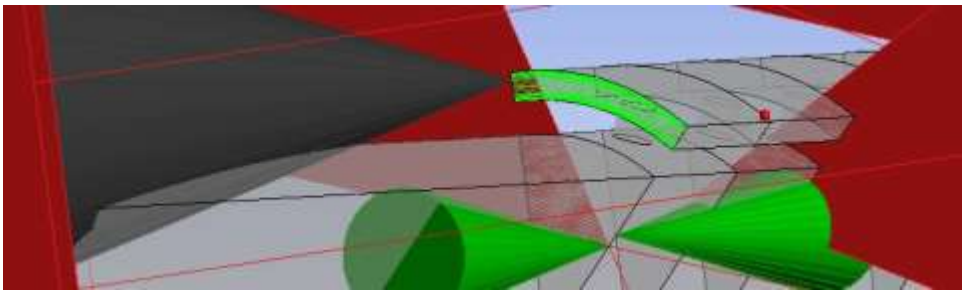

Shows LIT0020 1/8 REVA (ANSYS A) Boundary Air Inlet as mass flow rate

Assumption 2 – Pipe entrances and exits cannot be controlled by inlets or outlets so more geometry is added

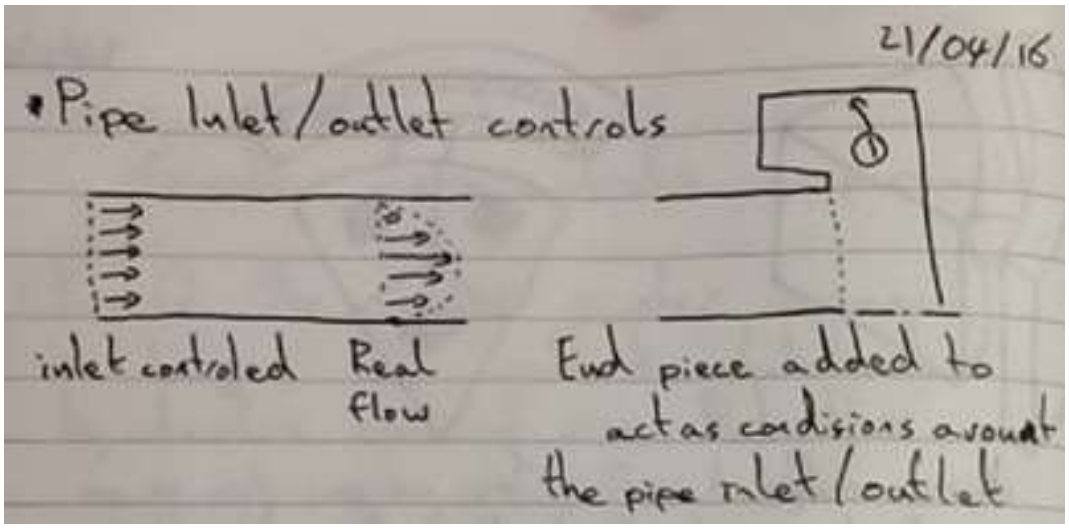

This shows how flow patterns are controlled by the inlet but they differ from the natural flow pattern

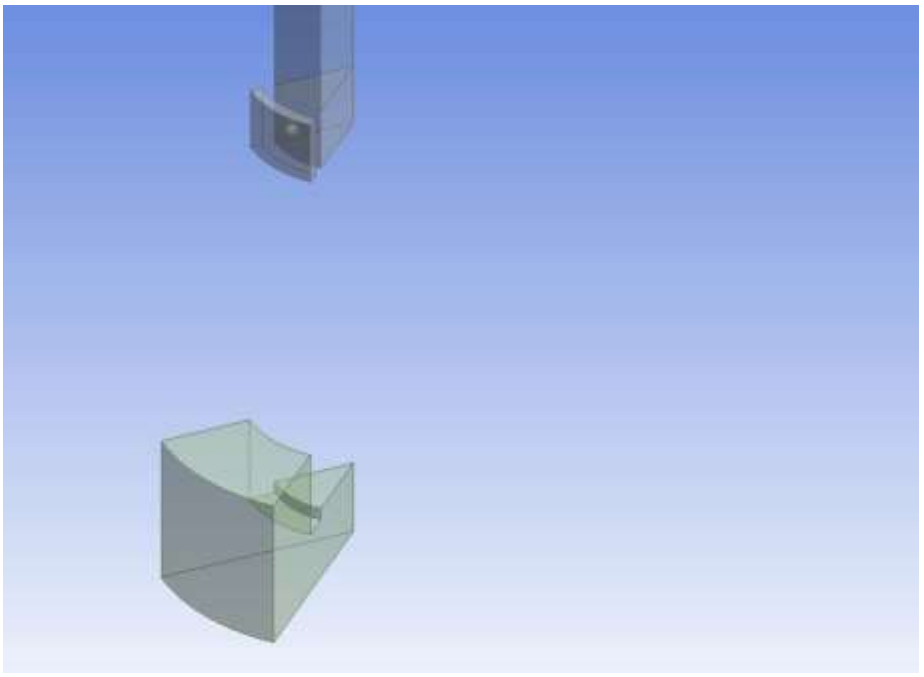

Shows LIT0020 1/8 REVA (ANSYS A b) With Base meshed

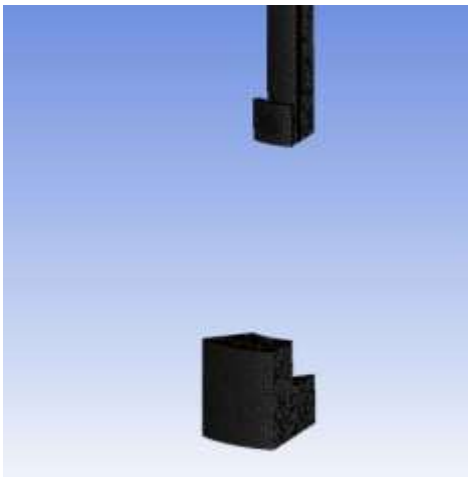

Shows LIT0020 1/8 REVA (ANSYS A b) With Base meshed

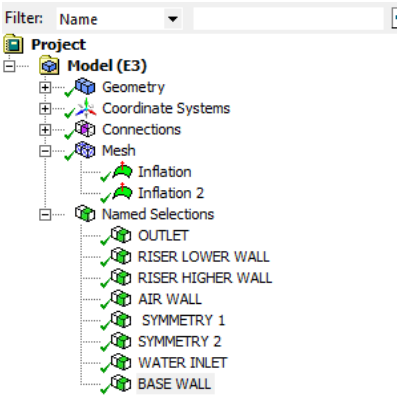

Shows LIT0020 1/8 REVA (ANSYS A b) Face Names

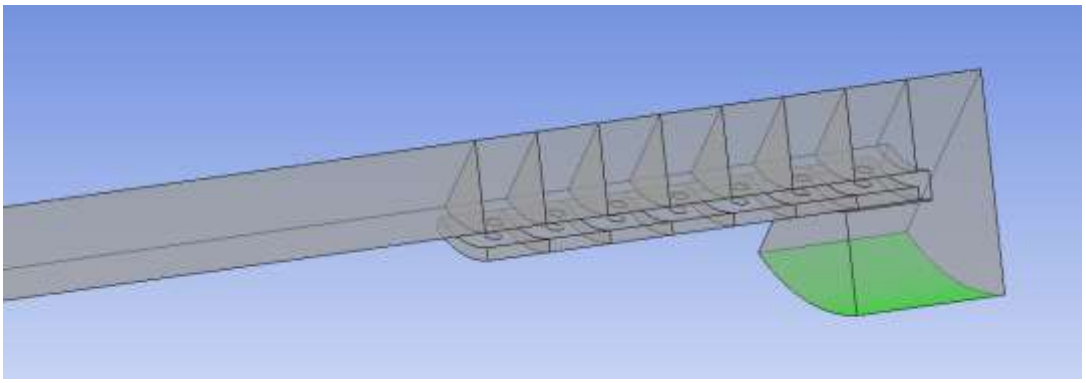

Shows LIT0020 1/8 REVA (ANSYS A b) Water Inlet

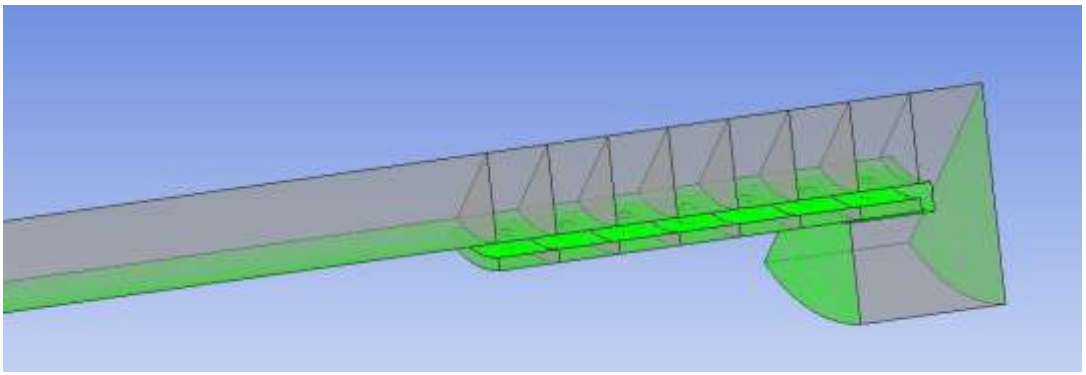

Shows LIT0020 1/8 REVA (ANSYS A b) Walls

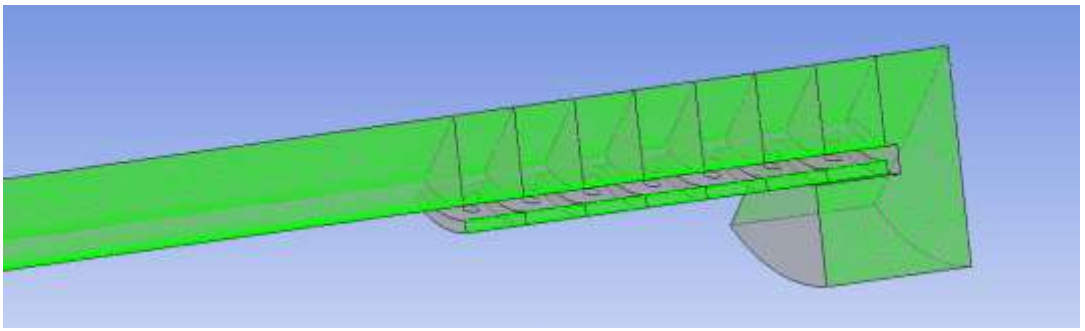

Shows LIT0020 1/8 REVA (ANSYS A b) Mirror

Adding Pressure to the Problem

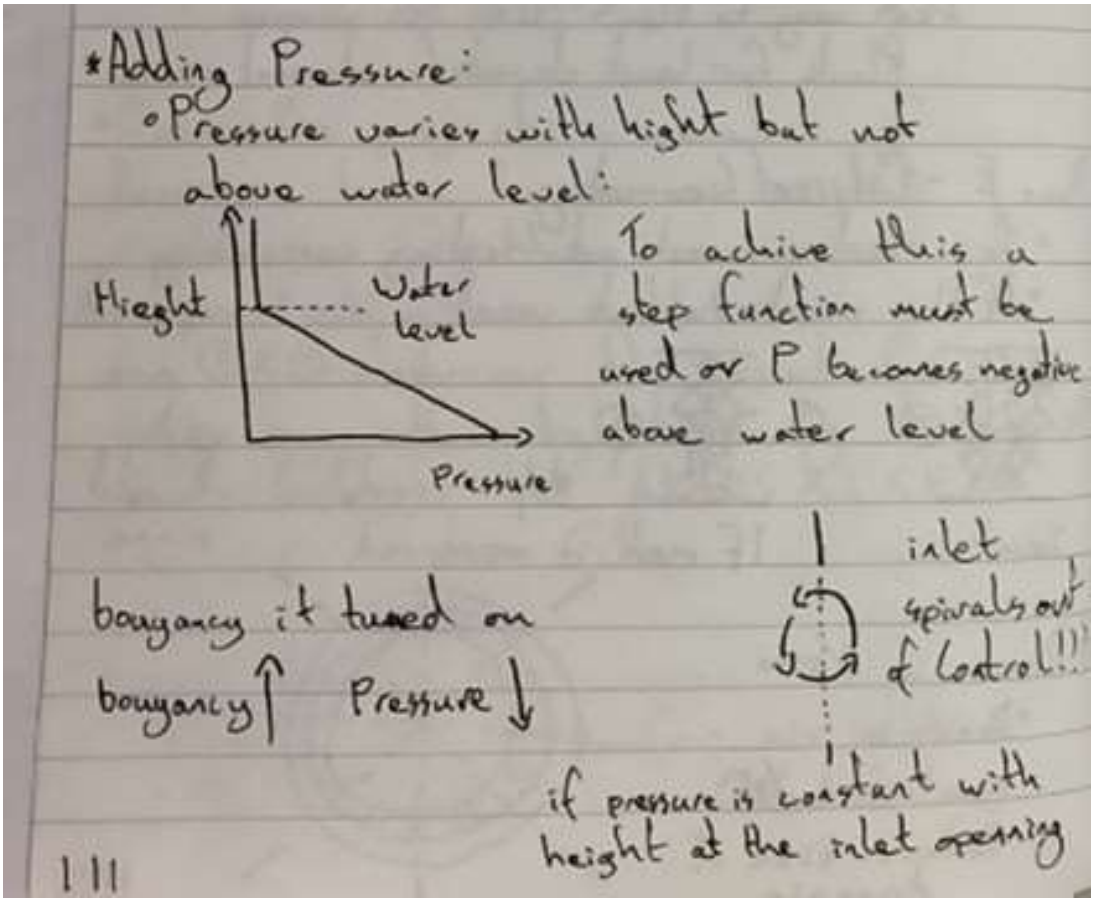

This shows how pressure must change with height throughout the domain. Without this the flow will become unbalanced and rotational at the water inlet due to buoyancy being switched on.

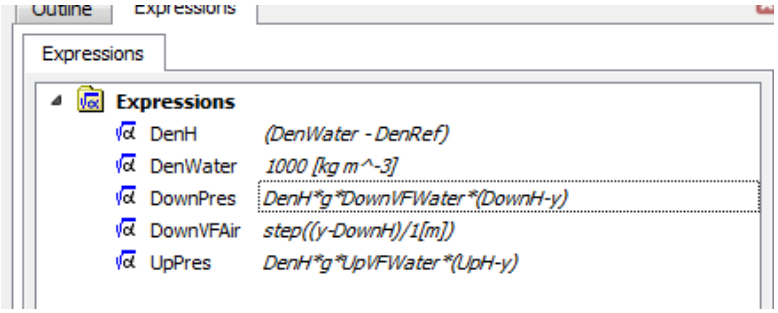

Shows LIT0020 1/8 REVA (ANSYS A b) Some expressions added

Adding More Geometry

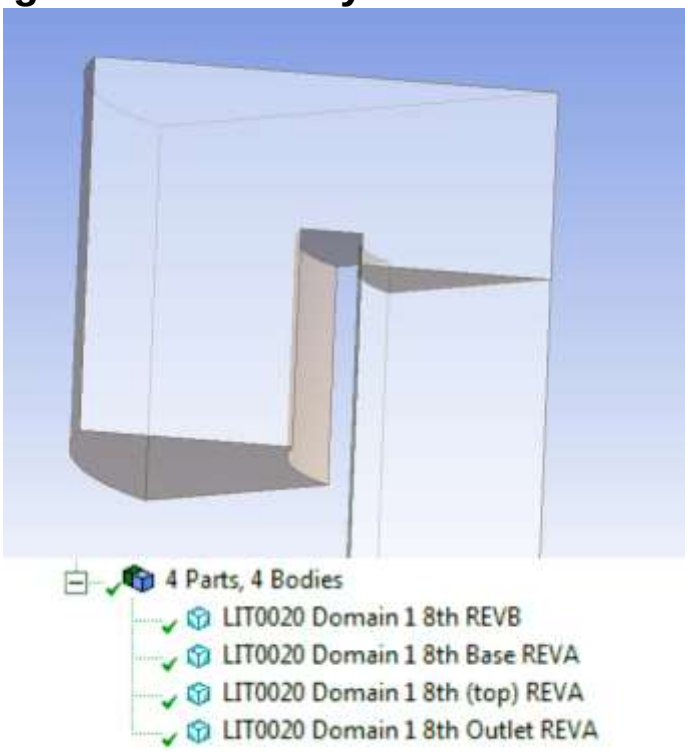

Shows LIT0020 1/8 REVA (ANSYS A b) With Top Outlet Added – Note the riser was shortened by 2 mm to do this.

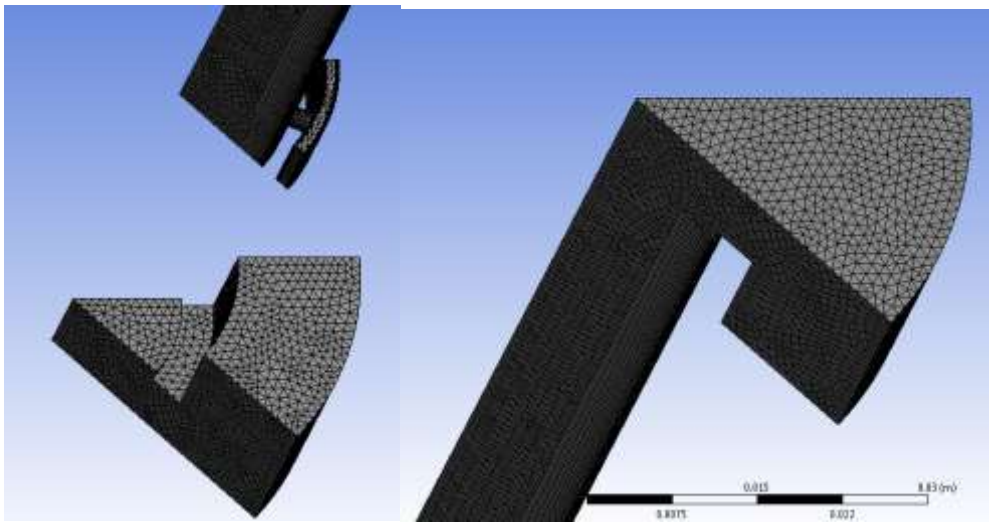

Shows LIT0020 1/8 REVA (ANSYS A b) With Meshing added

Selecting Run Models

Assumption 3 – Air is incompressible

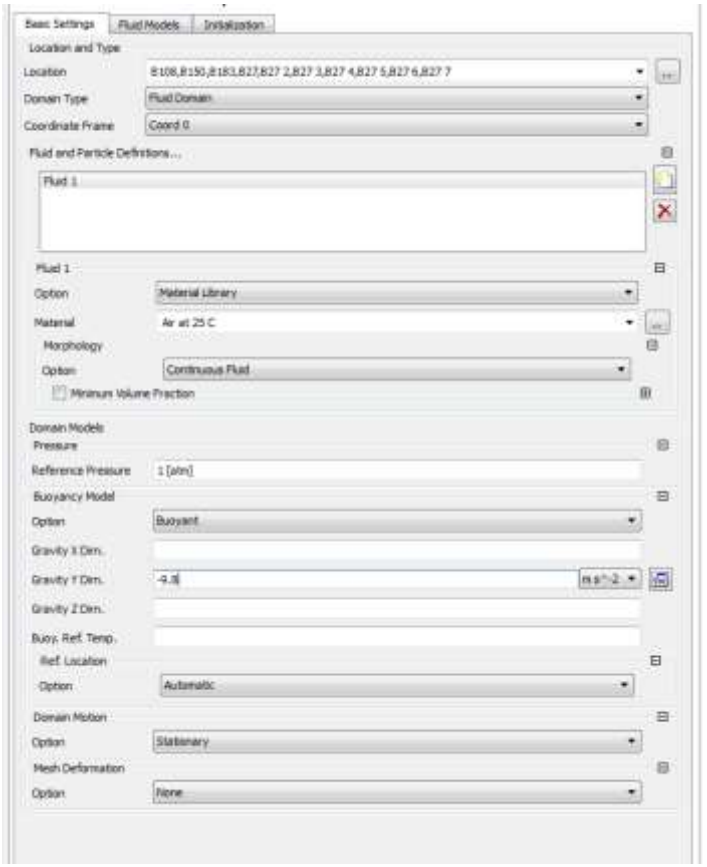

Shows LIT0020 1/8 REVA (ANSYS A b) With Buoyancy defined; This accounts for compressible flow

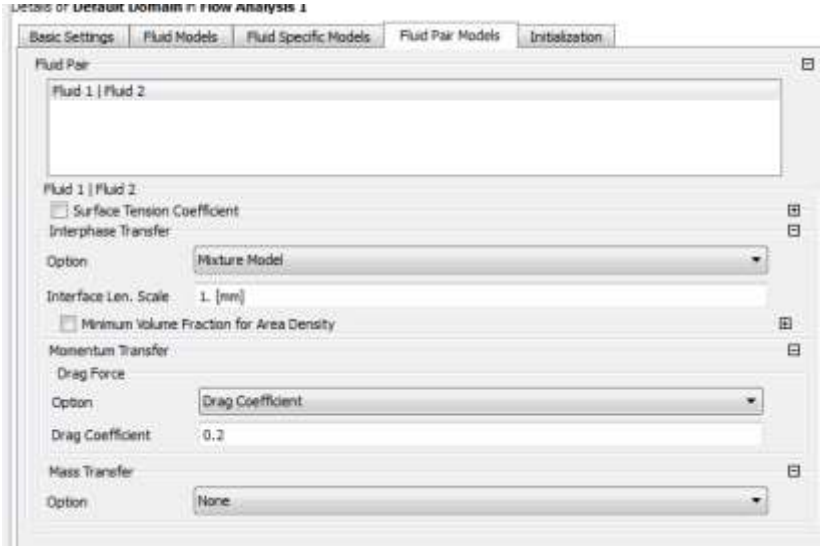

Shows LIT0020 1/8 REVA (ANSYS A b) With Mixture flow (found from LIT0030)

And Drag Coefficient set to 0.2 – LIT0031

	A	B
1	Property	Value
2	General	
3	Component ID	Setup 3
4	Directory Name	CFX-2
5	Physics Status	ERROR: In Analysis 'Flow Analysis 1' - Domain 'Default Domain': The boundary 'Wall' contains duplicate 2D regions. INFORMATION: In Analysis 'Flow Analysis 1' - Domain 'Default Domain': It is recommended that a homogeneous turbulence model is used for inhomogeneous multiphase simulations with more than one continuous phase.
6	Notes	
7	Notes	
8	Used Licenses	
9	Last Update Used Licenses	

Shows LIT0020 1/8 REVA (ANSYS A b) Is used with planes specified twice – this is as domains have been mirrored.

ADDITION OF ONE FACE CONNECTION:

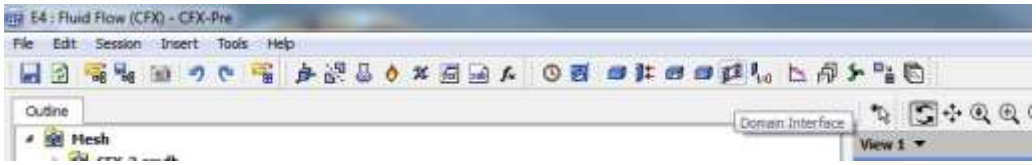

Second Revision Created (F)

Domain Interface Tool Select

GGC model

This links domains which were not mirrored by interpolation – Requires more calculations but should not affect results

Set Water Inlet to an opening; Flow can happen both ways at this point.

Assumption 4 – Pressure must change with height in the domain

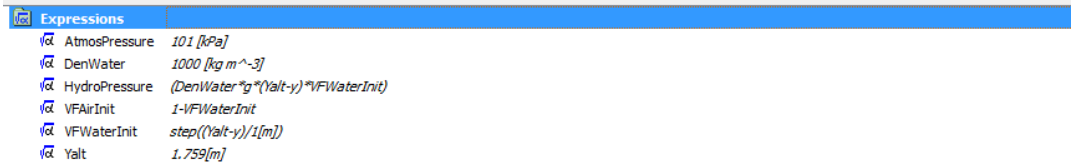

Shows changes to expressions to add surface pressure, pressure and outlet opening also changed. VFWaterInit adds a step function to ensure that the pressure does not become negative when above Yalt.

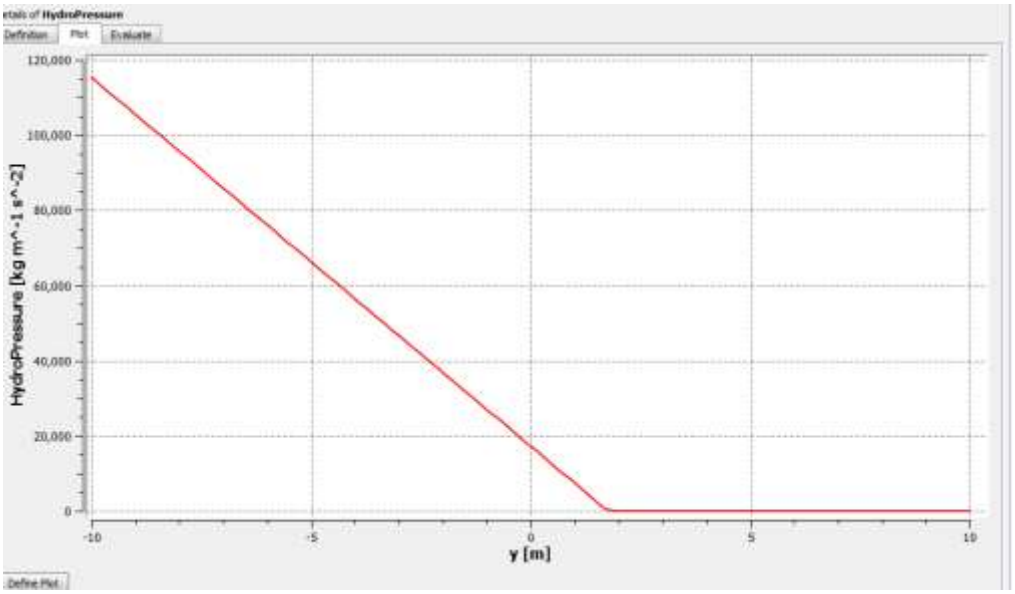

Shows hydrostatic pressure plotted.

Run F

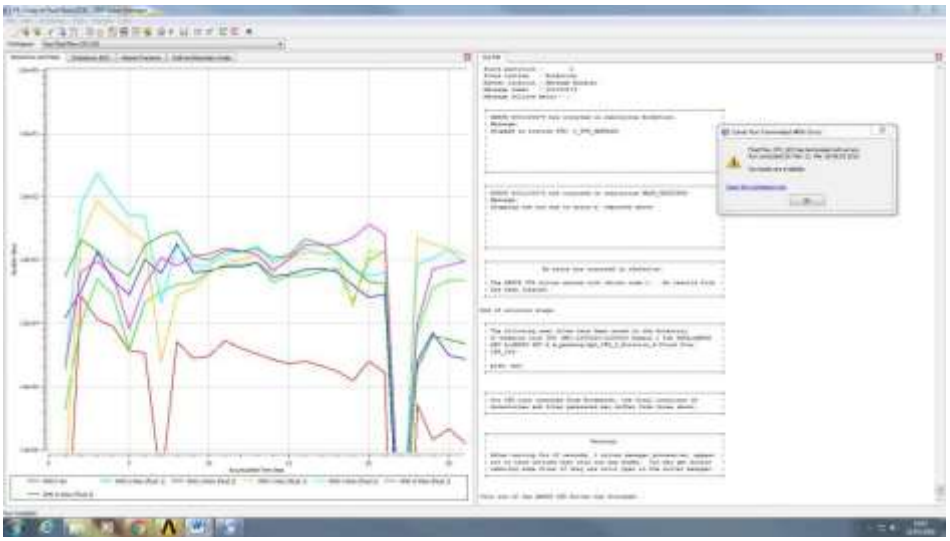

RUN FAILED

Inserted code for pressure related to high of domain or it will circle in and out again depended on

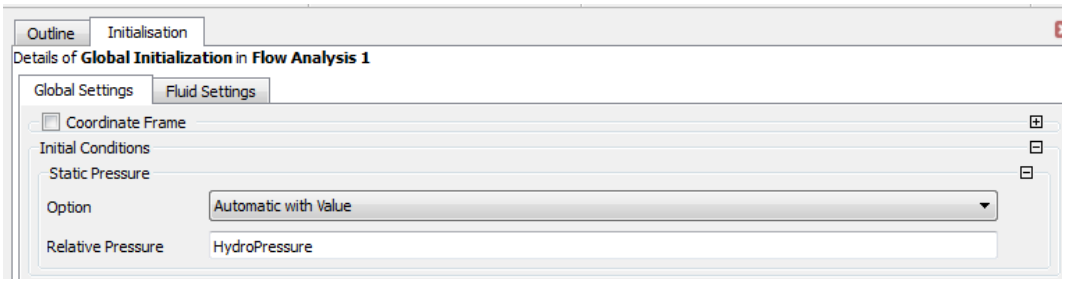

Initial set up will be implemented so that the system runs more gradually at the start; there is not a massive pressure difference leading to instability before the water is balanced in the system.

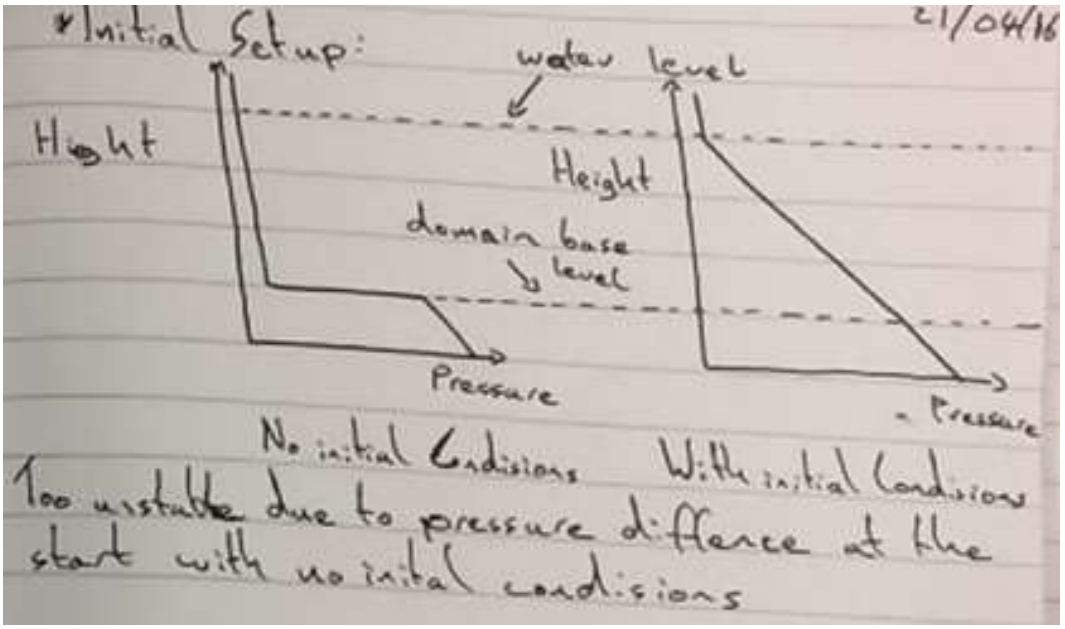

Shows the pressure jump at the start of the run caused by no initial conditions, this makes the run crash almost immediately as water is forced into the riser unopposed by the external pressure.

First Pressure Test Run

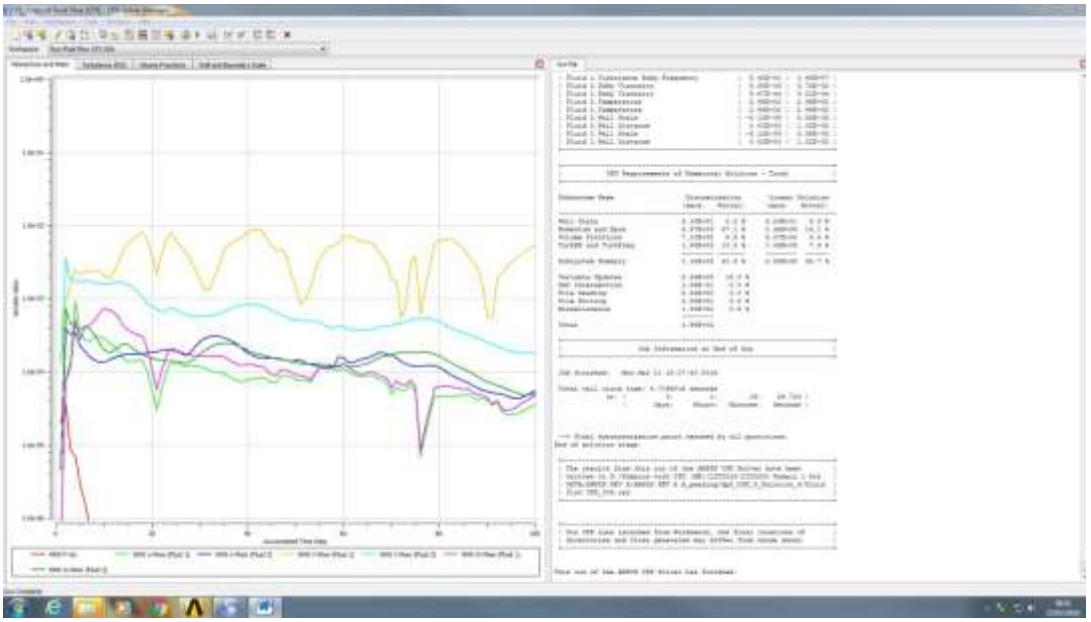

Shows CFD first run - The lines show it is unstable

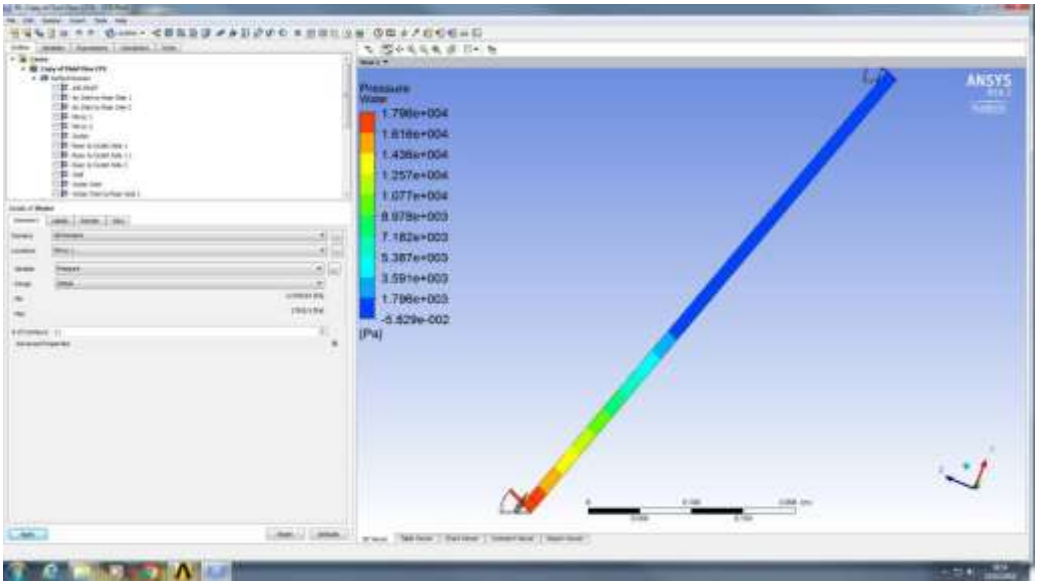

Shows pressure gradient as expected

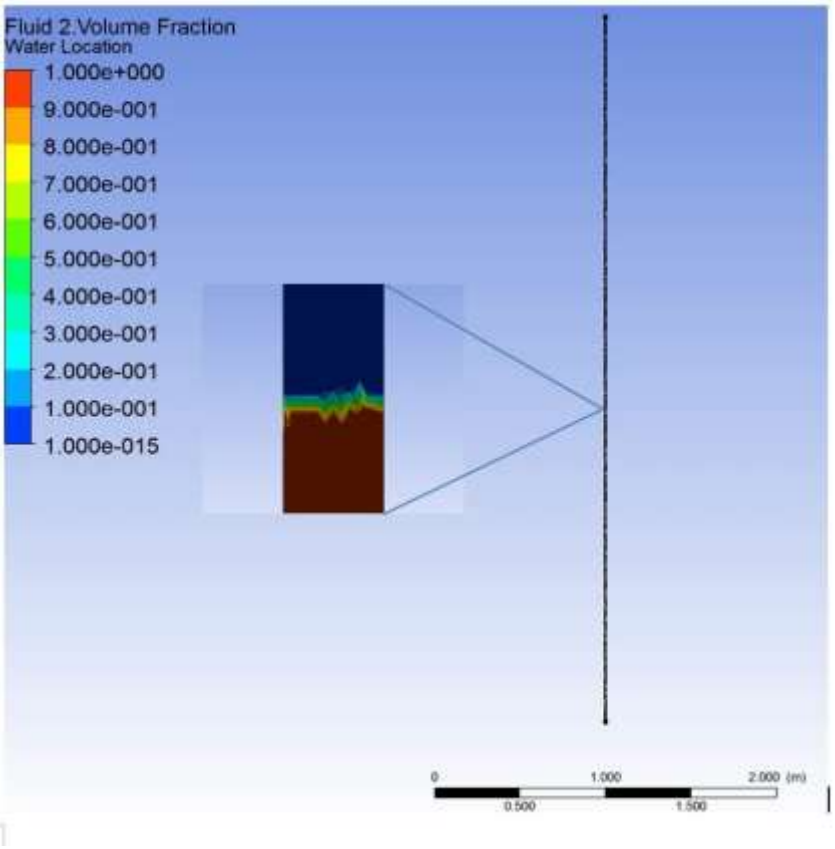

Shows location of water top in CFD Run

The Addition of an Air Inlet

Run G

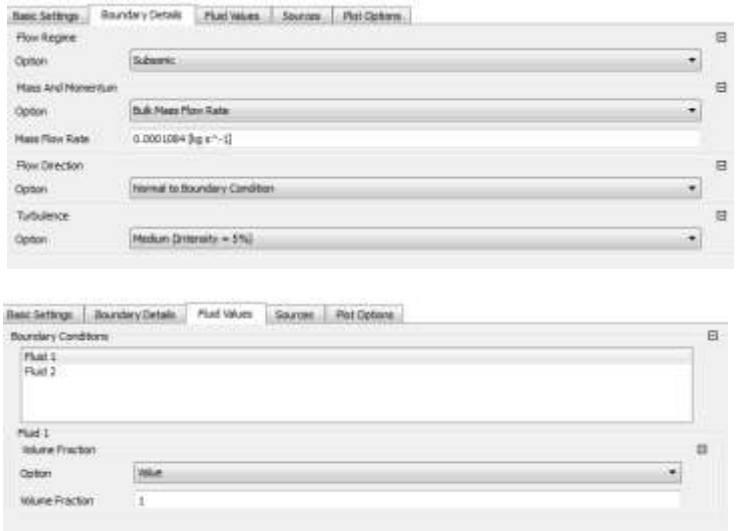

Shows work Air Inlet added

Run H

Shows when the Run stopped working (53rd iteration tried to divide by zero, error code: ERROR #00110027).

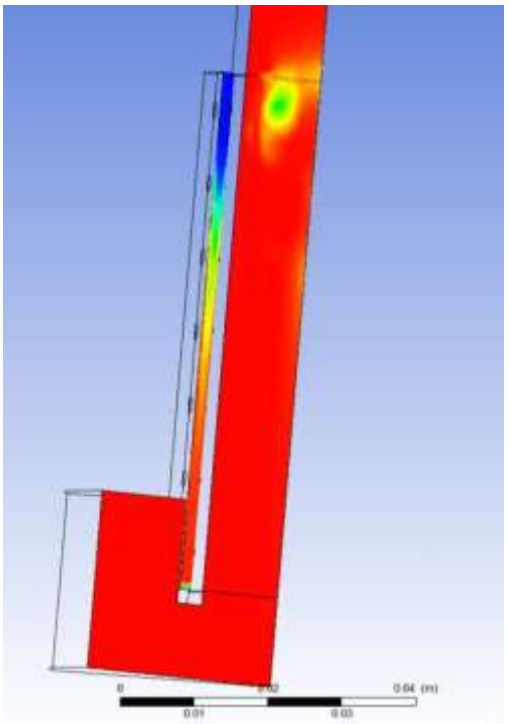

Shows Location of water by density

Velocity seems reasonable (about 6ms^-1).

Run again, crashed at 53 iterations for the same reason.

Run I

Will now be run to 50 iterations to see why it is going wrong before it crashed at 53 iterations.

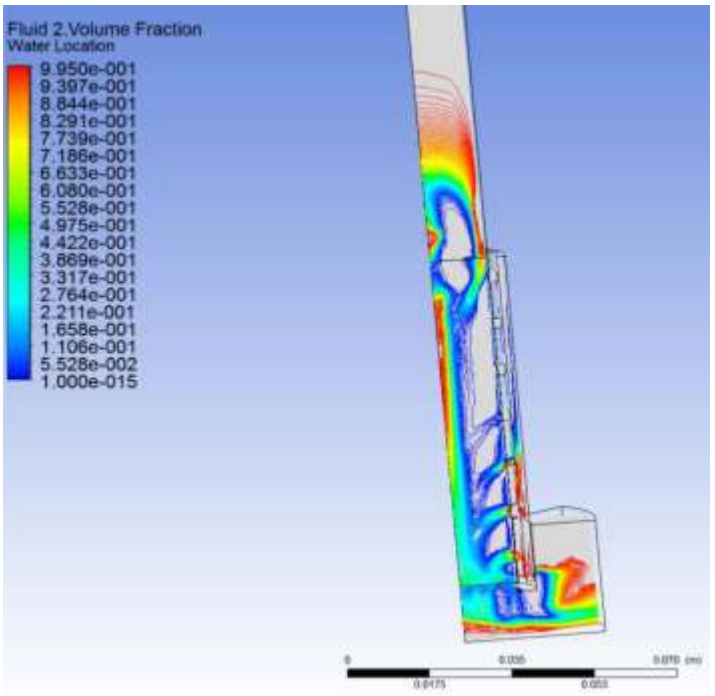

This shows the volume fraction of contours; it is not working quite how it should, this instability may be because the physics are transient. The run ended normally before it would have crashed on the 53rd iteration.

Transient Runs

Run J

Assumption 5 – The Problem is transient

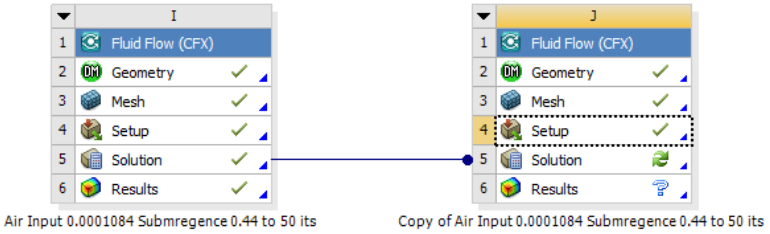

Because air lift pumps are a moving problem changing over time a transient run will be conducted. The results of this will allow evaluation of what is actually happening in the model. Transient runs required are the problem is always moving so the results will never balance.

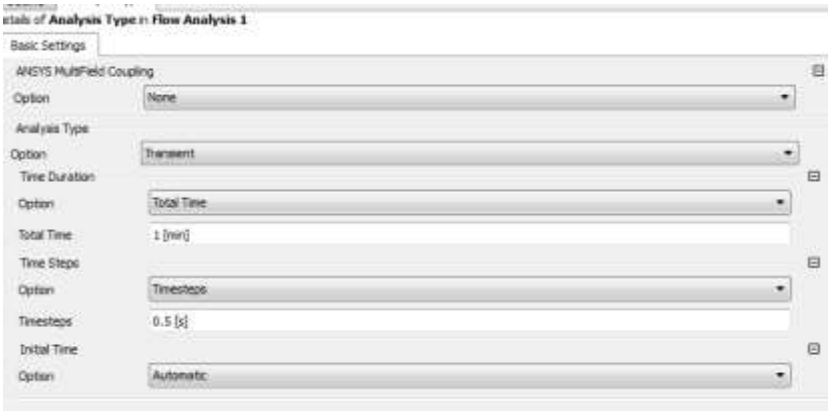

Setting up the time step, this will require iteration however the plan is to start simple and add in more detail by shortening the time pre step as required.

As the osolation is not known the time step length is predicted to start.

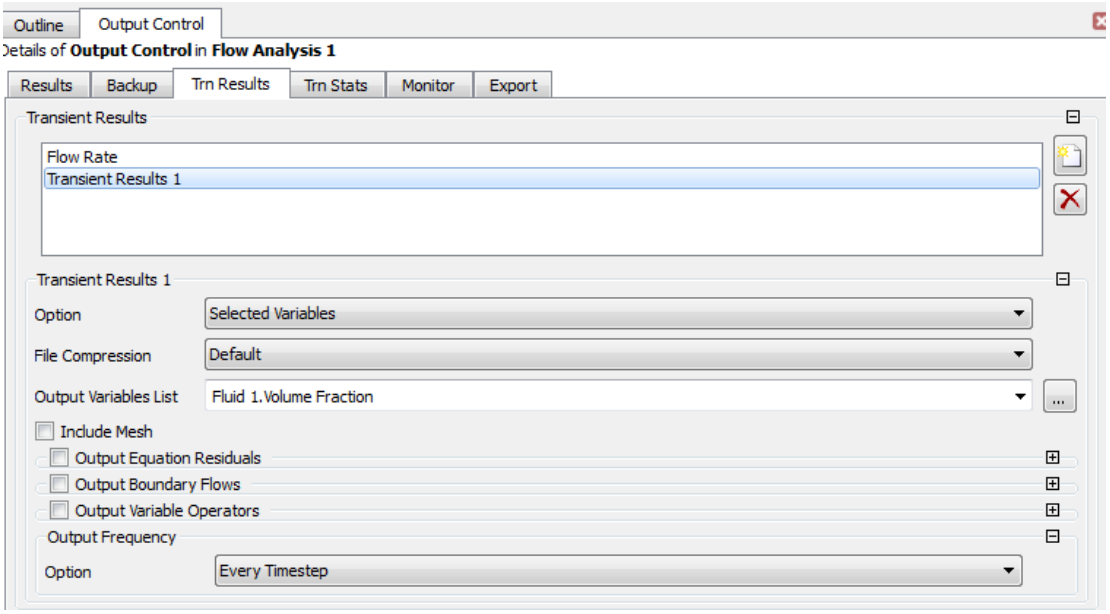

The Results of interested are selected

```
+--------------------------------------------------------------------+
| ERROR #001100279 has occurred in subroutine ErrAction.             |
| Message:                                                           |
| Stopped in routine FPX: C_FPX_HANDLER                              |
+--------------------------------------------------------------------+
```

Run Failed with error #001100279 – This is due to the run diverging because of a lack in stability. This can be improved by; smaller time steps, better initial conditions, tighter convergence etc.

Run K

Crashed run copied and the following measures have been teken to improve numerical stability:

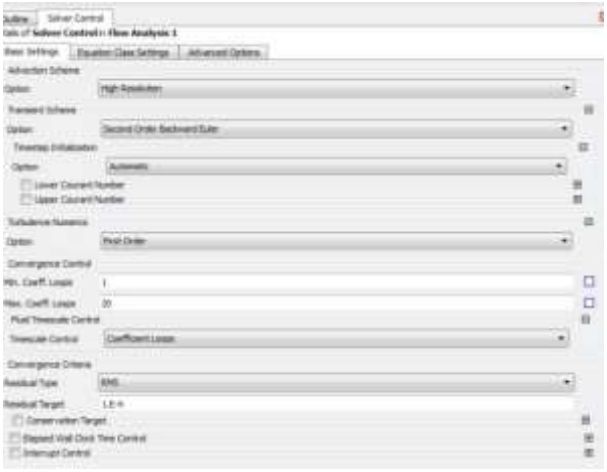

Increased iterations allowing the solver more time to balance each time step

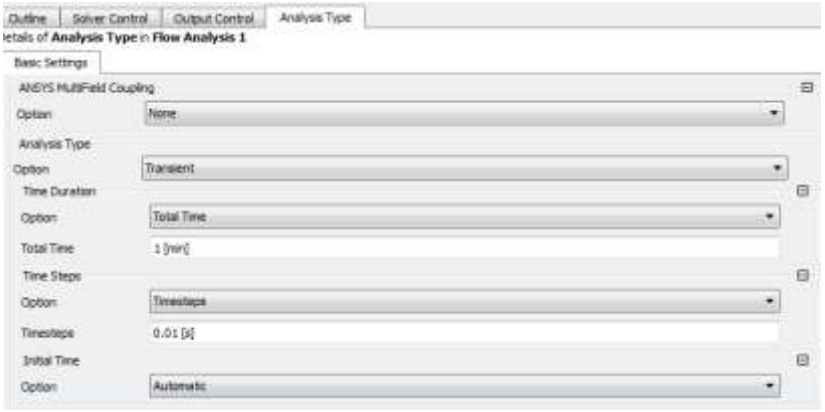

The time step has been reduced; this means that the initial predictions for each time step will be better as less has changed due to the shortened time between them.

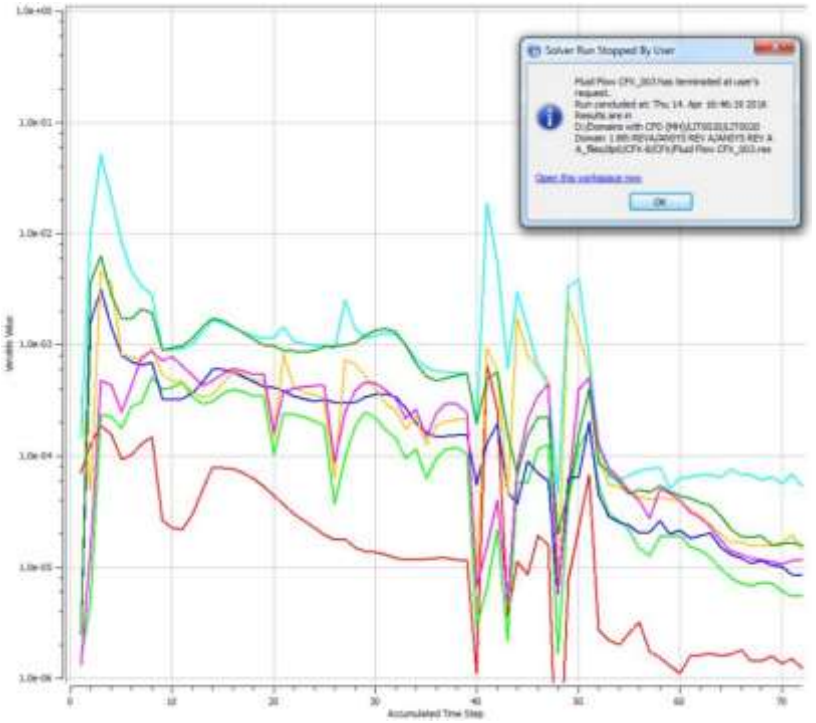

Simulation paused to view results. Simulation seems to be running better now it is not trying to find a steady state solution this is shown by the convergence settling out when transient runs are started.

Assumption 6 – Transient is working

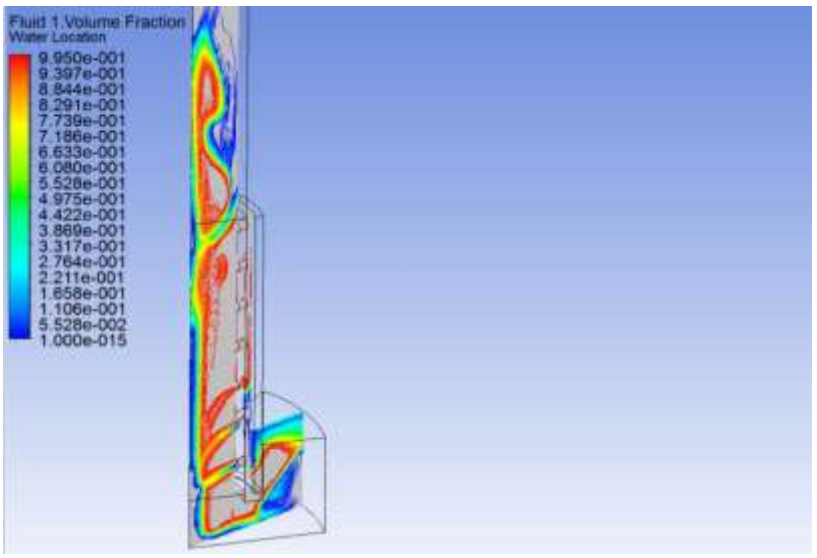

Screen shot from Ansys results file. This is not working quite how is should be at the moment and the model will be reviewed to find the problem.

Run L

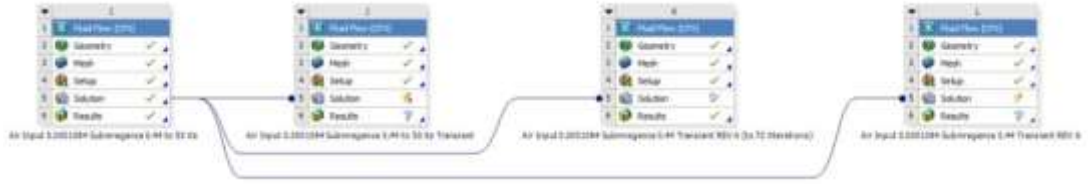

New run set so old data is not lost if the CFD crashes at a later time step

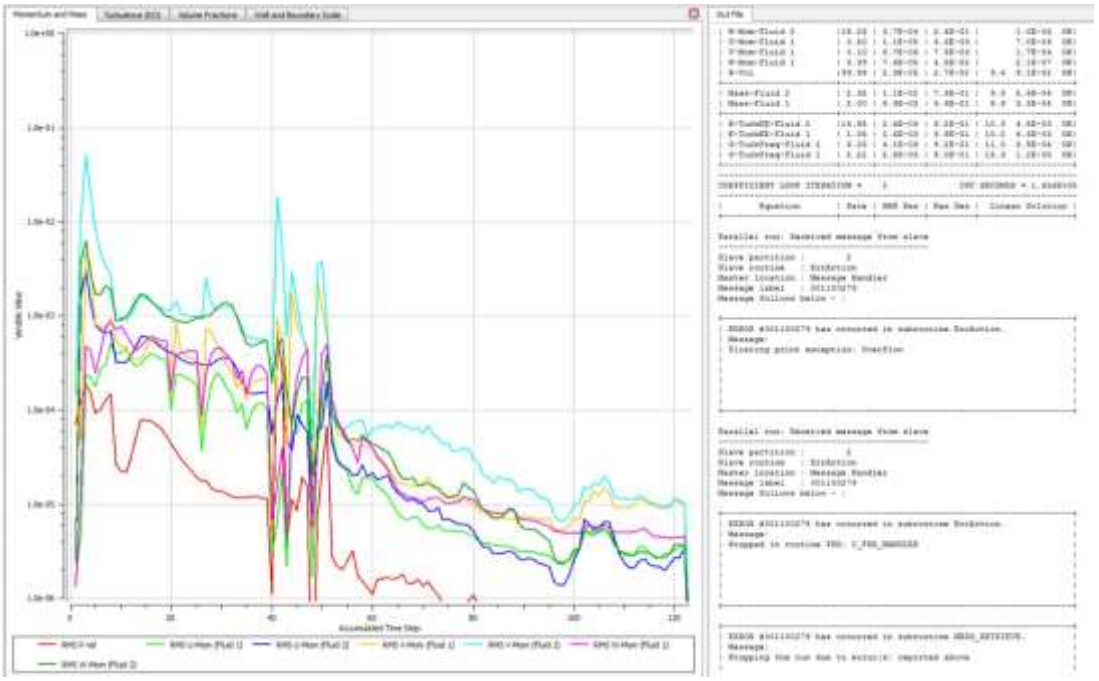

Run Crashed with error code: #001100279. However you can see from the movements towards convergence the transient runs are the correct path.

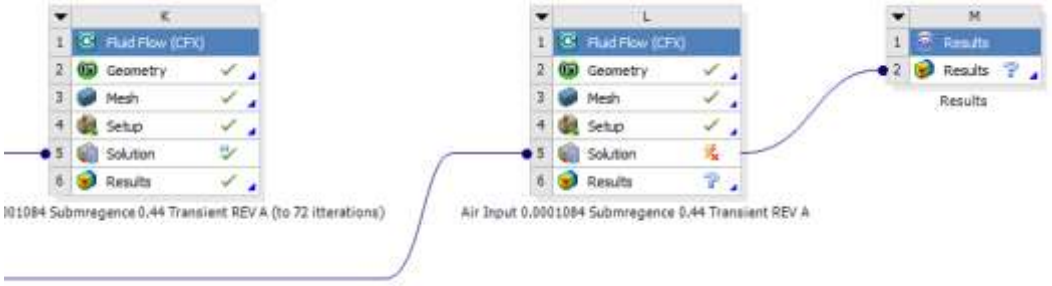

Attempts to salvage the run data have not worked.

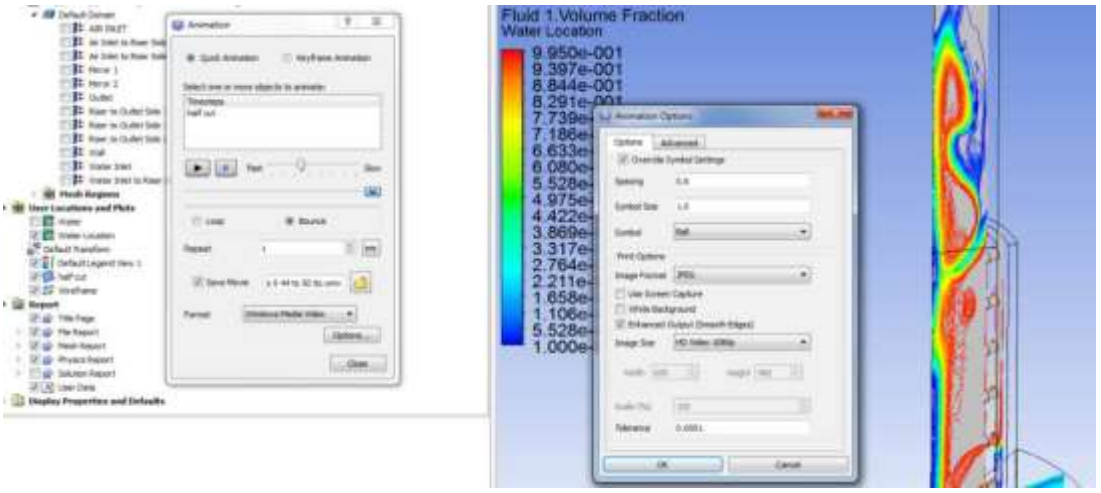

Shows the steps to create the video of the paused run.

Shows the location that the video will be saved to.

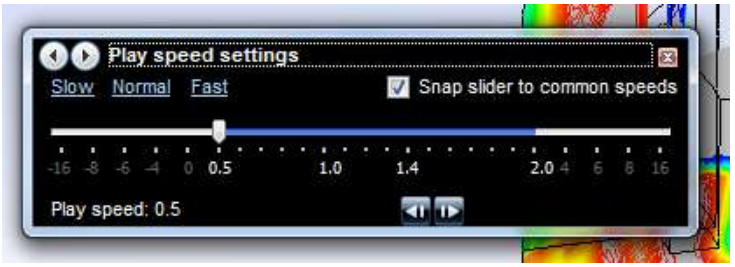

Slow down the play speed so what is going on can be seen

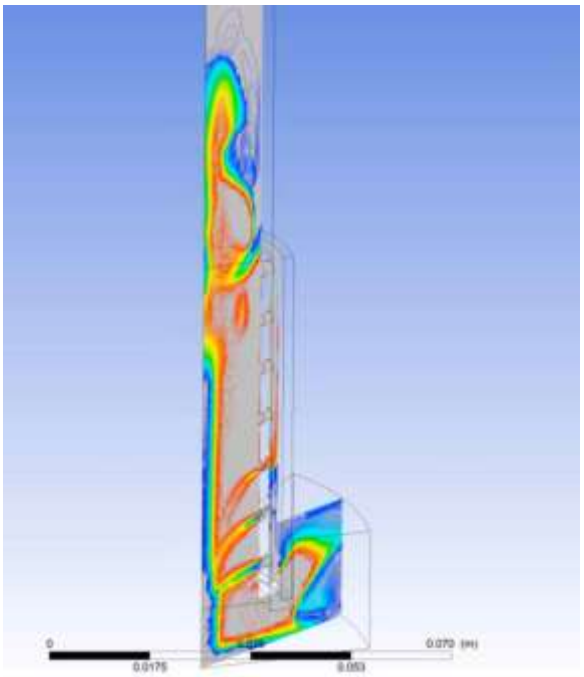

Starts with water filling air tube but by the end air only flows thought the bottom inlet pipe and some of it leaves thorough the bottom riser.

Could Changing the Drag Coefficient Work:

Run N

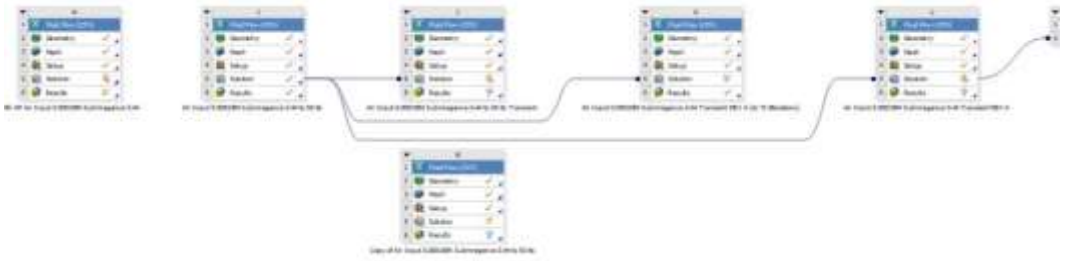

New CFD has been setup so that Cd can be changed

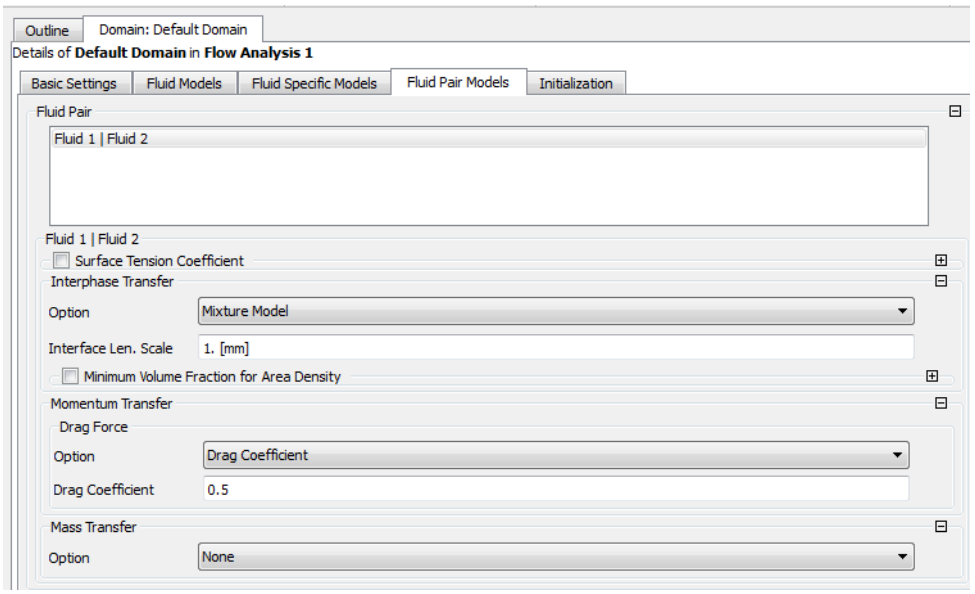

Drag coefficient is estimated to be 0.5 for this run.

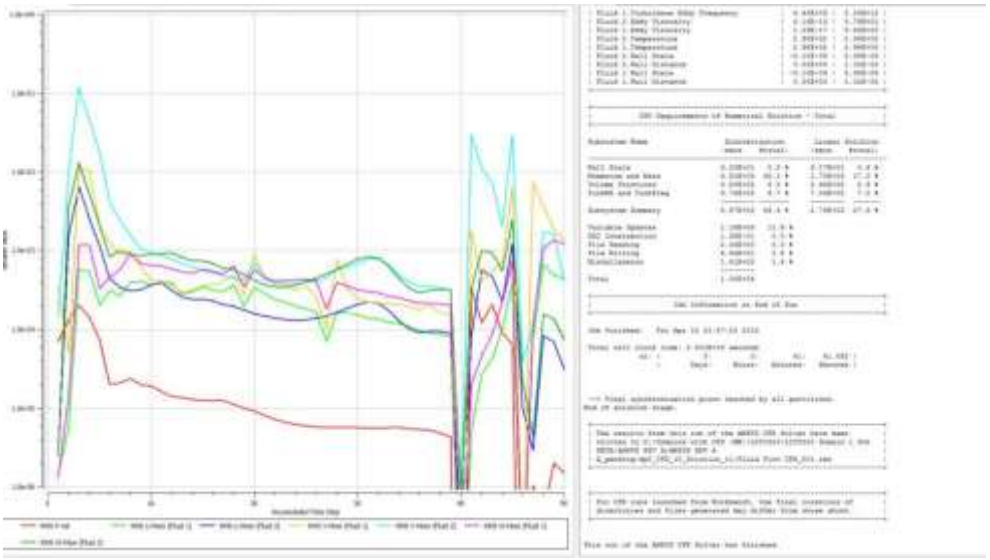

The steady state run completed normally

Run O

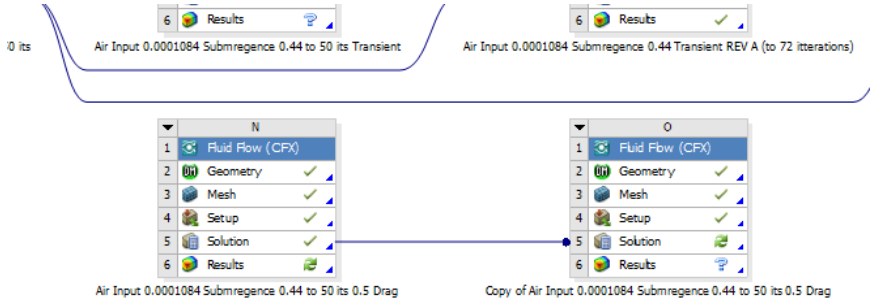

The results are then fed into a transient run with the same settings as last time.

Simulation crashed due to mathematical instability error #001100279

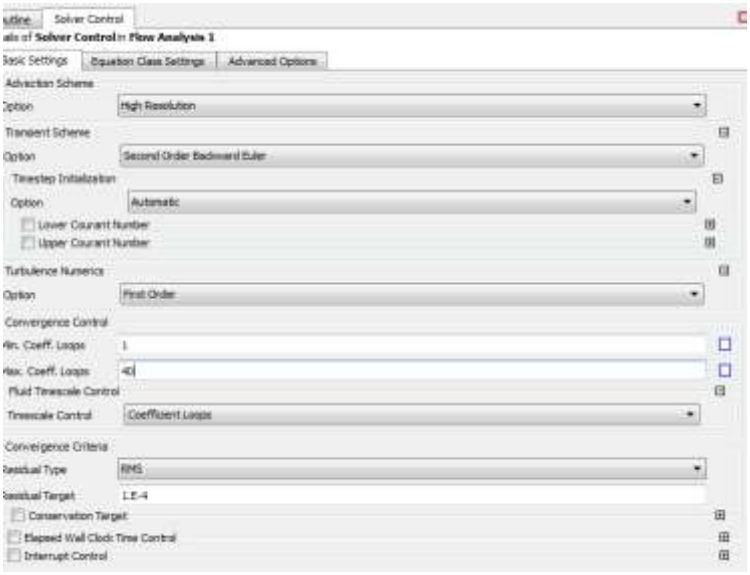

The number of loop iterations available is increased to give the run more opportunity to find stability.

Run failed, Loop iterations should not be above about 6. Therefore it is felt that increasing them further would be a mistake.

Review of CFD This Far:

This shows the record of runs created this far, Shown in full in Appendix G.

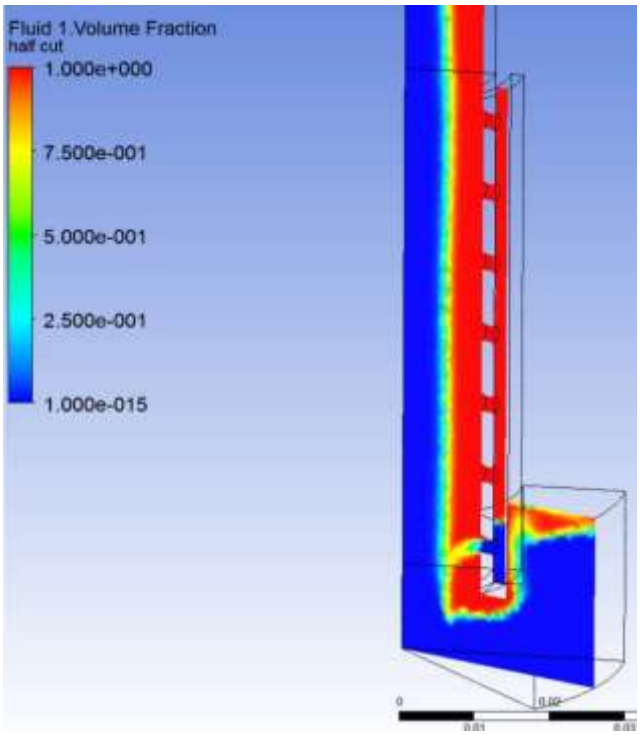

Why is the air escaping though the bottom of the riser? Is it entering too fast?

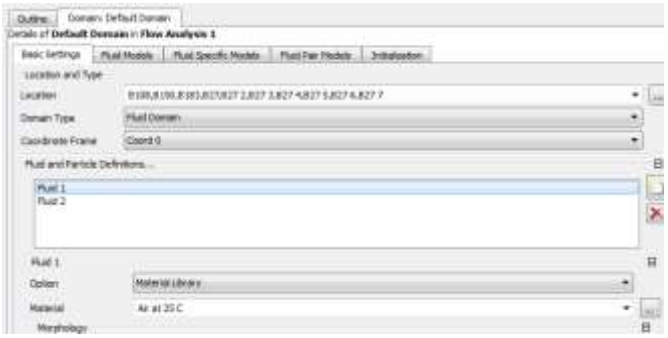

Air at 25 C is specified

This has a fixed density so it will not be compressed; this is wrong as it means the volume of air entering the system is very large.

For further runs this should be modelled as air following the ideal gas rule

Assumption 7 – Air should be changed to an ideal (compressible) gas

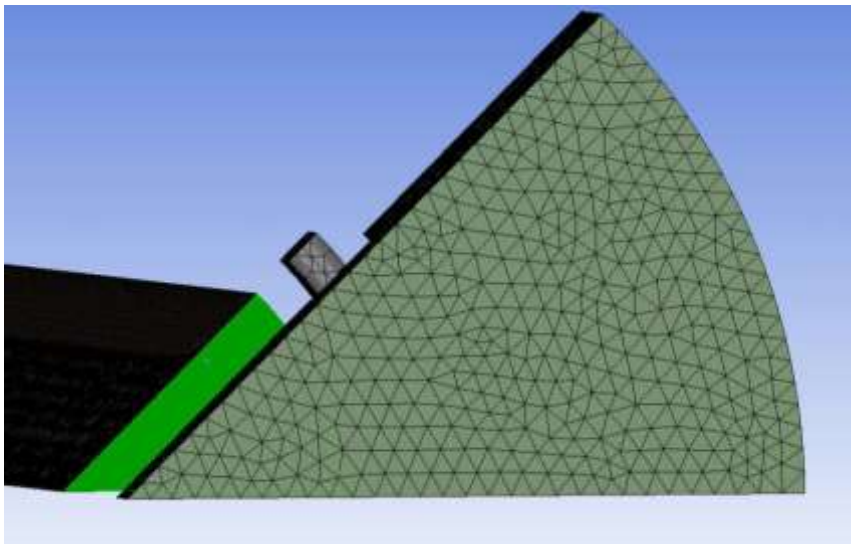

The rise tube contains most of the models mesh, to reduce elements therefore computational time this should be swept. (The face to be swept is shown in light green.)

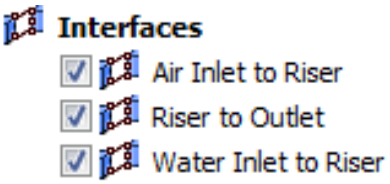

Interfaces can add to mathematical instability but cannot be helped for this geometry

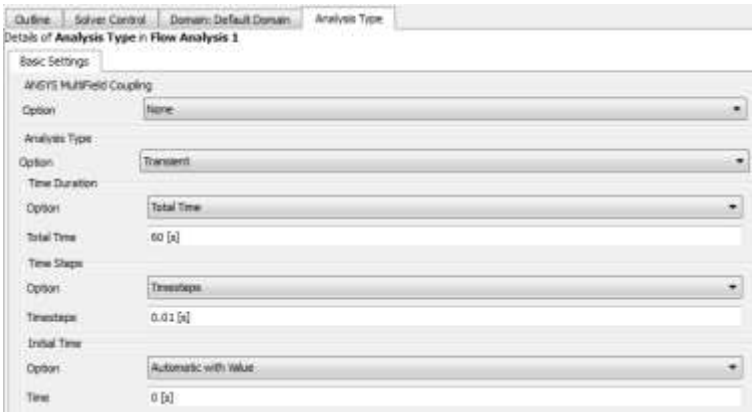

Time step is the biggest control of creating a stable model. A shorter time step adds stability.

Assumption 8 – Smaller time step needed to increase stability

Further Runs

Run P

Assumption 9 – sweeping the mesh in the riser geometry causing blocking will reduce the number of elements for the same mesh size.

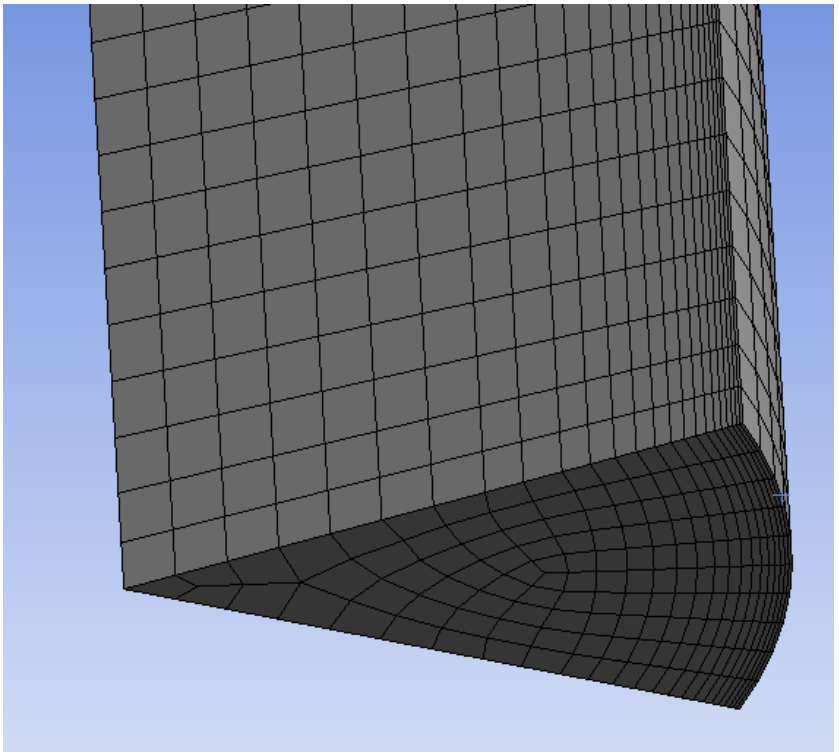

This shows the swept mesh being implemented on the riser component; this reduces the number of elements in the whole file by over 70%.

This can be done as the geometry is only one face extruded

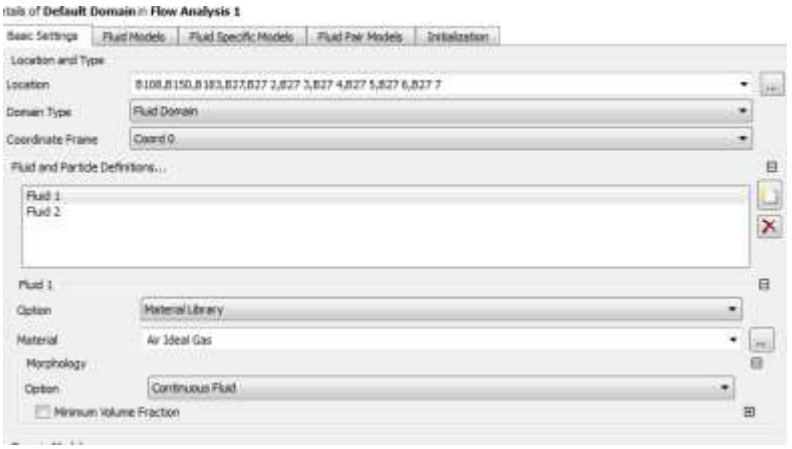

Shows Fluid one (Air) has been changed to an ideal gas

Shows the properties of ‘Air Idea Gas’

```
================================================================================
|                        Timestepping Information                              |
--------------------------------------------------------------------------------
|        Timestep        |   RMS Courant Number   |   Max Courant Number    |
+------------------------+------------------------+-------------------------+
|      1.0000E-02        |          33.21         |         999.99          |
--------------------------------------------------------------------------------
```

Courant Number from Run K is far too high; time step must be greatly reduced to solve this.

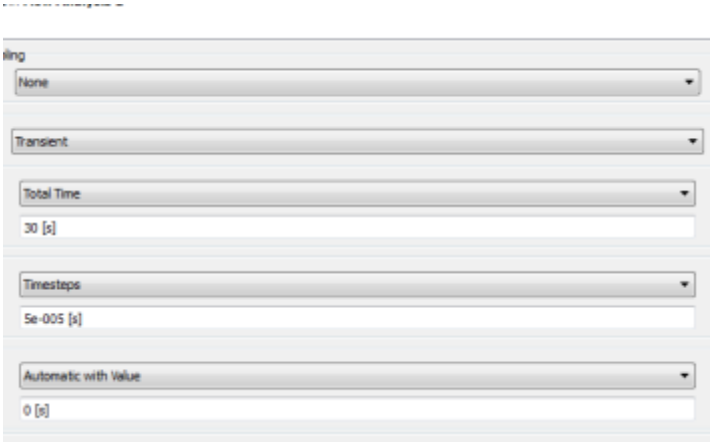

Time step reduced using the formula Courant Number = (Velocity * delta t)/element size with Courant Number = 999.99 (from Run K) and Delta T being Time Step. Velocity and Element size are kept constant.

This means iteration loops are reduced back to 10

Run crashed immediately as the from being too mathematically unstable

Assumption – 10 This is due to changing the mesh and air values before running with the old Steady state results to start with

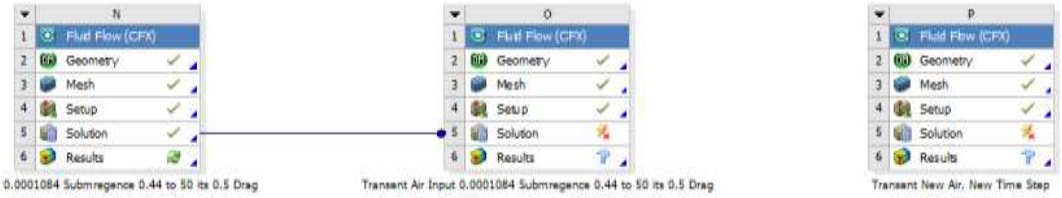

The solutions link form Run N to Run P is removed before running again

```
+--------------------------------------------------------------------+
|                                                                    |
| FATAL ERROR :                                                      |
|                                                                    |
| Initial values are required for all variables in TRANSIENT runs.   |
| In this simulation, no initial value was set for                   |
|                                                                    |
| Variable : Fluid 2.Velocity                                        |
| Domain   : Default Domain                                          |
|                                                                    |
| The value can be set using the Initialisation Branch in CFX Pre.   |
|                                                                    |
| To bypass this message and use default solver initial values,      |
| set the expert parameter "transient initialisation override = t"   |
|                                                                    |
+--------------------------------------------------------------------+
```

Run Crashed due to a Fatal Error. This is because all input data has been removed when deleting the link from the steady state run. It will not run as it is missing initial values for Fluid 2 Velocity (Water) which should be of zero.

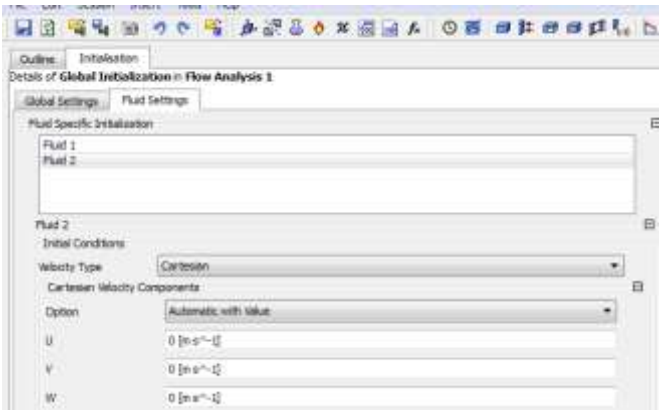

Fluid 2 (water) initial velocities set to zero; Fluid 1 (air) velocity was also set to zero.

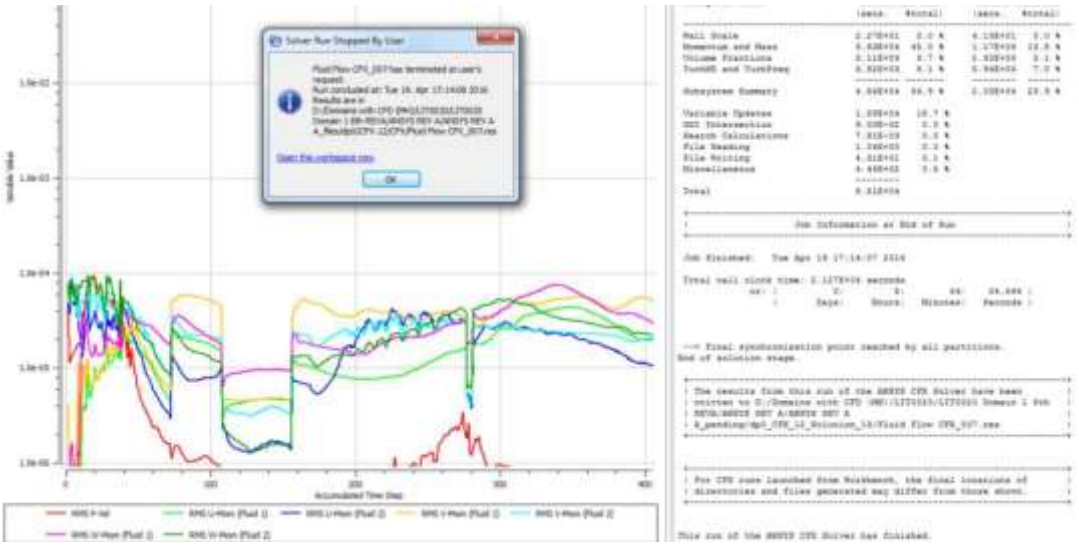

Run P is paused so we can review results. It can be seen from the graph that it is far more stable than before

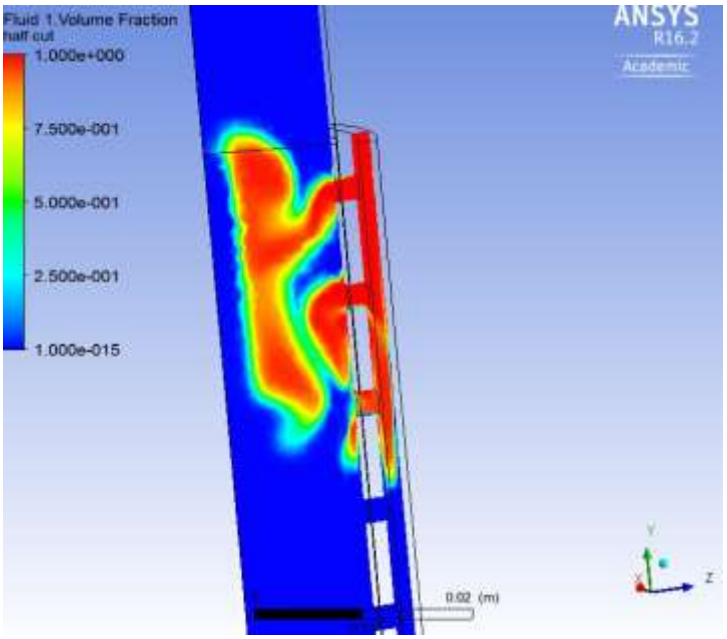

Shows Fluid 1 (air) fraction volume so far

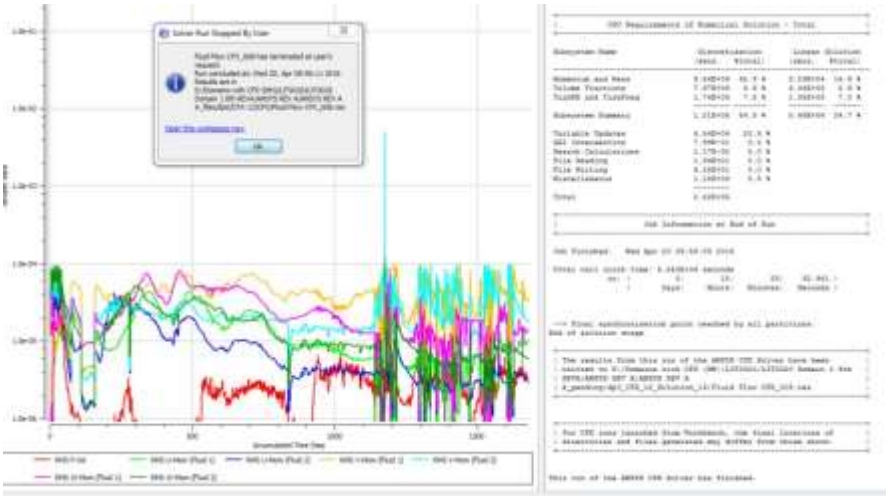

Run P is paused so we can review results.

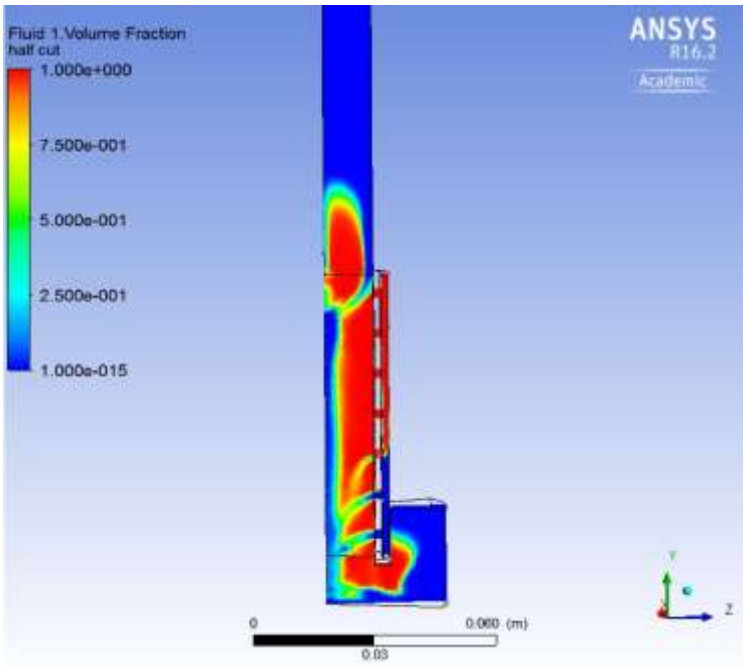

Run P will not work. This can be seen by the air having started to escape from the bottom of the riser. This could be because of incorrect mathematical set up or incorrect geometry.

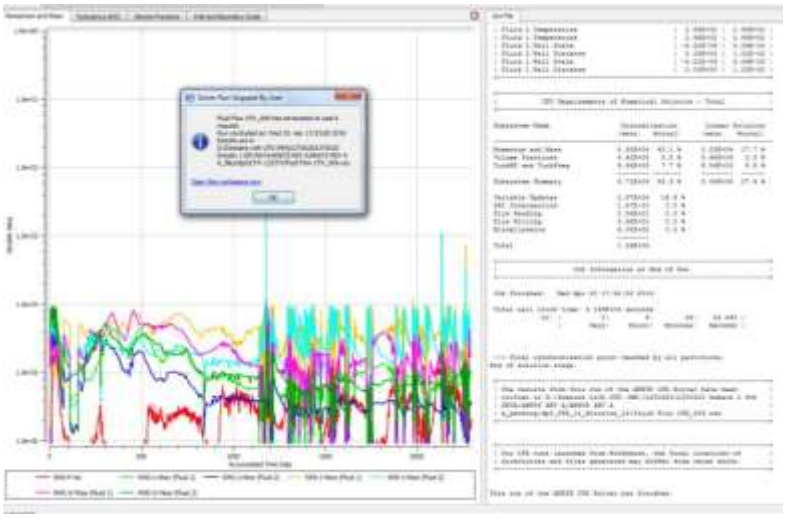

Run stopped after about 32 hours in total, about 2300 time steps have been solved. The total number of time steps required for 30 seconds is 600,000 (30/0.00005). This would mean it would take the run approximately 8,348 hours ((32/2300)*600,000), 348 days which is too long to be viable.

Assumption – 11 Losing Air is due to the lead of the riser before the air inlet not being long enough

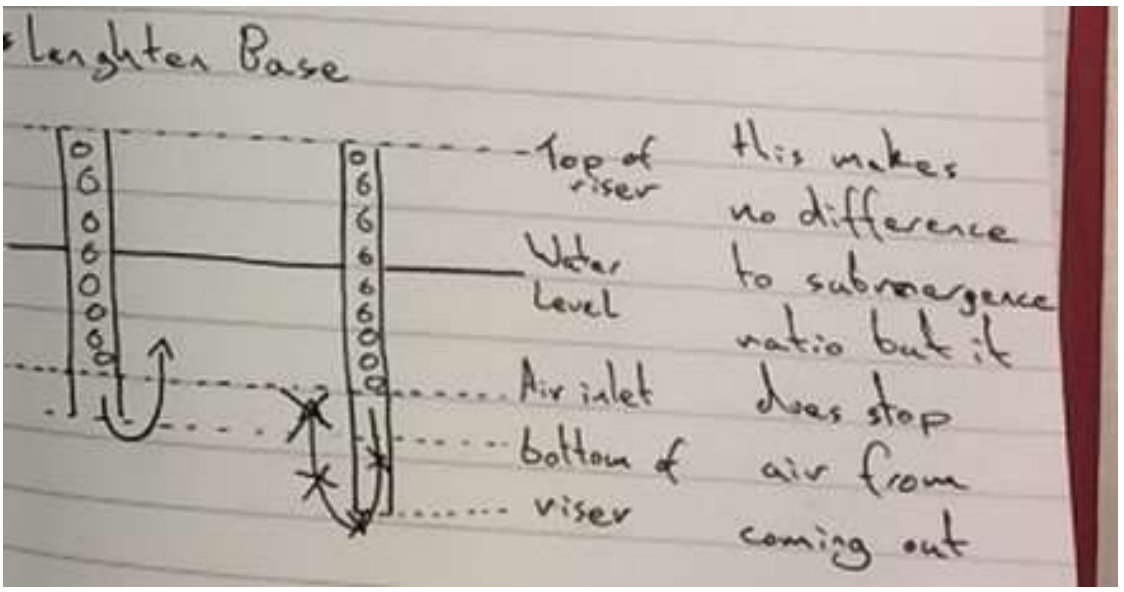

This shows how a longer base will give more time for the buoyancy force to take effect on the air before it has a chance to escape the riser.

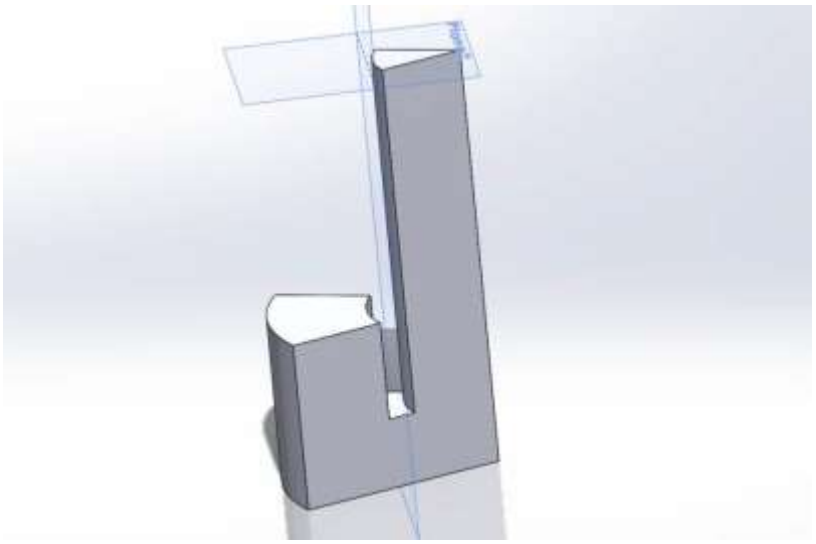

This shows the Base components dimensions being made longer. This was the simplest way of increasing the risers run in length. Note this has no impact on the pressure at the start of the air lift section

Run Q

This is a duplicate of Run P with the longer base section shown above

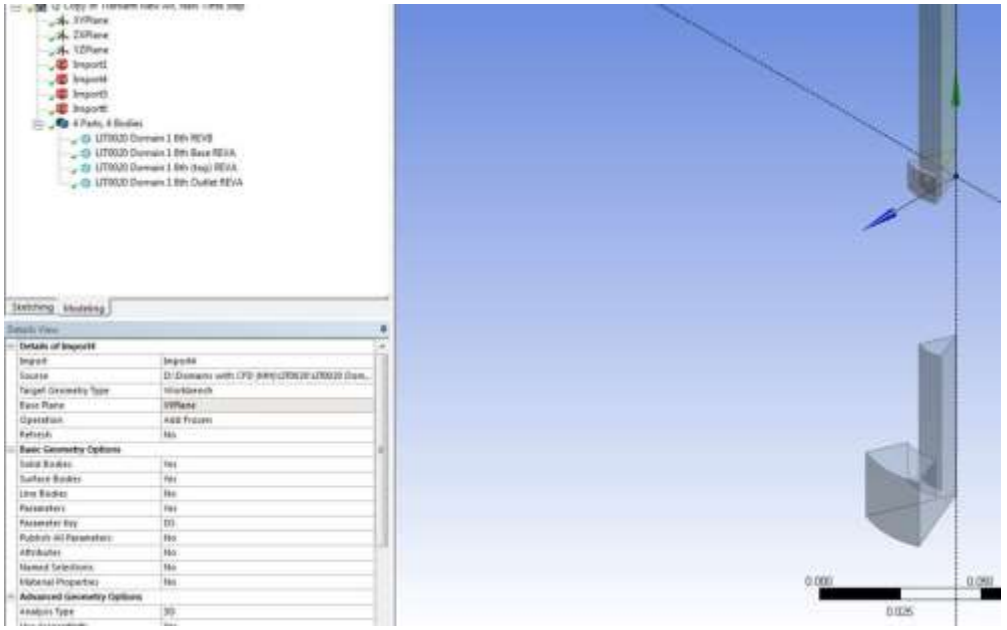

New lengthened Base being implemented. As this was achieved by editing the Solid Works file it only required getting Ansys to re-read the file, this is done by editing the import settings. This added 48 mm to the riser length with no change to the submergence ratio because it is below the point of air injection. The only change is that the length of the riser is increased by 1.2% this will increase friction but due to the small increase this is considered to be negligible.

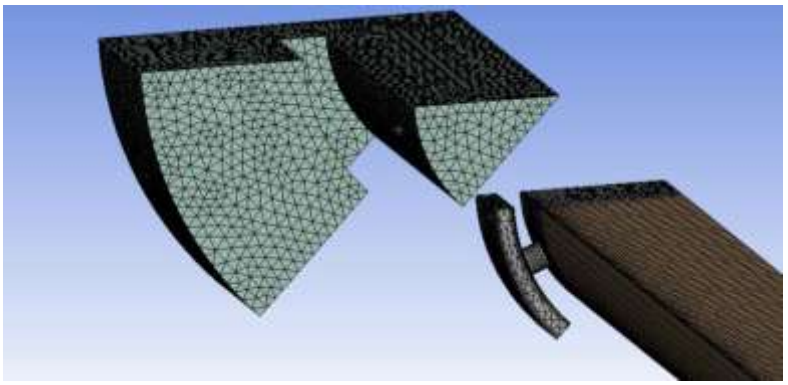

Shows new geometry Meshed

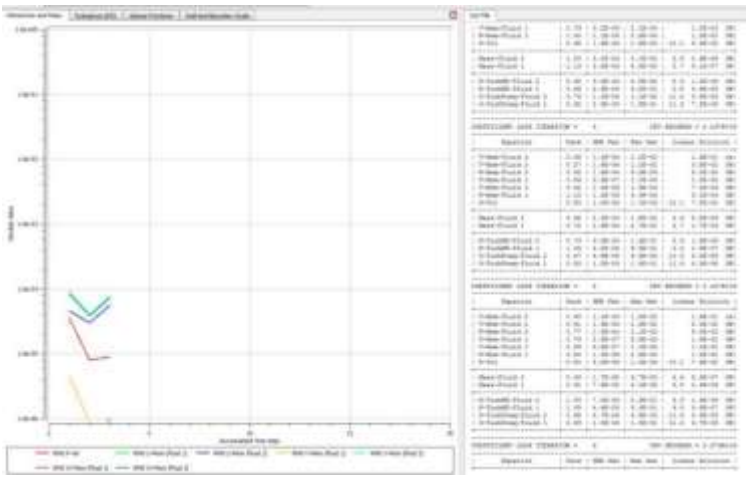

Having done this the run was started. No further changes where required as all of the setup data remained from Run P, the run which Run Q was originally a duplicate of.

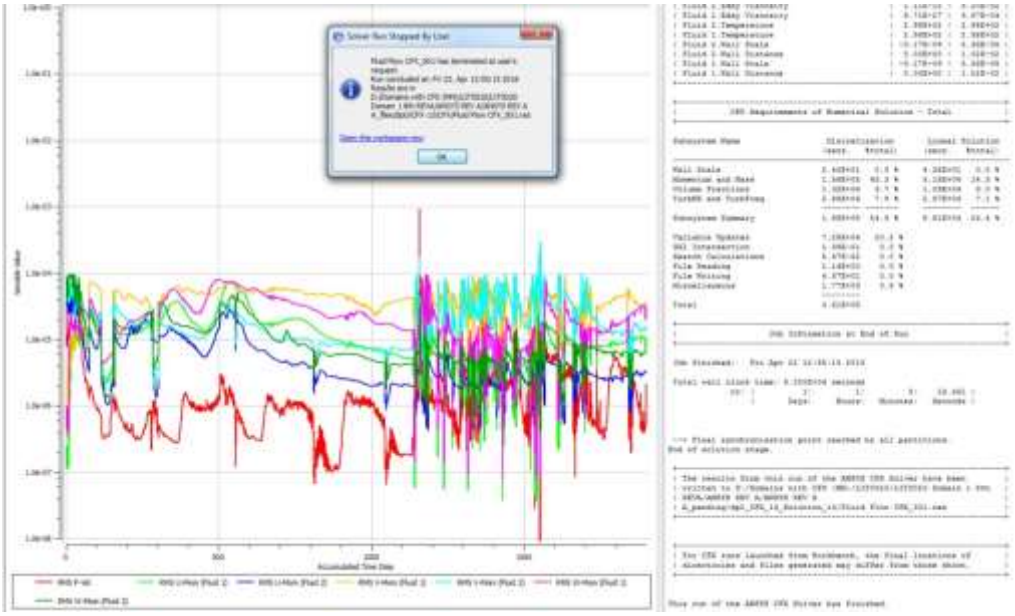

Run paused on 1899 time steps after 13 hours.

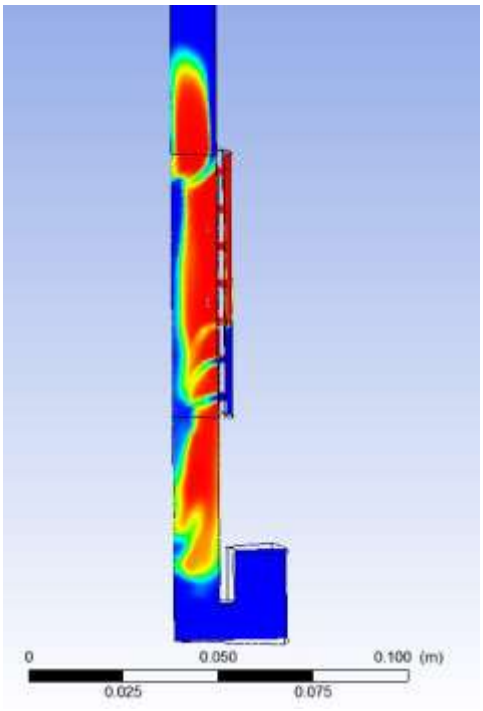

Domain does not appear to be long enough still. Should the air being pumped in start at a slow flow rate and slowly be increased over time until balanced flow is established?

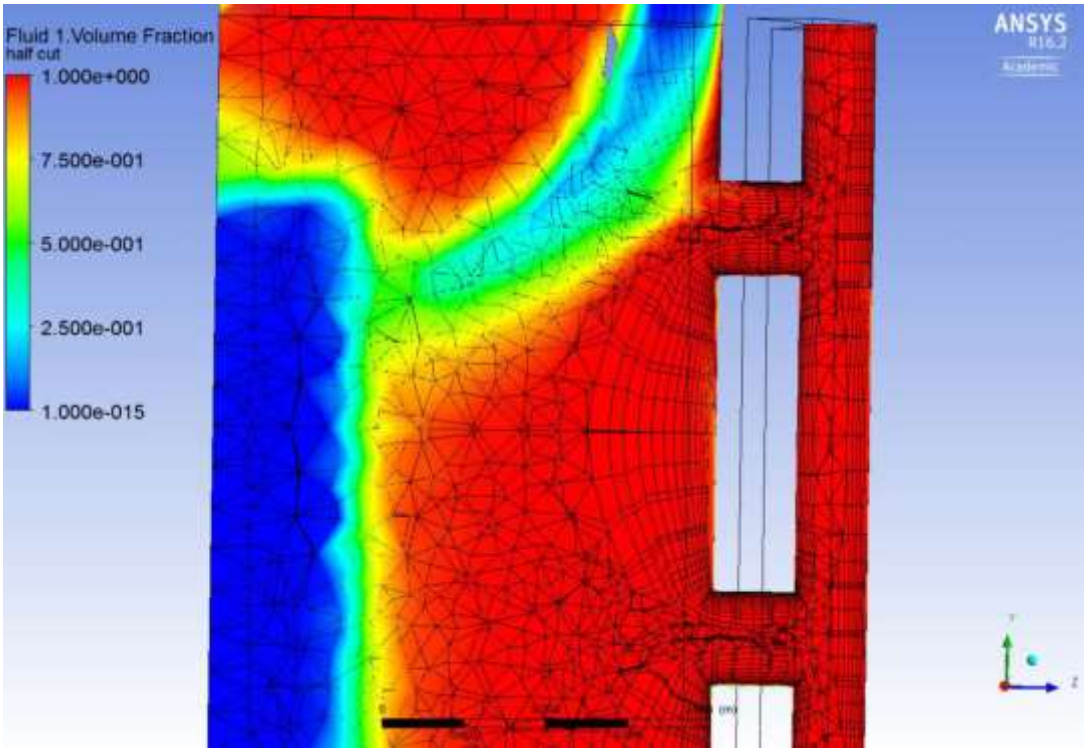

Shows that the mesh is too course as the bubbles shape is being affected by the shape of the mesh. For now a finer mesh cannot be run as run times are already excessive.

Assumption 12 - the air flow must be increased gradually from 0 flow to the know balanced flow point

Run R

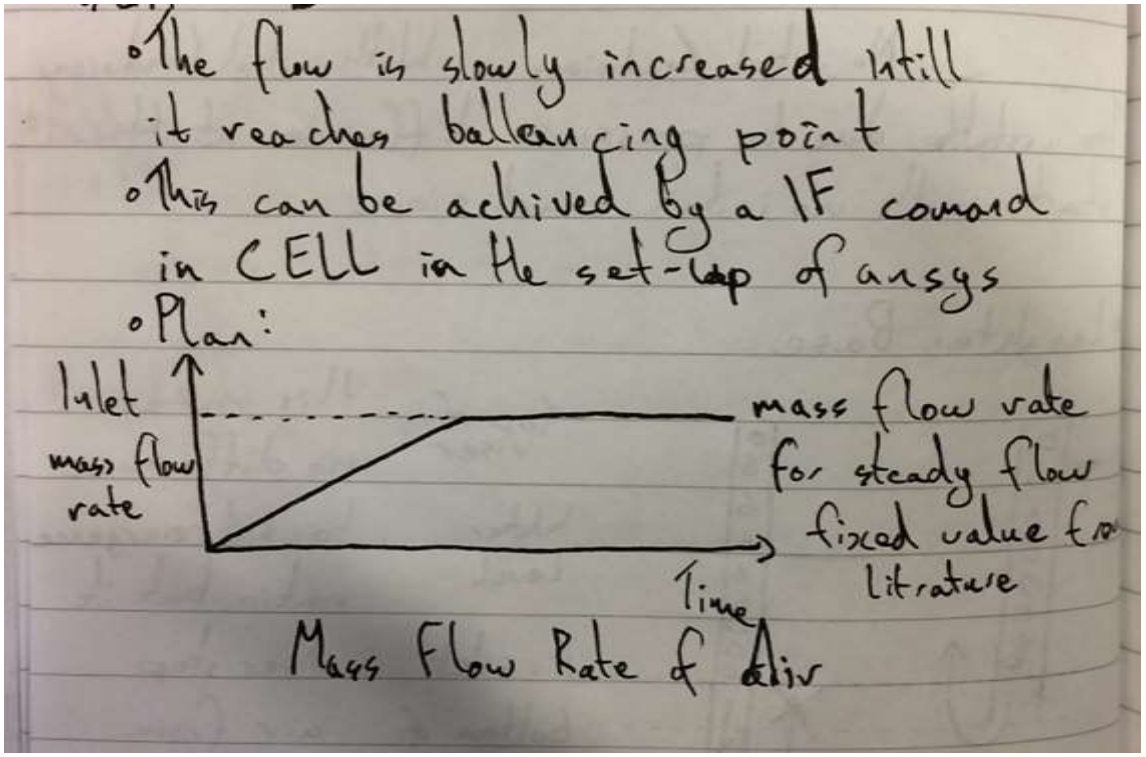

This shows the planed Air Mass Flow rate increasing over time, the rate of increase will be calculated to ensure that full flow rate is achieved after one minuet (this is an estimated time)

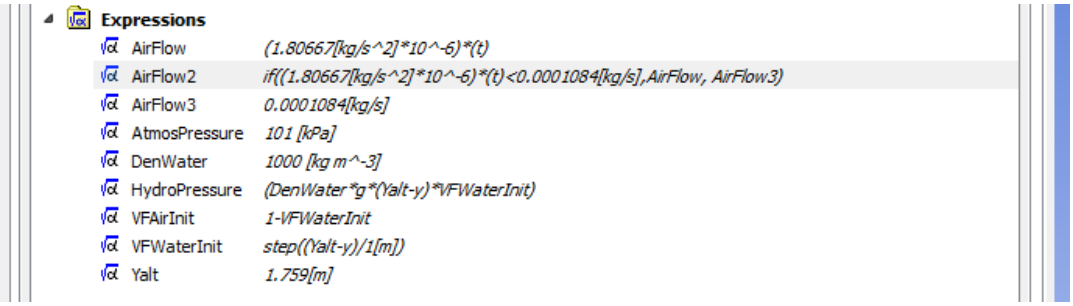

To achieve this the ending air mass flow rate of 0.0001084 kg/s is divided by 60, this means flow rate must increase by 1.80667*10^-6 kg s^-2 (0.0001084/60). Note; AirFlow, AirFlow2 or Airflow3 are added to the expressions list above

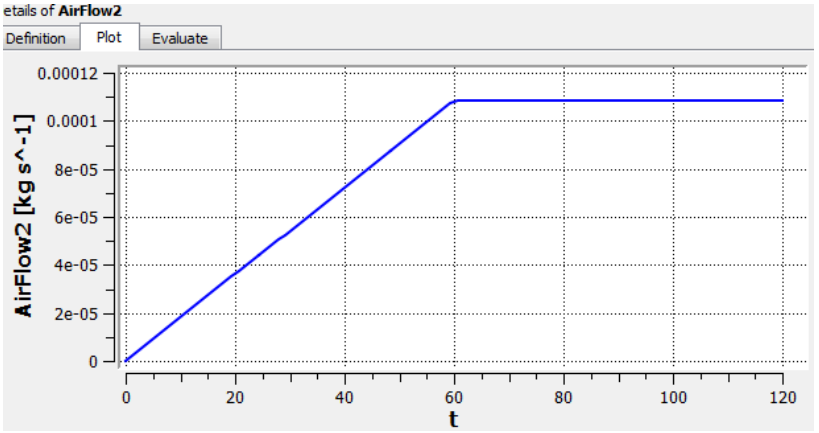

Then an ‘If’ function must be used to ensure that when the flow rate = 0.0001084 kg/s at around 1 minuet it remains constant. The inlet mass flow rate is shown over time modelled above.

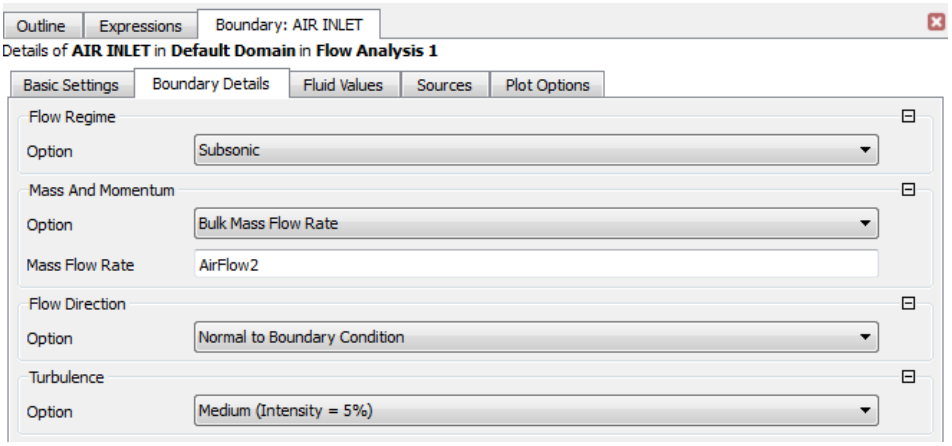

This is applied to the inlet

This is implemented for Run R a copy of Run Q

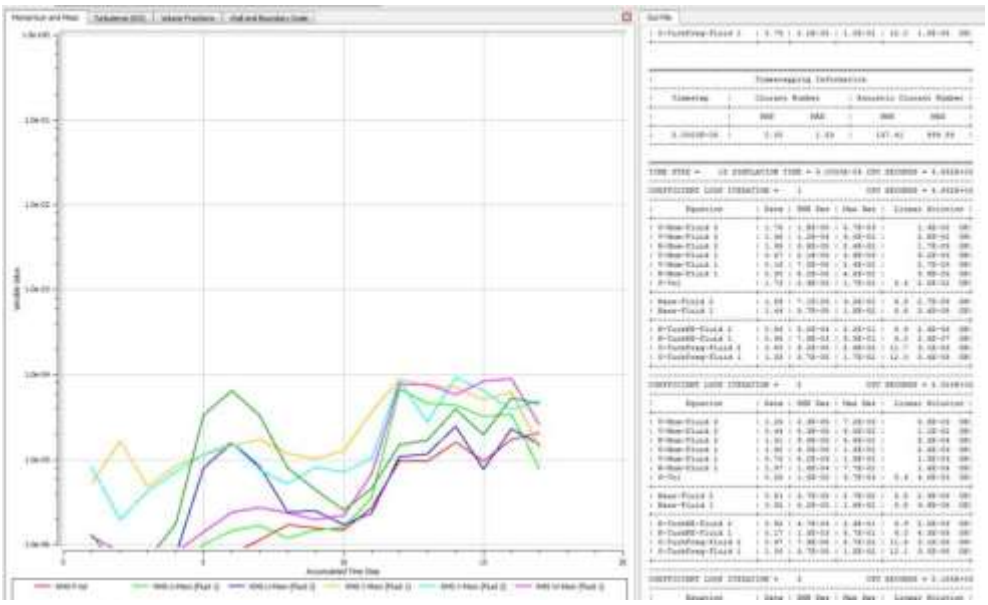

Run R started

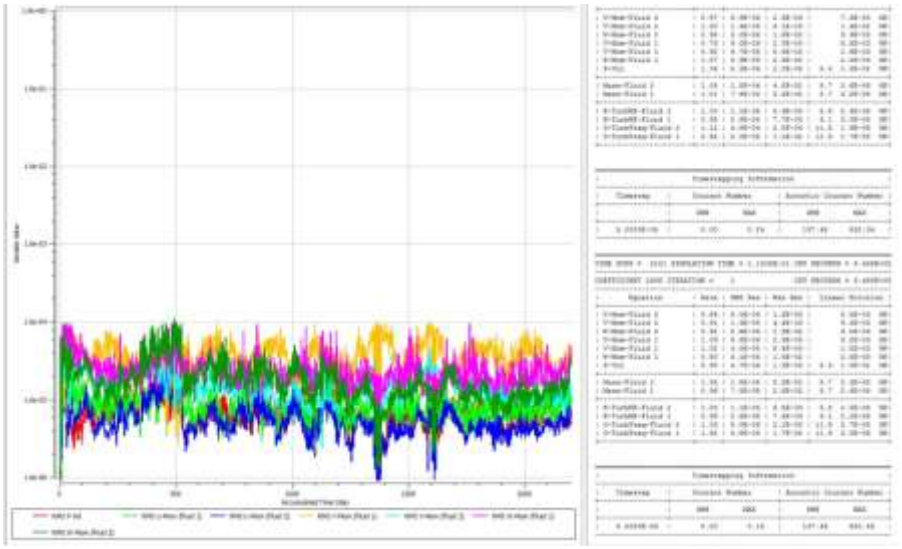

Run R after 2200 time steps, not courant number is now small as the flow is small, but this will increase as the speed of air increases over time

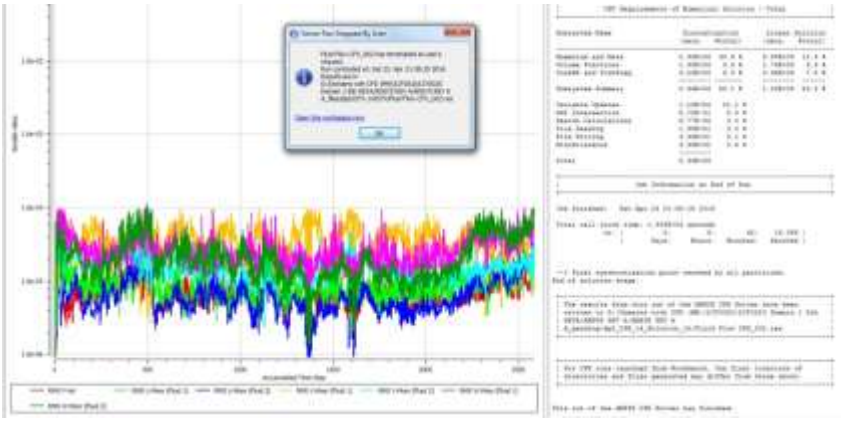

Run Paused to allow for Saturday night computer shutdown in SMB 107b

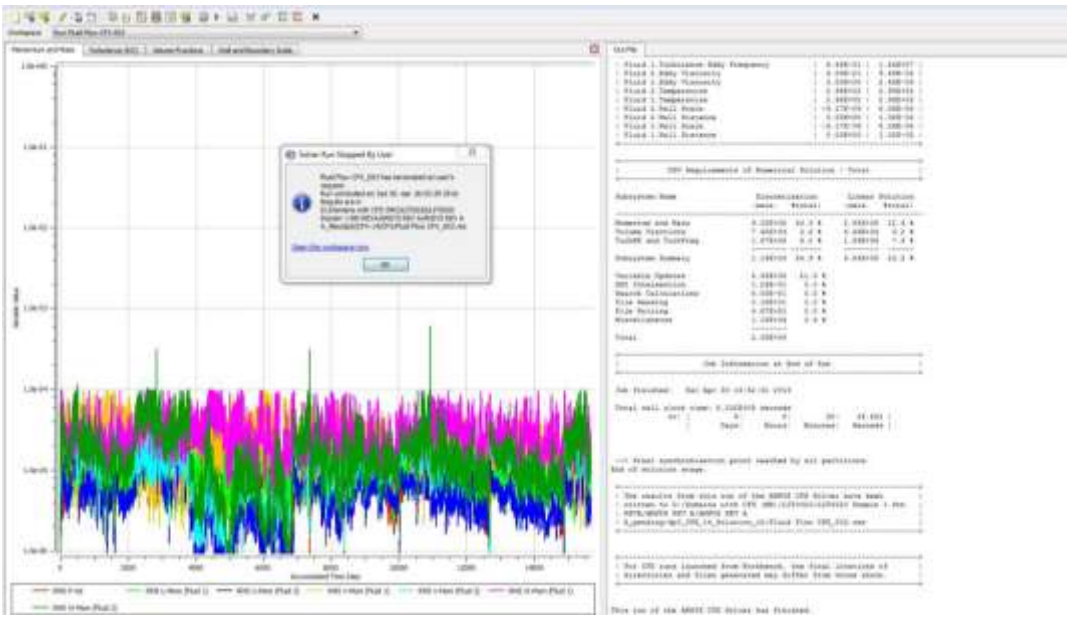

Run R stopped by the user after 6 days and 30 minutes. At this point it had completed 15671 iterations. With the time step of 5*10^-5 this means it has completed 0.73 seconds of the simulation in total.

5 minuets = 300 seconds (1/0.73*6days) = 8.22 days per second. 8.22*300 Seconds = 2465 days for a 5 minuet simulation. This is not viable.

Results show air flows upwards. At slower flows this means that the base could potentially be reduced to its former height.

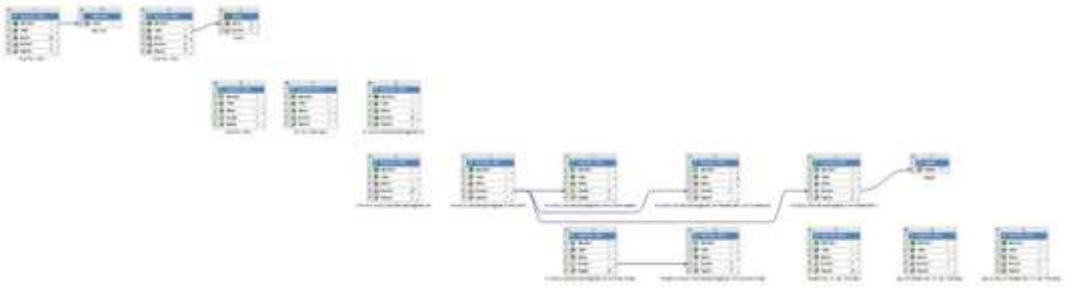

This shows all of the runs used in the project and how they are linked.

Mathematical Modelling

This document shows screenshots of the model created from the equations of (Kinsky, 1982), (Stenning & Martin, 1968), (Brkic, 2011) and (Kassaba, Kandila, Wardaa, & Ahmedb, 2009) outlined in (Kassaba, Kandila, Wardaa, & Ahmedb, 2009) method for using the (Stenning & Martin, 1968) equation. The construction and theory behind this model is discussed fully in Appendix H.

The Model

Inputs				
Name	Symbol	Formula	Value	Units
Riser Height	L	n/a	4.116	m
Riser Diameter	D	na	0.0245	m
Pipe Roughness	ε	n/a	0.002	m^3
Gravitational Constant	g	n/a	9.81	m s^-2
Liquid Density	ρwater	n/a	1000	kg m^-3
Dynamic Viscosity of Liquid	μ	n/a	1.002	kg m s^-1
Submregence Ratio	H/L	n/a	0.442	n/a
Water Depth	H	H/L*L	1.81927	m
Water Mass Flow Rate	Qml	Qvl/ρwater	n/a	kg s^-1
Water Volumetric Flow Rate	Ql	Vl*A or Qvl/ρwater	0.00027	m^3 s^-1
Water Velocity at water inlet (No Air in Column)	Vl	n/a	0.5778	m/s
Value to Goal Seek				
Coefficient of Friction	f	Estimate then Goal Seek	0.65579	n/a
Gas Volume Flow Rate	Qg	Estimate then Goal Seek	0.00017	kg s^-1
Outputs				
Riser Cross-Sectional Area	A	π*((D/2)^2	0.00047	m^2
Static Head	P	ρwater*g*H	17847.1	N m^-2
Slip Ratio	s	1.2+(0.2*(Qg/Ql))+((0.35*A*((g*D)^0.5)))/Ql))	1.62178	n/a
LHS Friction Coefficent	LHS (f)	1/(f^0.5)	1.23486	n/a
Reynolds Number of Water	Re	(ρwater*Vl*D)/μ	14.1279	n/a
RHS Friction Coefficient	RHS (f)	*-2*(log10((ε/(3.71*D))+(2.51/(Re*(f^0.5)))))	1.23455	n/a
Line For Goal Seek	Finding f	LHS (f) - RHS (f) must be zero	0.00031	n/a
LHS (Final Equation)	LHS (FE)	(H/L)-(1/(1+(Qg/(s*Ql))))	1.09716	n/a
RHS (Final Equation)	RHS (FE)	((Ql^2)/(2*g*L*(A^2)))*((((4*f*L)/D)+1)+((((4*f*L)/D)+2)*(Qg/Ql)))	2.96818	n/a
Line For Goal Seek	Finding Qg	LHS (FE) - RHS (FE) must be zero	-1.87102	n/a

Figure 1 – The Mathematical Model Proving Experimental Data from (Stenning & Martin, 1968) (Goal Seek Cells *Shown In Red) Data Available in Appendix F*

Bibliography

Brkic, D. (2011). New explicit correlations for turbulent flow friction factor. *Nuclear Engineering and Design*, 4055–4059.

Kassaba, S. Z., Kandila, H. A., Wardaa, H. A., & Ahmedb, W. H. (2009, 02). Air-lift pumps characteristics under two-phase flow conditions. *International Journal of Heat and Fluid Flow, 30*(1), 88–98.

Kinsky, R. (1982). *Applied Fluid Dynamics* (1 ed.). Sydney: McGraw-Hill Book Company.

Stenning, A. H., & Martin, C. B. (1968). An Analytical and Experimental Study of Air-Lift Pumpo Performance. *A Journal of Engineering for Power*, 106 - 110.

Project Gantt Charts

This document displays and comments on all revisions to the project Gantt charts. These have been updated at points when the project timeline required changing. The reasons for each revision are explained. Overall the project has been delivered on time with a healthy spread of work. The main discrepancy in workload spread is due the project tasks being changed to adapt to comments arising from the interim report. Nine revisions have been made with the Gantt charts being used as a tool for mitigating the risk of failing to meet its deadlines. The Gantt charts can also be verified by entries into the project logbook.

Table of Contents

Gantt Chart Design

The Gantt charts have been designed with the following factors considered:

- Accuracy of the Chart:
    - As timings for tasks are approximate and tasks may change the chart is restricted to tasks undertaken per week. Further definition is not viable,
- Mixture of tasks to avoid tasks to becoming repetitive:

- This will allow better focus on the project to be maintained,
- This also allows progress to be maintained even if difficulties are encountered,

- Considering the critical timeline:
  - Tasks which must be completed before other tasks can be undertaken are given priority to avoid major holdups,
- When considering project timing the mark scheme was considered. This is was for the initial Gantt chart REV01 and in shown in Table 1.

From the project definition outlined in the Interim report (Appendix A) the following sections and sub-sections were found. These are then considered against the mark scheme. From this the importance of each section with regards to the amount marks allocated to it was identified. This was used when allocating the number of weeks to spend on each task.

Weighting: - approximated from mark schemes				
Section	Sub Section	Interim Report	Final Report	Poster
1. Planning		30	10	0
	1.1 Project organisation	10	4	
	1.2 Gantt chart	10	2	
	1.3 Review of plan	10	4	
2. Background knowledge		35	20	0
	2.1 reviewing literature	18	12	
	2.2 construction of basic working model	8	2	
	2.3 Review into FSCL applications	9	6	
3. Scale Modelling		10	10	0
	3.1 feasible design scale model	5	1	
	3.2 design/manufacture of model	5	2	
	3.3 Testing of model		2	
	3.4 Recording of results		5	
4. CFD Modelling		5	10	0
	4.1 Local Area	5	1	
	4.2 modelling		2	
	4.3 model iteration		2	
	4.4 test results		5	
5. Results		0	20	0
	5.1 Comparing model		10	
	5.2 comparing results		10	
6. report*		10	30	0
	6.1 compiling the report	5	20	
	6.2 finalising the report	5	10	
7. Poster		0	0	100
	7.1 Poster			50
	7.2 Presentation			50

8. Log Book*	10	0	0
9. Submission of work	0	0	0
Total	100	100	100

Table 1 – Table to Show Key Sections of the Project and Their Weighting In the Mark Scheme

Reasons for Revisions

Table 2 shows the revision numbers, dates of revision and reasons for the revision.

Revisions Directory	Date	Reason for Revision
REV01	30/09/2015	First revision
REV02	07/10/2015	Improved to account for interim report date (04/12/15)
REV03	14/10/2015	Improved to account for a university trip to Alabama
REV04	26/11/2015	Improved to account for the removal of physical Testing and adjusted with knowledge of work from the first 9 weeks
REV05	16/12/2015	Addition of working model design and manufacture
ALL	26/11/2015	Revision numbers added to ALL Gantt charts for ease of identification
REV06	22/01/2016	Improved to account for the new project direction after meeting with DH and JGJ on 22/01/16 and no work during Christmas
REV07	17/03/2016	Improved to account for evolving timings as more is known about CAD - Past adjusted to account for real work done
REV08	12/04/2016	Adjusted to allow more time for CFD
REV09	29/04/2016	Adjusted to account for subtle changes during the final project stages

Table 2 – Record of Revisions To the Project Gantt chart

Gantt Chart Revisions

This section shows all revisions of the Gantt charts, these are printed on A3 pages so they can be easily read.

REV 01

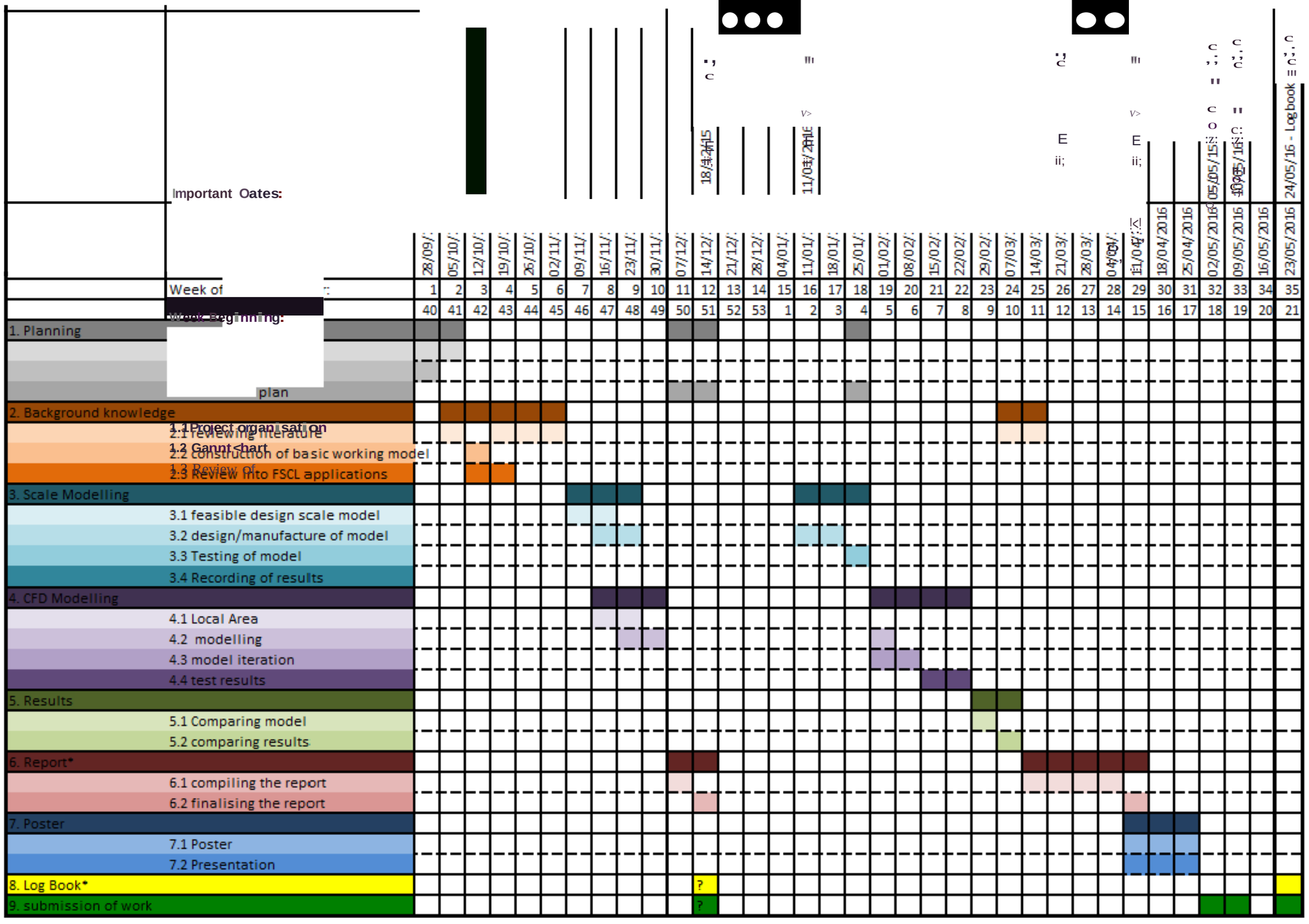
Important Oates:
Week of
Week beginning:
plan
1.1Project organisation
2.1 reviewing literature
1.2 Gannt chart
2.2 construction of basic working model
1.3 Review of
2.3 Review into FSCL applications
28/09/
05/10/
12/10/
19/10/
26/10/
02/11/
09/11/
16/11/
23/11/
30/11/
07/12/
14/12/
21/12/
28/12/
04/01/
11/01/
18/01/
25/01/
01/02/
08/02/
15/02/
22/02/
29/02/
07/03/
14/03/
21/03/
28/03/
18/04/2016
25/04/2016
16/05/2016
23/05/2016
24/05/16 - Logbook
1 2 3 4 5 6 7 8 9 10 11 12 13 14 15 16 17 18 19 20 21 22 23 24 25 26 27 28 29 30 31 32 33 34 35
40 41 42 43 44 45 46 47 48 49 50 51 52 53 1 2 3 4 5 6 7 8 9 10 11 12 13 14 15 16 17 18 19 20 21
1. Planning
2. Background knowledge
3. Scale Modelling
3.1 feasible design scale model
3.2 design/manufacture of model
3.3 Testing of model
3.4 Recording of results
4. CFD Modelling
4.1 Local Area
4.2 modelling
4.3 model iteration
4.4 test results
5. Results
5.1 Comparing model
5.2 comparing results
6. Report*
6.1 compiling the report
6.2 finalising the report
7. Poster
7.1 Poster
7.2 Presentation
8. Log Book*
9. submission of work
?
?

REV02

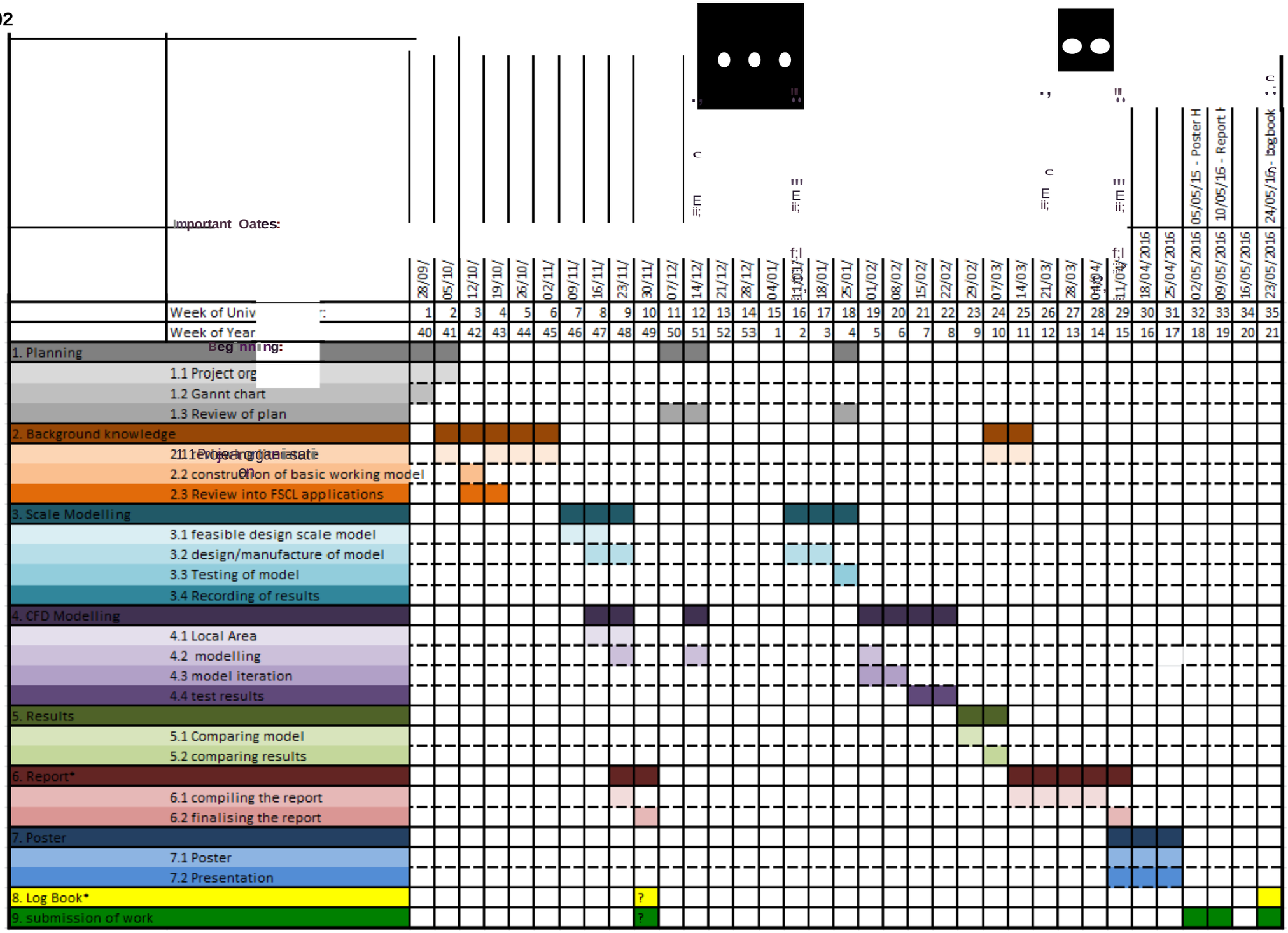

Appendix E

Table 4- Gantt Chart Revision 02

REV03

	Important Dates:																																		
	Week Beginning:	28/09/2015	05/10/2015	12/10/2015	19/10/2015	26/10/2015	02/11/2015	09/11/2015	16/11/2015	23/11/2015	30/11/2015	07/12/2015	14/12/2015	21/12/2015	28/12/2015	04/01/2016	11/01/2016	11/01/2016	18/01/2016	25/01/2016	01/02/2016	08/02/2016	15/02/2016	22/02/2016	29/02/2016	07/03/2016	14/03/2016	21/03/2016	28/03/2016	04/04/2016	11/04/2016	11/04/2016	18/04/2016	25/04/2016	02/05/2016	09/05/2016	16/05/2016	23/05/2016
	Week of University	1	2	3	4	5	6	7	8	9	10	11	12	13	14	15	16	17	18	19	20	21	22	23	24	25	26	27	28	29	30	31	32	33	34	35
	Week of Year	40	41	42	43	44	45	46	47	48	49	50	51	52	53	1	2	3	4	5	6	7	8	9	10	11	12	13	14	15	16	17	18	19	20	21
1. Planning																																				
	1.1Project organisation																																			
	1.2 Gannt <hart																																			
	1.3 Review of plan																																			
2. Background knowledge																																				
	2.1 reviewing literature																																			
	2.2 construction of basic working model																																			
	2.3 Review into FSCL applications																																			
3. Scale Modelling																																				
	3.1 feasible design scale model																																			
	3.2 design/manufacture of model																																			
	3.3 Testing of model																																			
	3.4 Recording of results																																			
4. CFD Modelling																																				
	4.1 Local Area																																			
	4.2 modelling																																			
	4.3 model iteration																																			
	4.4 test results																																			
5. Results																																				
	5.1 Comparing model																																			
	5.2 comparing results																																			
6. Report*																																				
	6.1 compiling the report																																			
	6.2 finalising the report																																			
7. Poster																																				
	7.1 Poster																																			
	7.2 Presentation																																			
8. Log Book*											?																									
9. submission of work											?																									

REV 04

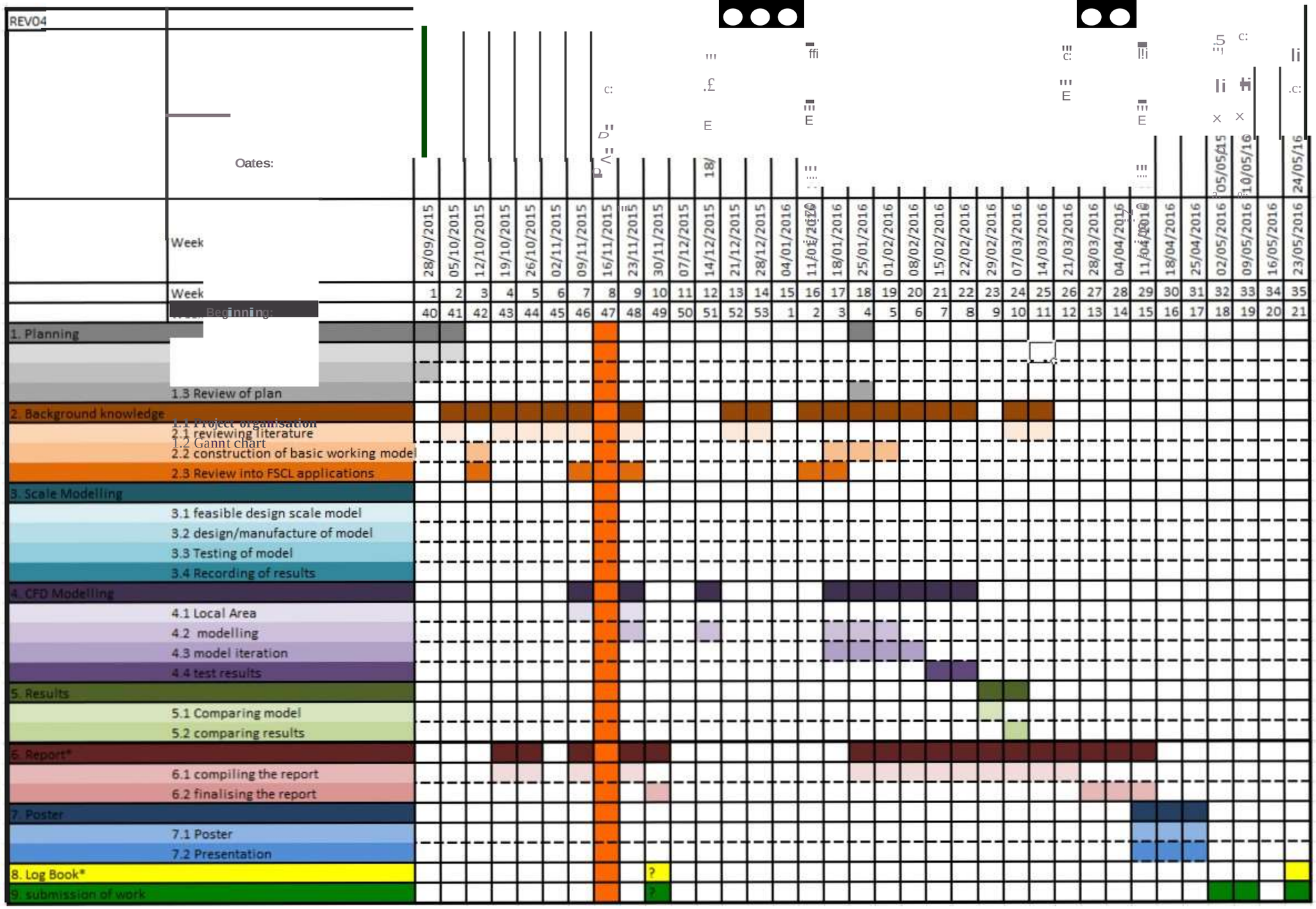

Appendix E

Table 15-Gartt Chart Revision 04

Appendix E

REV05

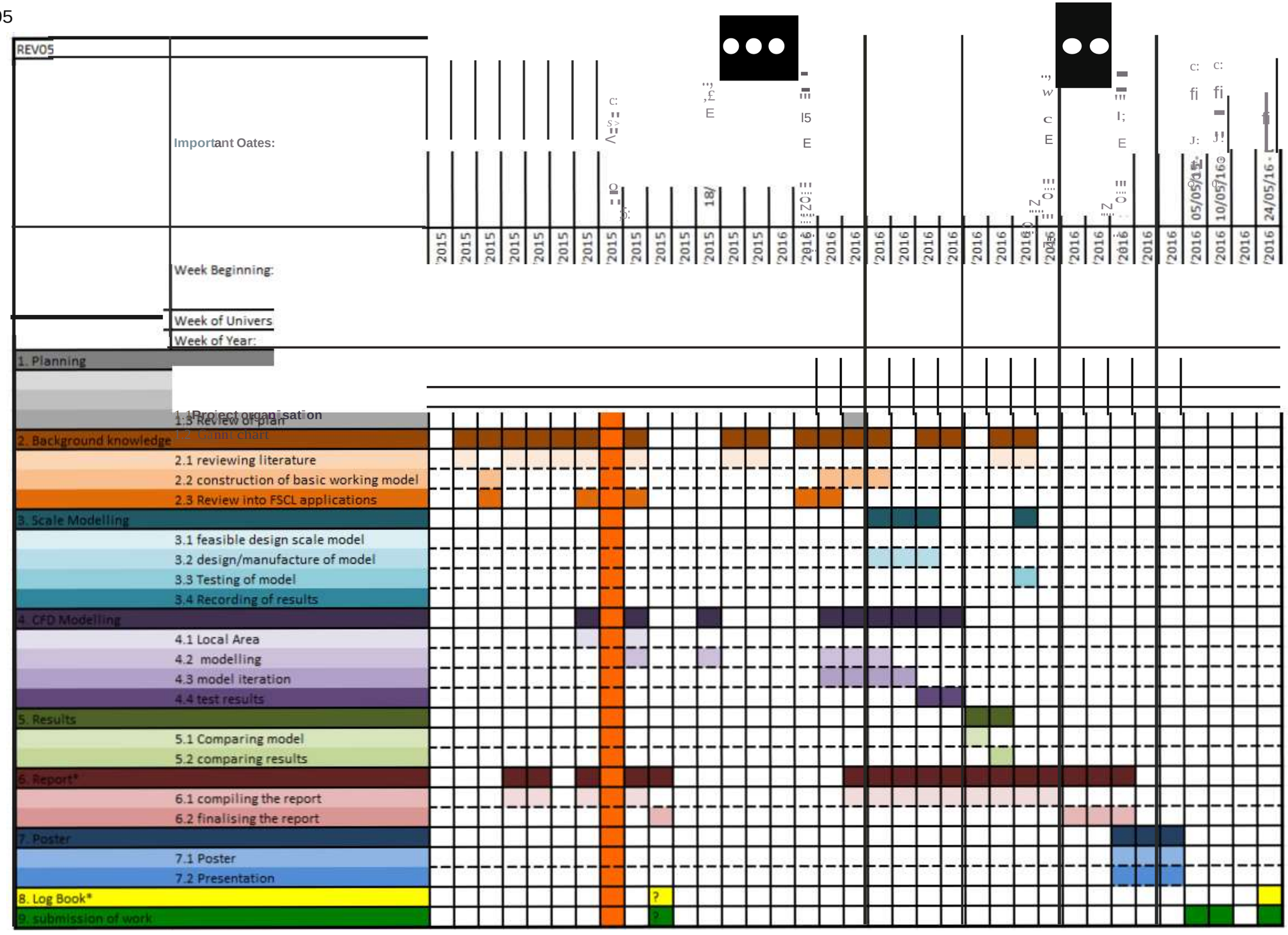

Table 7-Gartt Chart Revision 05

Appendix E

REV06

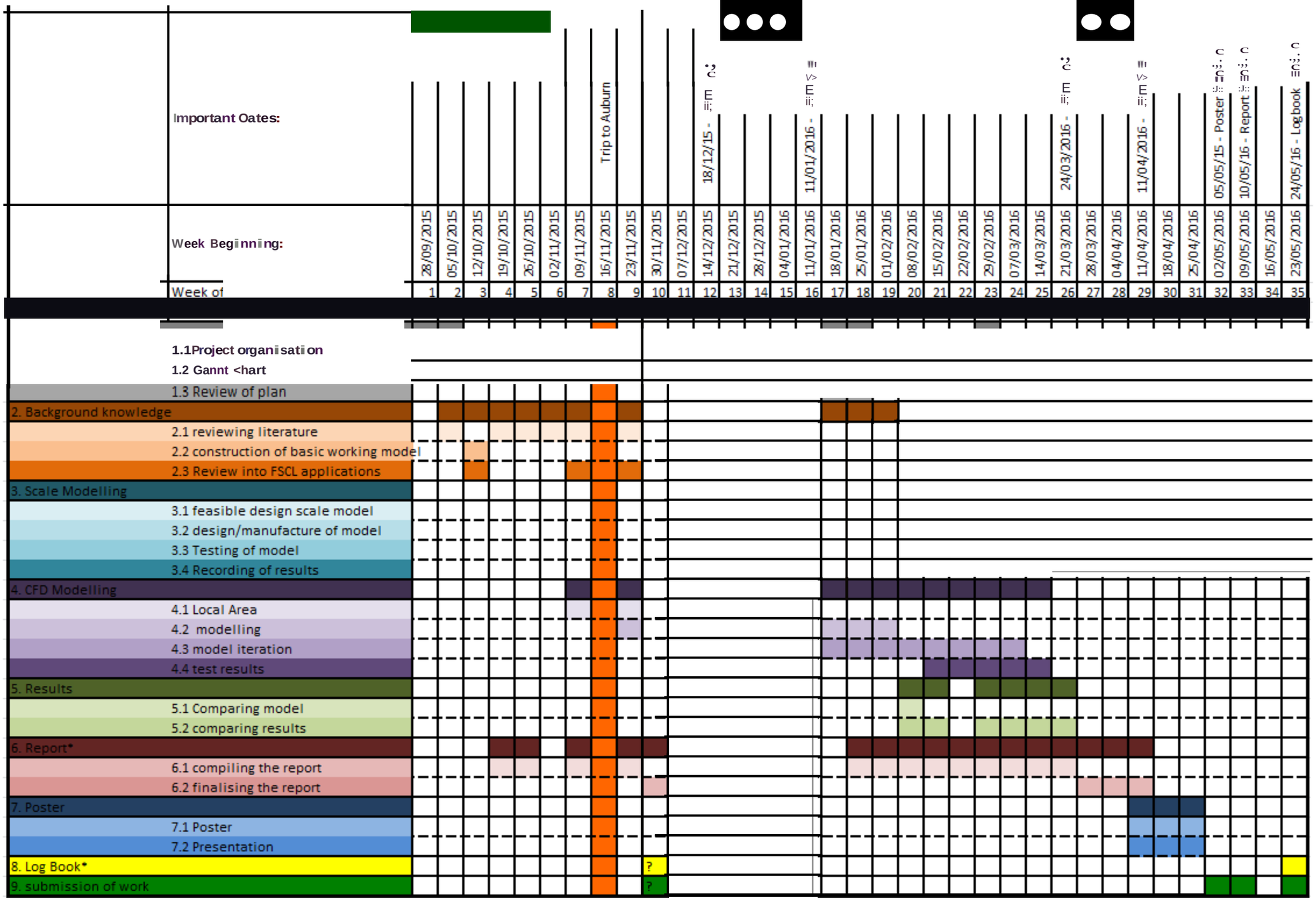

Table 8-Gartt Chart Revision 05

Table 8- Gantt Chatt Revision 06

Table 9-Gartt Chart Revision 05

Appendix E

REV07

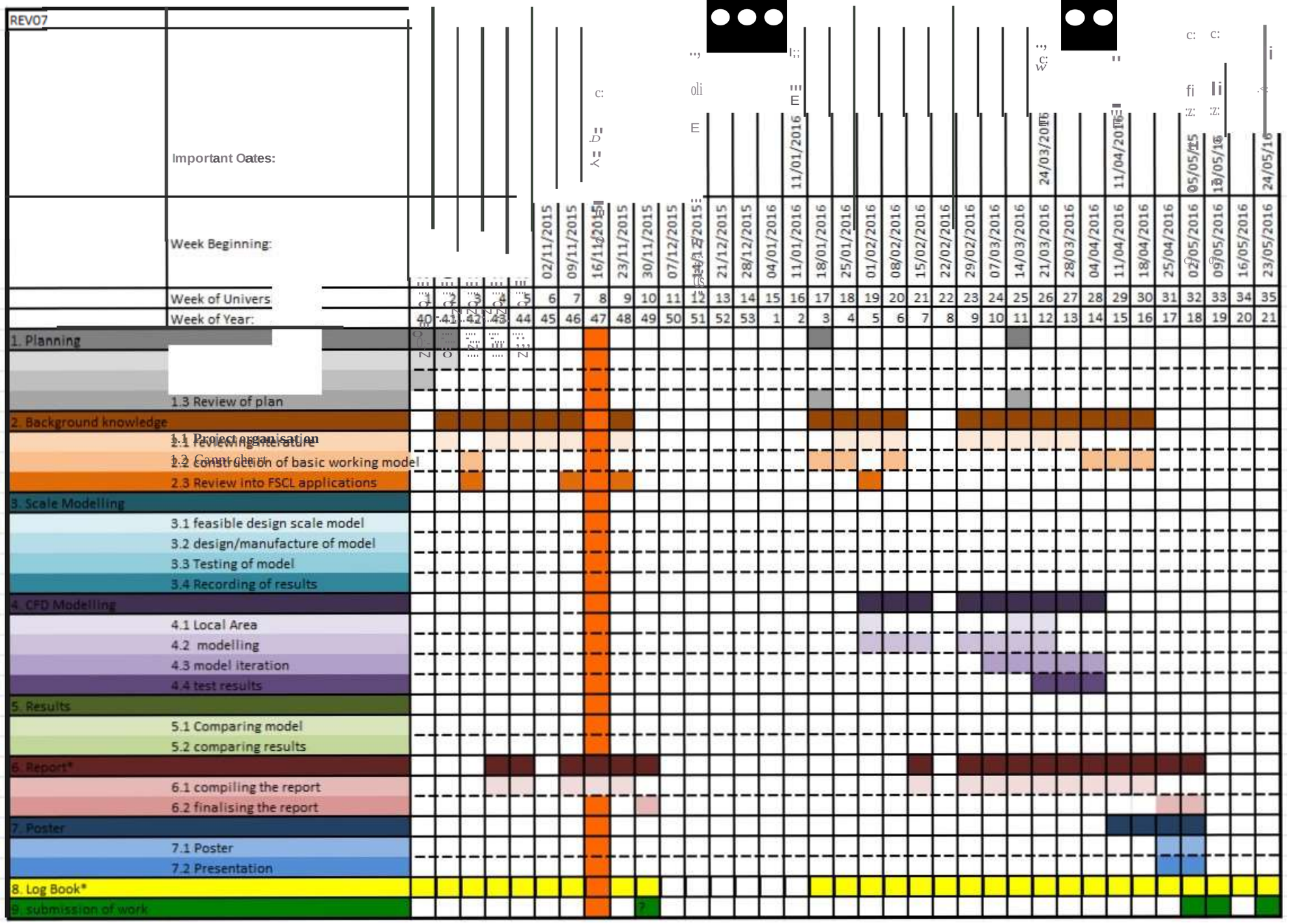

Table 9-Gartt Chart Revision 07

Appendix E

REV 0S

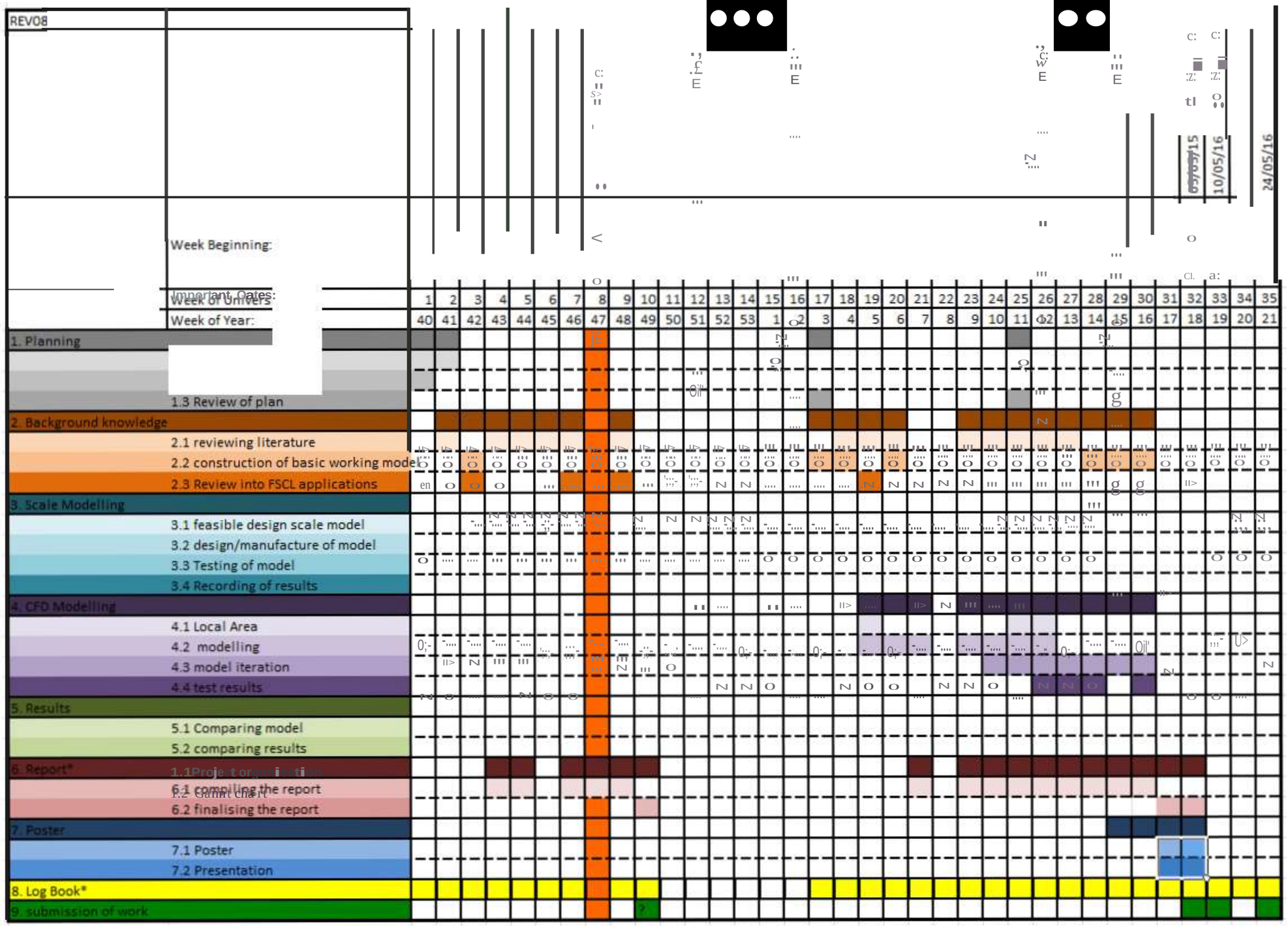

Table 10-Gartt Chart Revision 07

Appendix E

Table 10-Gartt Chart Revision 08

Table 11-Gartt Chart Revision 07

Appendix E

REV09

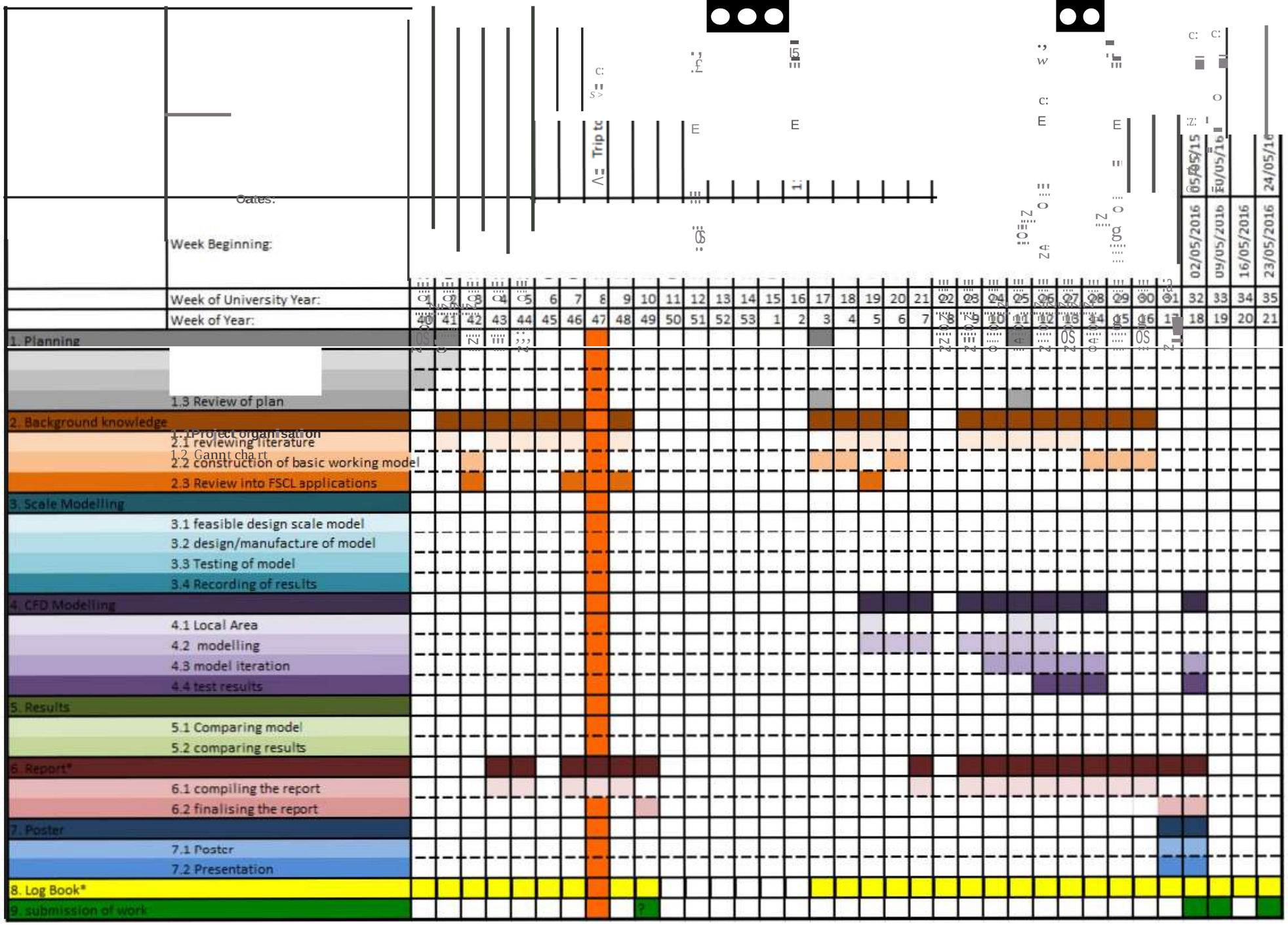

Appendix E

Table 11-Gartt Chart Revision 09

Appendix E

Conclusion

To simplify this section only Gantt chart REV 01 (Table 3) will be compared to REV 09 (Table 11). All of the smaller changes are shown in Table 2. This section focuses on the two main areas of change, these being issues with predictions of timings and the change of project objectives following the interim report (Appendix A) which led to a time of no work as the direction of progression was not clear.

Prediction of Timings

Looking between REV 01 and 09 it appears that more time has been spent on the project than was anticipated. There are also far more tasks being conducted simultaneously during each week then were originally timetabled. The reasons for this are as follows:

- Complex task such as CFD require computer Run time where other tasks must be focused on instead,
- When a problem is encountered it may be necessary to wait to consult a lecturer, while waiting another task has been undertaken to best use time,
- It became apparent from trying to write the interim report after collecting all of the data it is easier to run tasks simultaneously,
- Some predictions proved inaccurate particularly for tasks which had not been undertake before, such as CFD model construction, this was in part due to the extra learning skills which this requires,
- Some weeks less work was achieved, as other university work was required. This was a key factor shortly before Easter when students from Auburn University visited in relation to a design project.

To control these unknowns the project scope has been changed to a wider investigation into what is the best method for Fugro to pursue modelling Airlift pumps with for their application. The complexity of the problem is also reflected in the reports theoretical as apposed to mathematical findings with a large section of further work suggested to allow a model to eventually be made.

Change in Project Objectives

The largest change during the project was as a result of the interim report. Feedback form this was that more engineering had to be undertaken. Unfortunately this meant that over Christmas no work could be done on the project as the future direction was unknown. After exams in January a meeting was held with the project supervisor and moderator. During this meeting it was decided to include a study into creating a CFD model. At this point REV 06 was created to account for this change in project tasking.

Unfortunately delayed over Christmas and around the January exams have not been recovered resulting in the outcome of the project having to be reduced during April as the deadline approached. To reflect this, the project name was changed to: Fugro Seacore; Airlift Pump Modelling Proposal.

Overview

With all things considered it is felt that the Gantt charts have been a useful tool in project management. They have enabled the quick identification of areas that could have been undertaken differently informing the conclusion of this Appendix. This was a very good way of staying on schedule and should be revised regularly particular if broad estimate had to be made at the point of writing. The data shown is fully reflected by the logbook entries.

Validation Data

This document explains the method behind selecting and recovering suitable validation data for both the mathematical and CFD models. Unfortunately this data is not used to validate the final results because the models were not fully developed however it does shows a clear process and could be used if the project was developed further.

Table of Contents

Data Collection Methodology

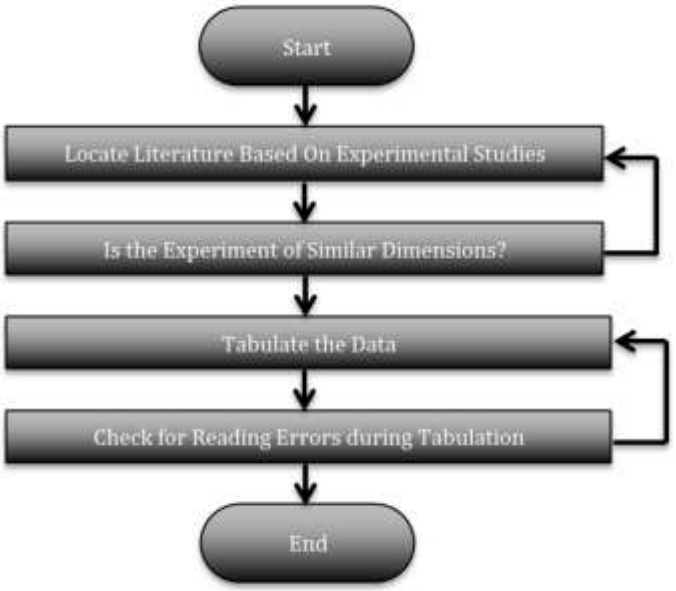

Figure 1 – Raw Data Harvesting Process

Figure 1 shows how raw data, which can be used for CFD validation, was collected.

All validation data has been taken from peer reviewed literature to ensure that it is reliable. It is also checked that similar dimensions are present as large differences may affect the models ability to be re-applied to other problems. For this reason only two-phase data is used.

The data is then tabulated by reading it from the graphs. To check for reading errors the data is them put back into graph form to check for reading mistakes shown by outlying data. This process can be of limited accuracy as stated earlier it will only be used to investigate if CFD can be used or not therefore full scale validation is not required.

It was chosen to use the (Stenning & Martin, 1968) experimental data for the tests. Using this data allows results from both their mathematical model and experimental data to be compared directly to the CFD results. The full tabulated results can be seen in the relevant section of this document for each source. Note that all data has been converted to SI units so it can be compared directly. Before the errors associated with the data extraction are considered it should be noted that the experimental data is only accurate to + or – 2% (Stenning & Martin, 1968) this is negligible when considered against the reading errors in the data harvesting.

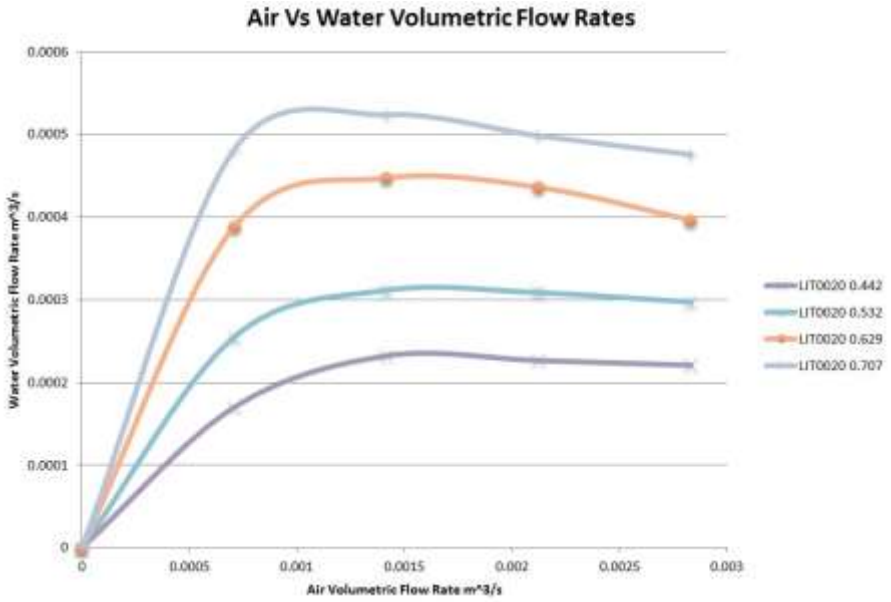

"Graph 1 – The Data Collected From (Stenning & Martin, 1968)*"*

Should more data be required for further validation results have also been taken from: (Fan, et al., 2013), (Tighzert, Brahimi, Kechroud, & Benabbas, 2013) and (Kassaba, Kandila, Wardaa, & Ahmedb, 2009). The geometry of the model will have to be changed to allow validation using each set of results. These have been chosen to broaden the range of cases that the CFD has been tested on should time allow. All of these results are shown in Graph 2. From these is can be seen how much the (Tighzert, Brahimi, Kechroud, & Benabbas, 2013) – LIT0007 results differ due to the negative submergence ratio and different scale of test.

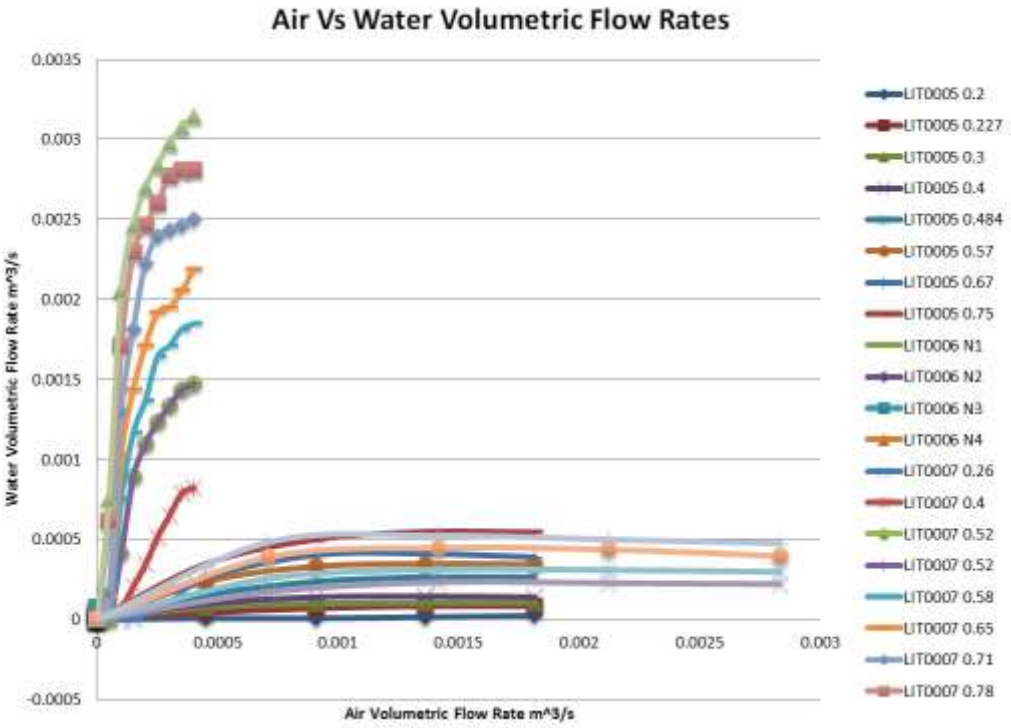

"Graph 2 – The Data Collected from: (Fan, et al., 2013)*,* (Tighzert, Brahimi, Kechroud, & Benabbas, 2013) *and* (Kassaba, Kandila, Wardaa, & Ahmedb, 2009)*"*

The Data Collected:

Here the raw data is shown organised into sections titled by the literature it has been taken from. The data is converted into SI units. As in Appendix B, the same literature code is used in the format LitXXXX. In the code the X locations are populated with numbers. Each number represents a piece of reference material. This is used throughout the project as a fast way of sighting reference material for editing and in the logbook. This was all controlled by an information directory spread sheet.

The literature codes in Table 1 are as follows;

- Lit0005 - (Kassaba, Kandila, Wardaa, & Ahmedb, 2009)
- Lit0006 - (Fan, et al., 2013)
- Lit0007 - (Tighzert, Brahimi, Kechroud, & Benabbas, 2013)
- Lit0020 - (Stenning & Martin, 1968)

Lit0005 - (Kassaba, Kandila, Wardaa, & Ahmedb, 2009)

Domain Dimensions										
submergence Depth	H	m	0.75	0.85125	1.125	1.5	1.815	2.1375	2.5125	2.8125
submergence Ratio	L/H	n/a	0.2	0.227	0.3	0.4	0.484	0.57	0.67	0.75
Riser Height	L	m	3.75							
Riser Cross-sectional Area	A	m^2	0.00188574							

Riser Diameter	D	m	0.0245							
Riser Material			Plastic							
Air Inlet holes										
height from bottom		m	0.2							
Hole Diameter		m	0.003							
Rows		n/a	7							
Columns		n/a	8							
States				Density						
Liquid			Fresh Water	1000	kg/m^3					
Gas			Air	1.225	kg/m^3					

"Table 1 – Taken from Lit0005 (Kassaba, Kandila, Wardaa, & Ahmedb, 2009) Domain Dimensions"

Results	**From Graph**						
Submergence Ratio	L/H	n/a	0.2	0.2	0.2	0.2	0.2
Water Mass Flow Rate		kg/hr	0	25	25	50	80
Water Volumetric Flow Rate		m^3/s	0	6.944E-06	6.9444E-06	1.3889E-05	2.2222E-05
Air Mass Flow Rate		kg/hr	0	2	4	6	8
Air Volumetric Flow Rate		m^3/s	0	0.0004535	0.00090703	0.00136054	0.00181406
Submergence Ratio	L/H	n/a	0.227	0.227	0.227	0.227	0.227
Water Mass Flow Rate		kg/hr	0	150	250	300	300
Water Volumetric Flow Rate		m^3/s	0	4.167E-05	6.9444E-05	8.3333E-05	8.3333E-05
Air Mass Flow Rate		kg/hr	0	2	4	6	8
Air Volumetric Flow Rate		m^3/s	0	0.0004535	0.00090703	0.00136054	0.00181406
Submergence Ratio	L/H	n/a	0.3	0.3	0.3	0.3	0.3
Water Mass Flow Rate		kg/hr	0	270	350	370	370
Water Volumetric Flow Rate		m^3/s	0	0.000075	9.7222E-05	0.00010278	0.00010278
Air Mass Flow Rate		kg/hr	0	2	4	6	8
Air Volumetric Flow Rate		m^3/s	0	0.0004535	0.00090703	0.00136054	0.00181406
Submergence Ratio	L/H	n/a	0.4	0.4	0.4	0.4	0.4
Water Mass Flow Rate		kg/hr	0	350	500	520	500
Water Volumetric Flow Rate		m^3/s	0	9.722E-05	0.00013889	0.00014444	0.00013889
Air Mass Flow Rate		kg/hr	0	2	4	6	8
Air Volumetric Flow Rate		m^3/s	0	0.0004535	0.00090703	0.00136054	0.00181406
Submergence Ratio	L/H	n/a	4.84	4.84	4.84	4.84	4.84

Water Mass Flow Rate		kg/hr	0	550	850	950	950
Water Volumetric Flow Rate		m^3/s	0	0.0001528	0.00023611	0.00026389	0.00026389
Air Mass Flow Rate		kg/hr	0	2	4	6	8
Air Volumetric Flow Rate		m^3/s	0	0.0004535	0.00090703	0.00136054	0.00181406
Submergence Ratio	L/H	n/a	0.57	0.57	0.57	0.57	0.57
Water Mass Flow Rate		kg/hr	0	850	1190	1250	1240
Water Volumetric Flow Rate		m^3/s	0	0.0002361	0.00033056	0.00034722	0.00034444
Air Mass Flow Rate		kg/hr	0	2	4	6	8
Air Volumetric Flow Rate		m^3/s	0	0.0004535	0.00090703	0.00136054	0.00181406
Submergence Ratio	L/H	n/a	0.67	0.67	0.67	0.67	0.67
Water Mass Flow Rate		kg/hr	0	950	1450	1480	1400
Water Volumetric Flow Rate		m^3/s	0	0.0002639	0.00040278	0.00041111	0.00038889
Air Mass Flow Rate		kg/hr	0	2	4	6	8
Air Volumetric Flow Rate		m^3/s	0	0.0004535	0.00090703	0.00136054	0.00181406
Submergence Ratio	L/H	n/a	0.75	0.75	0.75	0.75	0.75
Water Mass Flow Rate		kg/hr	0	1250	1800	1970	1960
Water Volumetric Flow Rate		m^3/s	0	0.0003472	0.0005	0.00054722	0.00054444
Air Mass Flow Rate		kg/hr	0	2	4	6	8
Air Volumetric Flow Rate		m^3/s	0	0.0004535	0.00090703	0.00136054	0.00181406

"Table 2 – Taken from Lit0005 (Kassaba, Kandila, Wardaa, & Ahmedb, 2009) Experimental Results Converted to SI Units"

Lit0006 - (Fan, et al., 2013)

Domain Dimensions						
Submergence Depth	H	m	-2.1			
Submergence Ratio	L/H	n/a	1.07420495			
Riser Height	L	m	28.3			
Riser Cross-sectional Area	A	m^2	0.50265482			
Riser Diameter	D	m	0.4			
Riser Material			Plastic			
Air Inlet holes			N1	N2	N3	N4
Height from Bottom		m	20	20	20	20
Hole Diameter		m	0.0005	0.002	0.002	0.0005
Formation		n/a	Cross	Cross	Circular	Circular
Number		n/a	384	24	24	384

States				Density		
Liquid			Fresh Water	998.5	kg/m^3	
Gas			Air	1.225	kg/m^3	

"Table 3 – Taken from Lit0006 (Fan, et al., 2013) *Domain Dimensions"*

Results										
Air inlet holes	L/H	n/a	N1	N1	N1	N1	N1	N1	N1	
Water Mass Flow Rate		m^3/hr	0	78	102	145	180	215	270	
Water Volumetric Flow Rate		m^3/s	0	2.1699E-05	2.8376E-05	4.0338E-05	5.0075E-05	5.9812E-05	7.5113E-05	
Air Mass Flow Rate		nm^3/hr	0	2	2.9	4.4	11	15	35	
Air Volumetric Flow Rate		m^3/s	0	4.5351E-31	6.576E-31	9.9773E-31	2.4943E-30	3.4014E-30	7.9365E-30	
Air inlet holes	L/H	n/a	N2	N2	N2	N2	N2	N2		
Water Mass Flow Rate		m^3/hr	0	155	220	260	290	285		
Water Volumetric Flow Rate		m^3/s	0	4.312E-05	6.1203E-05	7.2331E-05	8.0677E-05	7.9286E-05		
Air Mass Flow Rate		nm^3/hr	0	8.6	12.2	22.3	28	34		
Air Volumetric Flow Rate		m^3/s	0	1.9501E-30	2.7664E-30	5.0567E-30	6.3492E-30	7.7098E-30		
Air inlet holes	L/H	n/a	N3	N3	N3	N3	N3	N3	N3	
Water Mass Flow Rate		m^3/hr	0	88	140	180	240	245	280	
Water Volumetric Flow Rate		m^3/s	0	2.4481E-05	3.8947E-05	5.0075E-05	6.6767E-05	6.8158E-05	7.7895E-05	
Air Mass Flow Rate		nm^3/hr	0	2.8	6.5	12.2	22	28.8	33	
Air Volumetric Flow Rate		m^3/s	0	6.3492E-31	1.4739E-30	2.7664E-30	4.9887E-30	6.5306E-30	7.483E-30	
Air inlet holes	L/H	n/a	N4	N4	N4	N4	N4	N4	N4	N4
Water Mass Flow Rate		m^3/hr	0	130	90	100	140	140	190	190
Water Volumetric Flow Rate		m^3/s	0	3.6165E-05	2.5038E-05	2.782E-05	3.8947E-05	3.8947E-05	5.2857E-05	5.2857E-05
Air Mass Flow Rate		nm^3/hr	0	2.7	6	10	17	21	35	38
Air Volumetric Flow Rate		m^3/s	0	6.1224E-31	1.3605E-30	2.2676E-30	3.8549E-30	4.7619E-30	7.9365E-30	8.6168E-30

"Table 4 – Taken from Lit0006 (Wahba, et al., 2014) *Experimental Results Converted to SI Units"*

Lit0007 - (Tighzert, Brahimi, Kechroud, & Benabbas, 2013)

Domain Dimensions										
Submergence Depth	H	m	0.806	1.24	1.612	1.798	2.015	2.201	2.418	2.604
submergence Ratio	L/H	n/a	0.26	0.4	0.52	0.58	0.65	0.71	0.78	0.84
Riser Height	L	m	3.1							
Riser Cross-sectional Area	A	m^2	0.00342119							
Riser Diameter	D	m	0.033							
Riser Material										
Air Inlet holes										
Height from Bottom		m	0							
Hole Diameter		m	0.001	3.14159E-06						
Rows		n/a	8	Total area of holes						
Columns		n/a	10	0.000251327	m^2					
States				Density						
Liquid			Fresh Water	1000	kg/m^3					
Gas			Air	1.225	kg/m^3					

"Table 5 – Taken from Lit0007 (Tighzert, Brahimi, Kechroud, & Benabbas, 2013) *Domain Dimensions"*

Results	**From Graph**										
Submergence Ratio	L/H	n/a	0.26	0.26	0.26	0.26	0.26	0.26	0.26	0.26	0.26
Water Flow Rate		m/s	0	0	0	0	0.01	0.02	0.03	0.05	0.07
Water Volumetric Flow Rate		m^3/s	0	0	0	0	3.4212E-05	6.8424E-05	0.00010264	0.00017106	0.00023948
Air Flow Rate		m/s	0	0.2	0.4	0.6	0.8	1	1.2	1.4	1.6
Air Volumetric Flow Rate		m^3/s	0	5.02655E-05	0.00010053	0.0001508	0.00020106	0.00025133	0.00030159	0.00035186	0.00040212
Submergence Ratio	L/H	n/a	0.4	0.4	0.4	0.4	0.4	0.4	0.4	0.4	0.4
Water Flow Rate		m/s	0	0	0.02	0.06	0.1	0.15	0.19	0.23	0.24
Water Volumetric Flow Rate		m^3/s	0	0	6.8424E-05	0.00020527	0.00034212	0.00051318	0.00065003	0.00078687	0.00082109
Air Flow Rate		m/s	0	0.2	0.4	0.6	0.8	1	1.2	1.4	1.6
Air Volumetric Flow Rate		m^3/s	0	5.02655E-05	0.00010053	0.0001508	0.00020106	0.00025133	0.00030159	0.00035186	0.00040212
Submergence Ratio	L/H	n/a	0.52	0.52	0.52	0.52	0.52	0.52	0.52	0.52	0.52
Water Flow Rate		m/s	0	0	0.12	0.26	0.32	0.36	0.39	0.42	0.43
Water Volumetric Flow Rate		m^3/s	0	0	0.00041054	0.00088951	0.00109478	0.00123163	0.00133427	0.0014369	0.00147111
Air Flow Rate		m/s	0	0.2	0.4	0.6	0.8	1	1.2	1.4	1.6
Air Volumetric Flow Rate		m^3/s	0	5.02655E-05	0.00010053	0.0001508	0.00020106	0.00025133	0.00030159	0.00035186	0.00040212
Submergence Ratio	L/H	n/a	0.58	0.58	0.58	0.58	0.58	0.58	0.58	0.58	0.58

Water Flow Rate		m/s	0	0	0.22	0.34	0.4	0.48	0.5	0.53	0.54
Water Volumetric Flow Rate		m^3/s	0	0	0.00075266	0.00116321	0.00136848	0.00164217	0.0017106	0.00181323	0.00184744
Air Flow Rate		m/s	0	0.2	0.4	0.6	0.8	1	1.2	1.4	1.6
Air Volumetric Flow Rate		m^3/s	0	5.02655E-05	0.00010053	0.0001508	0.00020106	0.00025133	0.00030159	0.00035186	0.00040212
Submergence Ratio	L/H	n/a	0.65	0.65	0.65	0.65	0.65	0.65	0.65	0.65	0.65
Water Flow Rate		m/s	0	0.04	0.3	0.42	0.5	0.56	0.57	0.6	0.64
Water Volumetric Flow Rate		m^3/s	0	0.000136848	0.00102636	0.0014369	0.0017106	0.00191587	0.00195008	0.00205272	0.00218956
Air Flow Rate		m/s	0	0.2	0.4	0.6	0.8	1	1.2	1.4	1.6
Air Volumetric Flow Rate		m^3/s	0	5.02655E-05	0.00010053	0.0001508	0.00020106	0.00025133	0.00030159	0.00035186	0.00040212
Submergence Ratio	L/H	n/a	0.71	0.71	0.71	0.71	0.71	0.71	0.71	0.71	0.71
Water Flow Rate		m/s	0	0.05	0.38	0.53	0.65	0.7	0.71	0.72	0.73
Water Volumetric Flow Rate		m^3/s	0	0.00017106	0.00130005	0.00181323	0.00222378	0.00239484	0.00242905	0.00246326	0.00249747
Air Flow Rate		m/s	0	0.2	0.4	0.6	0.8	1	1.2	1.4	1.6
Air Volumetric Flow Rate		m^3/s	0	5.02655E-05	0.00010053	0.0001508	0.00020106	0.00025133	0.00030159	0.00035186	0.00040212
Submergence Ratio	L/H	n/a	0.78	0.78	0.78	0.78	0.78	0.78	0.78	0.78	0.78
Water Flow Rate		m/s	0	0.18	0.5	0.67	0.72	0.76	0.81	0.82	0.82
Water Volumetric Flow Rate		m^3/s	0	0.000615815	0.0017106	0.0022922	0.00246326	0.00260011	0.00277117	0.00280538	0.00280538
Air Flow Rate		m/s	0	0.2	0.4	0.6	0.8	1	1.2	1.4	1.6

Air Volumetric Flow Rate		m^3/s	0	5.02655E-05	0.00010053	0.0001508	0.00020106	0.00025133	0.00030159	0.00035186	0.00040212
Submergence Ratio	L/H	n/a	0.84	0.84	0.84	0.84	0.84	0.84	0.84	0.84	0.84
Water Flow Rate		m/s	0	0.22	0.6	0.72	0.79	0.83	0.87	0.9	0.92
Water Volumetric Flow Rate		m^3/s	0	0.000752663	0.00205272	0.00246326	0.00270274	0.00283959	0.00297644	0.00307907	0.0031475
Air Flow Rate		m/s	0	0.2	0.4	0.6	0.8	1	1.2	1.4	1.6
Air Volumetric Flow Rate		m^3/s	0	5.02655E-05	0.00010053	0.0001508	0.00020106	0.00025133	0.00030159	0.00035186	0.00040212

"Table 6 – Taken from Lit0007 (Tighzert, Brahimi, Kechroud, & Benabbas, 2013) *Experimental Results Converted to SI Units"*

Lit0020 - (Stenning & Martin, 1968)

Domain Dimensions						
Submergence Depth	H	m	0.05732596	0.06899866	0.08157925	0.09169559
Submergence Ratio	L/H	n/a	0.442	0.532	0.629	0.707
Riser Height	L	m	4.116			
Riser Cross-Sectional Area	A	m^2	0.00188574			
Riser Diameter	D	m	0.0245			
Riser Material						
Air Inlet holes						
Height from bottom		m	0.03675			
Hole Diameter		m	0.00229688	2.296875		
Holes		n/a	56			
cfs to m^3/s		n/a	0.02831685			
States				Density		
Liquid			Fresh Water	1000	kg/m^3	
Gas			Air	1.225	kg/m^3	

"Table 7 – Taken from Lit0020 (Stenning & Martin, 1968) *Domain Dimensions"*

Results	From Graph						
Submergence Ratio	L/H	n/a	0.442	0.442	0.442	0.442	0.442
Water Mass Flow Rate		cfs (cubic feet per second)	0	0.006	0.0082	0.008	0.0078
Water Volumetric Flow Rate		m^3/s	0	0.0001699	0.0002322	0.00022653	0.00022087
Air Mass Flow Rate		cfs (cubic feet per second	0	0.025	0.05	0.075	0.1
Air Volumetric Flow Rate		m^3/s	0	0.00070792	0.00141584	0.00212376	0.00283168
Slip Ratio		n/a					
For 1 /8th							
Submergence Pressure	L/H*H*ρ*g	Pa	1.819272	17847.0583	17847.0583	17847.0583	17847.0583
Water Volumetric Flow Rate	X/8	m^3/s	0	2.1238E-05	2.9025E-05	2.8317E-05	2.7609E-05
Air Mass Flow Rate	(AV*ρ) / 8	kg/s	0	0.0001084	0.0002168	0.0003252	0.0004336
Submergence Ratio	L/H	n/a	0.532	0.532	0.532	0.532	0.532
Water Mass Flow Rate		cfs (cubic feet per second	0	0.009	0.011	0.0109	0.0105
Water Volumetric Flow Rate		m^3/s	0	0.00025485	0.00031149	0.00030865	0.00029733
Air Mass		cfs (cubic	0	0.025	0.05	0.075	0.1

Flow Rate		feet per second					
Air Volumetric Flow Rate		m^3/s	0	0.00070792	0.00141584	0.00212376	0.00283168
Slip Ratio							
For 1 /8th							
Submergence Pressure	L/H*H*ρ*g	Pa	21481.0747	21481.0747	21481.0747	21481.0747	21481.0747
Water Volumetric Flow Rate	X/8	m^3/s	0	3.1856E-05	3.8936E-05	3.8582E-05	3.7166E-05
Air Mass Flow Rate	(AV*ρ) / 8	kg/s	0	0.0001084	0.0002168	0.0003252	0.0004336
Submergence Ratio	L/H	n/a	0.629	0.629	0.629	0.629	0.629
Water Mass Flow Rate		cfs (cubic feet per second	0	0.0137	0.0158	0.0154	0.014
Water Volumetric Flow Rate		m^3/s	0	0.00038794	0.00044741	0.00043608	0.00039644
Air Mass Flow Rate		cfs (cubic feet per second	0	0.025	0.05	0.075	0.1
Air Volumetric Flow Rate		m^3/s	0	0.00070792	0.00141584	0.00212376	0.00283168
Slip Ratio							
For 1 /8th							
Submergence Pressure	L/H*H*ρ*g	Pa	25397.7368	25397.7368	25397.7368	25397.7368	25397.7368
Water Volumetric Flow Rate	X/8	m^3/s	0	4.8493E-05	5.5926E-05	5.451E-05	4.9554E-05
Air Mass Flow Rate	(AV*ρ) / 8	kg/s	0	0.0001084	0.0002168	0.0003252	0.0004336
Submergence Ratio	L/H	n/a	0.707	0.707	0.707	0.707	0.707
Water Mass Flow Rate		cfs (cubic feet per second	0	0.017	0.0185	0.0176	0.0168
Water Volumetric Flow Rate		m^3/s	0	0.00048139	0.00052386	0.00049838	0.00047572
Air Mass Flow Rate		cfs (cubic feet per second	0	0.025	0.05	0.075	0.1
Air Volumetric Flow Rate		m^3/s	0	0.00070792	0.00141584	0.00212376	0.00283168
Slip Ratio							
For 1 /8th							
Submergence Pressure	L/H*H*ρ*g	Pa	28547.2177	28547.2177	28547.2177	28547.2177	28547.2177
Water Volumetric Flow Rate	X/8	m^3/s	0	6.0173E-05	6.5483E-05	6.2297E-05	5.9465E-05
Air Mass Flow Rate	(AV*ρ) / 8	kg/s	0	0.0001084	0.0002168	0.0003252	0.0004336

"Table 8 – Taken from Lit0020 (Stenning & Martin, 1968) *Experimental Results Converted to SI Units"*

Appendix F

Table 8 also shows the calculations made for the 1/8th CFD domains, geometry for these are shown in Appendix B.

Conclusion

While all of the data collected may not have been used in the final report, as models could not be completed, the data which has been collected shows that it would be posable to validate models with experimental data from previous papers. The quality of this data also shows that the collection methodology can be trusted.

Bibliography

Fan, W., Chen, J., Pan, Y., Huang, H., Chen-Tung, Chen, A., et al. (2013). Experimental study on the performance of an air-lift pump for artificial upwelling. *Ocean Engineering, 59*, 47–57.

Kassaba, S. Z., Kandila, H. A., Wardaa, H. A., & Ahmedb, W. H. (2009, 02). Air-lift pumps characteristics under two-phase flow conditions. *International Journal of Heat and Fluid Flow, 30*(1), 88–98.

Stenning, A. H., & Martin, C. B. (1968). An Analytical and Experimental Study of Air-Lift Pumpo Performance. *A Journal of Engineering for Power*, 106 - 110.

Tighzert, H., Brahimi, M., Kechroud, N., & Benabbas, F. (2013, 10). Effect of submergence ratio on the liquid phase velocity, efficiency and void fraction in an air-lift pump. *Journal of Petroleum Science and Engineering, 110*(1), 155–161.

Domain Geometry See Drawing For Dimensions	A	B	C	D	E	F	G	H	I
Litrature	LIT0020	LIT0020	LIT0020	LIT0020	LIT0020	LIT0020	LIT0020	LIT0020	LIT0020
Size	1/8	1/8	1/8	1/8	1/8	1/8	1/8	1/8	1/8
Rev	B	B	C	C	C	C	C	C	C
Notes									
Notes On Run	ICEM Mesh	ICEM Mesh	Set Up For Fluent	Fluent	ANSYS CFX	Presure Test	ANSYS CFX Flow	ANSYS CFX Flow	ANSYS CFX Flow
Mesh									
Number of mesh elements	-	-	2418589	2418589	2528944	2662420	2662420	2662420	2662420
Max Element Size	-	-	10mm	10mm	10mm	10mm	10mm	10mm	10mm
Note: Controlled using the 'Max Element Size' and 'Max Face Size' controls on the master meshing panel									
Global growth rate		-	1.2	1.2	1.2	1.2	1.2	1.2	1.2
Note: Global growth rate controlled on the master									
Curvature Normal Angle	-	-	18 degrees	18 degrees	18 degrees	18 degrees	18 degrees	18 degrees	18 degrees
Inflation Type	-	-	Smooth Transition	Smooth Transition	Smooth Transition	Smooth Transition	Smooth Transition	Smooth Transition	Smooth Transition
Transition Ratio	-	-	0.77	0.77	0.77	0.77	0.77	0.77	0.77
Growth Rate	-	-	1.2	1.2	1.2	1.2	1.2	1.2	1.2
Turbulence Modelling and Convergence Control									
Turbulence model	-	-	-	-	SST	SST	SST	SST	SST
Interphase Transfere	-	-	-	-	Mixture Model	Mixture Model	Mixture Model	Mixture Model	Mixture Model
Convergence criteria	-	-	-	-	1.00E-04	1.00E-04	1.00E-04	1.00E-04	1.00E-04
Drag Coefficent	-	-	-	-	2.00E-01	2.00E-01	2.00E-01	2.00E-01	2.00E-01
Timescale Control	-	-	-	-	Auto Timescale	Auto Timescale	Auto Timescale	Auto Timescale	Auto Timescale
Setup & Boundary Conditions									
Steady State or Transient	-	-	-	-	Steady State	Steady State	Steady State	Steady State	Steady State
Max Air Flow Rate (kg/s)	-	-	-	-	Wall	Wall	1.08E-04	1.08E-04	1.08E-04
Air Flow Rate Increase (kg/s^2)	-	-	-	-	-	-	-	-	-
Air Modled as	-	-	-	-	Air at 25 C	Air at 25 C	Air at 25 C	Air at 25 C	Air at 25 C
Submergence Ratio	-	-	-	-	-	0.44	0.44	0.44	0.44
Max Iterations	-	-	-	-	1.00E+02	1.00E+02	1.00E+02	1.00E+02	5.00E+01
Loop Iterations (Transient Only)	-	-	-	-	-	-	-	-	-
Total Time (Transient Only)	-	-	-	-	-	-	-	-	-
Time Step (Transient Only)	-	-	-	-	-	-	-	-	-
Initial Conditions From (Transient Only)	-	-	-	-	-	-	-	-	-
Solver Manager Controls									
Parallel Processing	-	-	-	-	-	Yes	-	-	Yes
No of Partitions	-	-	-	-	-	4	-	-	4
Double Precision	-	-	-	-	-	No	-	-	No
Boundary layer resolution									
Maximum Y^+	N/A	N/A	N/A	N/A	N/A	N/A	N/A	N/A	N/A
Minimum Y^+	N/A	N/A	N/A	N/A	N/A	N/A	N/A	N/A	N/A
Average Y^+	N/A	N/A	N/A	N/A	N/A	N/A	N/A	N/A	N/A
Simulated Results									
Was It Run?	Not Run	Not Run	Not Run	Not Run	Not Run	Run	Not Run	Not Run	Run
Error Code (If Crashed)	-	-	-	-	-	-	-	-	-

J	K	L	M	N	O	P	Q	R
UT0020 1/8	UT0020 1/8	UT0020 1/8	UT0020 1/8	UT0020 1/8	UT0020 1/8	UT0020 1/8	UT0020 1/8	UT0020 1/8
C	C	C	C	C	C	C	D	D
Transient	Transient	Transient	Transient	ANSYS CFX Flow	Transient	Transient	Transient	Transient
2662420	2662420	2662420	2662420	2662420	2662420	792748	781724	781724
10mm	10mm	10mm	10mm	10mm	10mm	10mm	10mm	10mm
1.2	1.2	1.2	1.2	1.2	1.2	1.2	1.2	1.2
18 degrees	18 degrees	18degree$	18 degrees	18 degrees	18 degrees	18 degrees	18 degrees	18 degrees
Smooth Transition	Smooth Transition	Smooth Transition	Smooth Transition	Smooth Transition	Smooth Transition	Smooth Transition	Smooth Transition	Smooth Transition
0.77	0.77	0.77		0.77	0.77	0.77		0.77
SST	SST	SST	SST	SST	SST	SST	SST	SST
Mixture Model	Mixture Model	Mixture Model	Mixture Model	Mixture Model	Mixture Model	Mixture Model	Mixture Model	Mixture Model
1.00EQ 2.00E01	1.00EQ 2.00E01	1.00EQ 2.00E01	1.00EQ 2.00E01	1.00EQ 2.00E01	1.00EQ 2.00E01	1.00EQ 2.00E01	1.00EQ4 2.00E01	1.00EQ 2.00E01
Transient	Transient	Transient		Steady State	Transient	Transient	Transient	Transient
1.08EQ4	1.08EQ4	1.08EQ4		1.08EQ4	1.08EQ4	1.08EQ4	1.08EQ4	1.08EQ4
								1.81E06
Air at 2SC	Air at 2SC	Air at 2SC	Air at 2SC	Air at 2SC	Air at 2SC	Air Ideal Gas	Air Ideal Gas	Air Ideal Gas
0.44	0.44	0.44		0.44	0.44	0.44	0.44	0.44
				S.00E+01				
1.00E+01	2.00E+01	2.00E+01			2.00E+01	1.00E+01	1.00E+01	1.00E+01
60;	60;	60;			60;	3O ;	3O ;	3O ;
0.Ss	0.Ols	0.Ols			0.Ols	0.0000Ss	0.0000Ss	0.0000Ss
Run I	Run I	Run I			Run N	Initial Conditions	Initial Conditions	Initial Conditions
Yes	Yes	Yes		Yes	Yes	Yes	Yes	Yes
4	4	4		4	4	4	4	4
No	No	No		No	No	No	No	No
N/A	N/A	N/A	N/A	N/A	N/A	N/A	N/A	N/A
N/A	N/A	N/A	N/A	N/A	N/A	N/A	N/A	N/A
Crashed	Paused	Crashed	Not Run	Run	Crashed	Paused	Paused	Paused
Unstable Maths		Unstable Maths			Unstable Maths	Air Leaving through bottom af Riser	Air Leaving through bottom of Riser	Too Complex to Complete

Mathematical Modelling Manual

This document is split into two sections construction of the model and operation of the model.

Table of Contents

Construction of the Model

To find the best model for Fugro's requirements the following steps were taken:

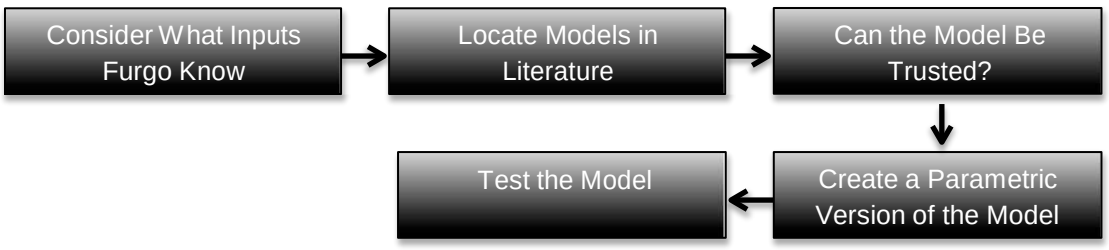

These are addressed by the titles in this section.

Consider What Inputs Fugro Know

This is important as the model chosen must be capable of making predictions using only known data. This is found using information first located during section 3.1 of the interim report (Appendix A). When designing two-phase Airlift pump, the unknown value is normally the water or air flow rate. The dimensions such as submergence ratio, riser diameter and riser height can be found using information such as Reeds' Nautical Almanac (Towle & Fishwick, 2015), navigational charts, hole depth and the dimensions of riser that the drill will allow. This is also shown the Figure 1 a plan of Fugro's Jersey project from (Hackwell, 2015).

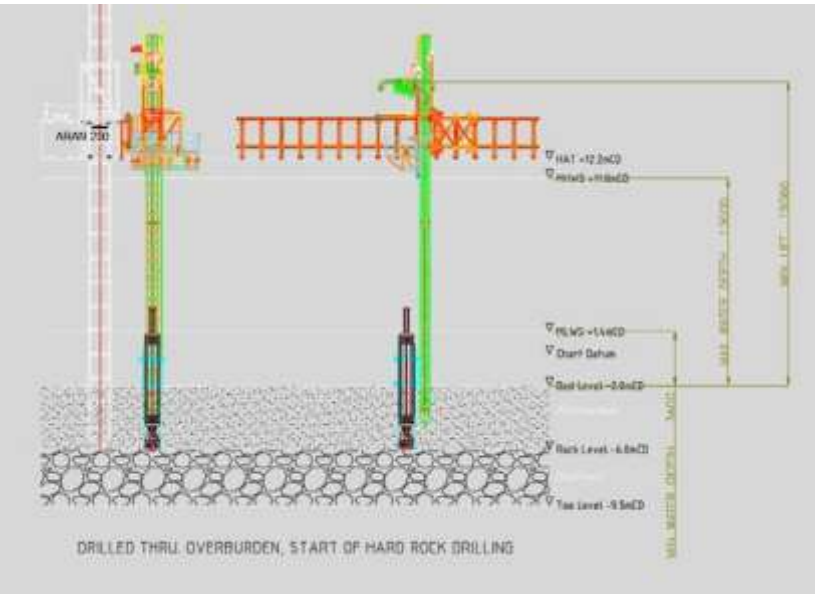

"Figure 1 – A Diagram of Fugro's Jersey Project Setup from (Hackwell, 2015)"

From this information it can be deduced that any model should only require the following inputs:

- Riser Height
- Submergence Ratio
- Riser Diameter
- Riser Roughness – Found from material of riser
- Liquid Density
- Liquid Dynamic Viscosity
- Liquid Flow Rate

This list forms a rough specification as to the inputs and required outputs of the model.

Locate the Model in Literature

This work was completed during section 2 of Appendix A. A number of prediction models are listed by (Wahba et al., 2014). Prediction methods for smaller diameter risers were considered by (Reinemann et al., 1990). (Yoshinaga & Sato, 1996) And (Mahrous, 2012) Produce far more complex three-phase models. With (Mahrous, 2012) also investigating the findings of many other papers.

The chosen model is that of (Stenning & Martin, 1968). This is further investigated by (Kassaba et al., 2009) who validates (Stenning & Martin, 1968) and then explain

how to use it to make predictions on Airlift pumps. (Wahba et al., 2014) Also mentions this model.

Can the Model Be Trusted?

As both (Stenning & Martin, 1968) and (Kassaba et al., 2009) appear in scientific papers, it is felt that the models can be trusted and will provide accurate predictions if used properly.

This model does not account for the expansion of air over the riser height. Pressure change as the water depth is reduced causes this. For this reason (Stenning & Martin, 1968) states that their equation is only accurate for airlift pumps in shallow water. This is could be adapted to account for greater depth by splitting the riser into small lengths over which the pressure change is small enough for the bubbles size not to change (Stenning & Martin, 1968).

Selection of this distance could be made using the ideal gas law; Eq. 1 (Laugier & Garai, 2007):

$$PPPP = mmm\text{}mm - [EEE\text{}1\ FFF\text{}FFmm$$

(Laugier & Garai, 2007)

Where pressure is calculated using the Eq. 2 from:

$$PP = \rho\rho\rho\rho\rho\rho\rho\rho\text{}FF \times gg \times HH - [\ EEE\text{}2$$

$$FFF\text{}FFmm \text{ (Kinsky, 1982)}$$

This shallow water estimate is very important because as the bubble size increases the overall density of the riser decreases. The bubble fraction increasing increases the velocity of water and therefore the Reynolds number stated by (Huppert & Hallworth, 2007) to determine the flow type. This is supported by bubble size being controlled by lateral forces (Frank et al., 2005). Figure 1 from (Kim et al., 2014) also shows that fraction volume between the two phases affects the flow type. This will also increase as the bubble expands within the riser.

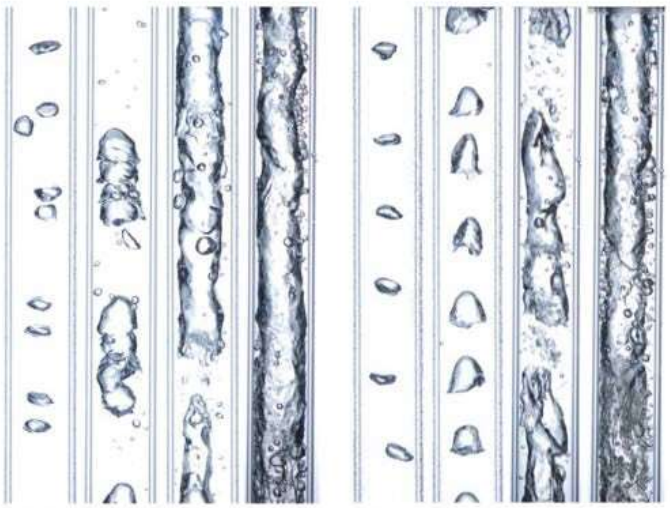

left (α= 0.8) right (α= 1.0)

"Figure 1 - Photographs of bubble pattern in Airlift pump with the tube diameter of 18 mm for several gas flow rates, of (a) 0.0234, (b) 0.234, (c) 1.403, and (d) 3.12 (left: α = 0.8, right: α = 1.0). Taken from (Kim et al., 2014)*"*

Create a Parametric Version of the Model

The following steps for using the (Stenning & Martin, 1968) model are taken from (Kassaba et al., 2009).

Step 1:

The geometrical parameters of L – riser height, D – riser diameter, ε - pipe roughness, *ρ* - water density and μ - viscosity, are known. Then the air or water mass flow rate may be found providing the other is known (Kassaba et al., 2009). For Fugro's application it is lightly that the flow rate of water to lift the particles will be known. This allows the gas flow rate required to achieve this to be predicted.

Step 2:

Select a static head H for a certain submergence ratio, this accounts for pressure at the water inlet.

$$PP = \rho\rho\rho\rho\rho\rho\rho\rho FF \times gg \times HH - [\,EEE 2\ FFF FFmm\ (\text{Kinsky}, 1982)]$$

Step 3:

Assume a value of water or air mass flow rate depending on which was not input at the start.

Step 4:

Compute the friction coefficient (f) from Colebrook Eq. 3, also calculate the slip ratio "*s*" (between 1.5 and 2.5 (Stenning & Martin, 1968)) this is found more accurately in Eq. 4.

$$\frac{1}{\sqrt{f}} = -2\log\left(\frac{\varepsilon\varepsilon}{3.71\times D} + \frac{2.51}{RRR\sqrt{f}}\right) \quad [\,EEE 3\ FFF FFmm\ (\text{Brkic}, 2011)]$$

$$s = 1.2 + \left(0.2 \times \frac{Q Q}{Q Q}\right) + \frac{0.35\times A \times (Q \times D)}{Q Q} - [\,EEE 4\ FFF FFmm\ (\text{Kassaba et al.}, 2009)]$$

Step 5:

Calculate the value of the left hand side and the right hand side of Eq. 5.

$$\frac{HH}{LL} \frac{1}{1+\frac{}{QQQ}} = \frac{}{\frac{Q Q^2}{2\times QQ\times L \times A^2}\left[\frac{4\times f}{DD}\frac{\times LL}{} + 1 + \left(\frac{4\times f}{DD}\frac{\times LL}{} + 2\right) \times \frac{Q Q}{Q Q}\right]}$$

[EEE 5 FFF $FFmm$ (Kassaba et al., 2009)]

Step 6:

Repeat steps 3–5 until the total difference between the left hand side and the right hand side of Eq. 5 becomes less than 0.001 (Kassaba et al., 2009).

Implementing the Formulae

The formulae above is placed into an excel spread sheet. This is made to be fully parametric bar the two goal seek cells shown in red in Figure 2. The cells are programmed to implement the formula from step 1 to 6.

Inputs				
Name	Symbol	Formula	Value	Units
Riser Hight	L	n/a	4.116	m
Riser Diameter	D	na	0.0245	m
Pipe Roughness	ε	n/a	0.002	m^3
Gravitational Constant	g	n/a	9.81	m s^-2
Liquid Density	ρwater	n/a	1000	kg m^-3
Dynamic Viscosity of Liquid	μ	n/a	1.002	kg m s^-1
Submregence Ratio	H/L	n/a	0.442	n/a
Water Depth	H	H/L*L	1.819272	m
Water Mass Flow Rate	Qml	Qvl/ρwater	n/a	kg s^-1
Water Volumetric Flow Rate	Ql	Vl*A or Qvl/ρwater	0.000272	m^3 s^-1
Water Velocity at water inlet (No Air in Column)	Vl	n/a	0.577802	m/s
Value to Goal Seek				
Coefficent of Friction	f	Estimate then Goal Seek	0.65579	n/a
Gas Volume Flow Rate	Qg	Estimate then Goal Seek	0.00017	kg s^-1
Outputs				
Riser Cross-Sectional Area	A	π*((D/2)^2	0.000471	m^2
Static Head	P	ρwater*g*H	17847.06	N m^-2
Slip Ratio	s	1.2+(0.2*(Qg/Ql))+((0.35*A*((g*D)^0.5)))/Ql))	1.621784	n/a
LHS Friction Coefficent	LHS (f)	1/(f^0.5)	1.23486	n/a
Reynolds Number of Water	Re	(ρwater*Vl*D)/μ	14.12789	n/a
RHS Friction Coefficent	RHS (f)	*-2*(log10((ε/(3.71*D))+(2.51/(Re*(f^0.5)))))	1.234554	n/a
Line For Goal Seek	Finding f	LHS (f) - RHS (f) must be zero	0.000306	n/a
LHS (Final Equation)	LHS (FE)	(H/L)-(1/(1+(Qg/(s*Ql))))	1.097155	n/a
RHS (Final Equation)	RHS (FE)	((Ql^2)/(2*g*L*(A^2)))*((((4*f*L)/D)+1)+((((4*f*L)/D)+2)*(Qg/Ql	2.968176	n/a
Line For Goal Seek	Finding Qg	LHS (FE) - RHS (FE) must be zero	-1.87102	n/a

Figure 2 – Image of Mathematical Modelling Spread Sheet

In Figure 2 the model, shown in Appendix D, has been populated with data from an experiment run by (Stenning & Martin, 1968) to which an accuracy of 2% was attached. The populated data is shown in the inputs column. These are all inputs, which will be available to Fugro when trying to predict airlift pump performance assuming that the velocity of liquid could be determined as the minimum velocity required to lift cuttings into the pump.

This was not required when populating Figure 2 with data from (Stenning & Martin, 1968) as the volumetric flow rate is given. After completing both Goal Seek tasks the gas flow rate is similar to that found by (Stenning & Martin, 1968). This shows that the model has been implemented correctly in the formulae.

Operation of the Model

Operation of the model is relatively simple. This requires populating the input values and conducting two goal seek operations to find the friction coefficient and gas volume flow rate. The friction coefficient must be found first as location of Qg relies on this. Further automation of this process has not been conducted because of the limits of the model and improvements, which are needed.

Limits of the Model

The main limitation of the model is its inability to predict anything but shallow airlift pumps (Stenning & Martin, 1968). This is as the model neglects to account for the expansion of the gas phase as pressure is reduced. This has been discussed in the 'can the model be trusted section'. This is shown graphically in Figure 3 taken from the logbook.

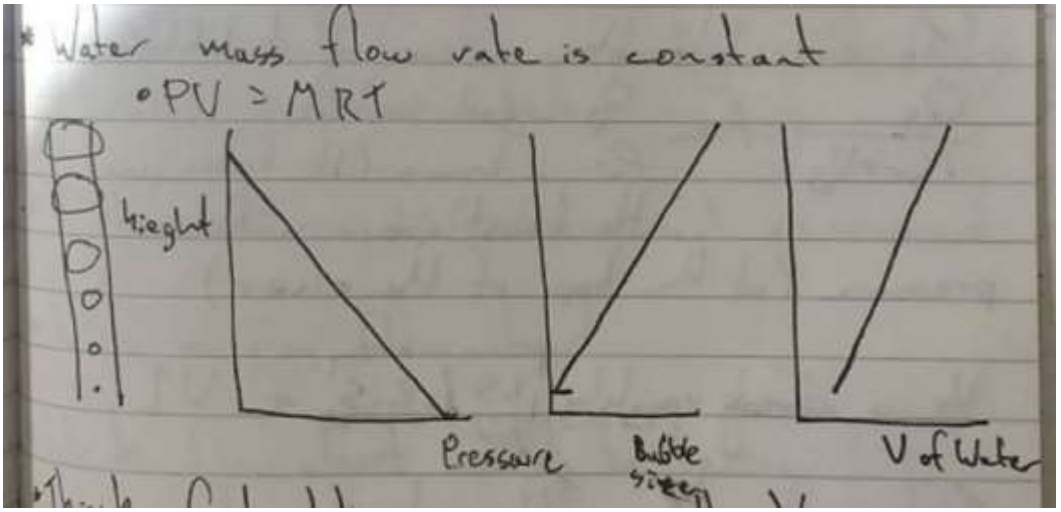

Figure 3 – Why Bubble Size Changes Over The Riser and What This Means

Another obvious flaw is that the model only accounts for two-phase flow however this could be accounted for by adding a coefficient to the model and determining the minimum water speed required at the water inlet to suck cuttings in.

The model is also unable to determine the type of flows possible listed by (Tighzert et al., 2013). The flow type defines a limiting factor of three-phase Airlift. This affects the liquid flow rate, which must be sufficient to carry drill cuttings.

Improvements to the Model

The problems with the (Stenning & Martin, 1968) can be addressed in a number of ways. (Stenning & Martin, 1968) Suggests that the model can be used to predict deeper Airlift scenarios by dividing the riser into short vertical sections. Over these sections the constant pressure and therefore bubble size can be assumed. The height of each riser section could be determined by considering Eq. 1.

The most accurate way of creating a fully reliable model for Fugro to use is by adapting the equation by adding coefficients and correction factors. This would be achieved using data from previous Airlift projects, which the company has conducted. This negates the need for large and expensive testing as the data is collected over real projects, which are already financed. This data is then used in modelling in a similar manor to the Holtrop resistance model.

Holtrop is a resistance prediction method used in the initial stages of ship design (Holtrop & Mennen, 1982). This was created from random and experimental data (Holtrop & Mennen, 1982), which could be provided from results of Fugro's previous

work. This would strengthen the model by making predictions based on regression analysis of trusted data.

Basing this method entirely on the Holtrop model would require too many tests to be performed. But incorporating the Stenning and Martin equation (Eq. 5) prediction on the effects of key dimensions can be made. This will mean less data is needed allowing a complete useable model to be implemented faster.

Further tests on the reliability of this model across a range of Airlift pumps of different dimensions can be made by inputting the data from other experimental papers such as (Fan et al., 2013), (Tighzert et al., 2013) and (Kassaba et al., 2009). Information from which this can be done is available in Appendix F.

Bibliography

Brkic, D., 2011. New explicit correlations for turbulent flow friction factor. *Nuclear Engineering and Design*, p.4055–4059.

Fan, W. et al., 2013. Experimental study on the performance of an air-lift pump for artificial upwelling. *Ocean Engineering*, 59, p.47–57.

Hackwell, 2015 Private Communications with Fugro GeoSevices, Project Design Engineer.

Holtrop, J. & Mennen, G., 1982. An Approximate Power Prediction Method. *Int. Shipbuild Progress*, 29, pp.166-71.

Huppert, H. & Hallworth, 2007. Bi-directional flows in constrained systems. *J. Fluid Mech.*, 578, pp.95-112.

Kassaba, S.Z., Kandila, H.A., Wardaa, H.A. & Ahmedb, W.H., 2009. Air-lift pumps characteristics under two-phase flow conditions. *International Journal of Heat and Fluid Flow*, 30(1), p.88–98.

Kim, S.-H., Sohn, C.-H. & Hwang, J.-Y., 2014. Effects of tube diameter and submergence ratio on bubble pattern and performance of air-lift pump. *International Journal of Multiphase Flow*, p.195–204.

Kinsky, R., 1982. *Applied Fluid Dynamics*. 1st ed. Sydney: McGraw-Hill Book Company.

Laugier, A., & Garai, J. (2007, 11). Derivation of the Ideal Gas Law. *Journal of Chamical Education, 84*(11), 1832-1833.

Mahrous, A.F., 2012. Numerical Study of Solid Particles-Based Airlift Pump Performance. *WSEAS Transactions on Applied and Theoretical Mechanics*, 7(3).

Reinemann, D.J., Parlange, J.Y. & Timmons, B.M., 1990. Theory of Small-Diameter Airlift Pumps. *International Journal for Multiphase Flow*, 16, pp.113-22.

Stenning, A.H. & Martin, C.B., 1968. An Analytical and Experimental Study of Air-Lift Pumpo Performance. *A Journal of Engineering for Power*, pp.106 - 110.

Tighzert, H., Brahimi, M., Kechroud, N. & Benabbas, F., 2013. Effect of submergence ratio on the liquid phase velocity, efficiency and void fraction in an air-lift pump. *Journal of Petroleum Science and Engineering*, 110(1), p.155–161.

Wahba, E.M. et al., 2014. On the Performance of Air-Lift Pumps: From Analytical Models to Large Eddy Simulation. *Journal of Fluids Engineering*, pp.on-line.

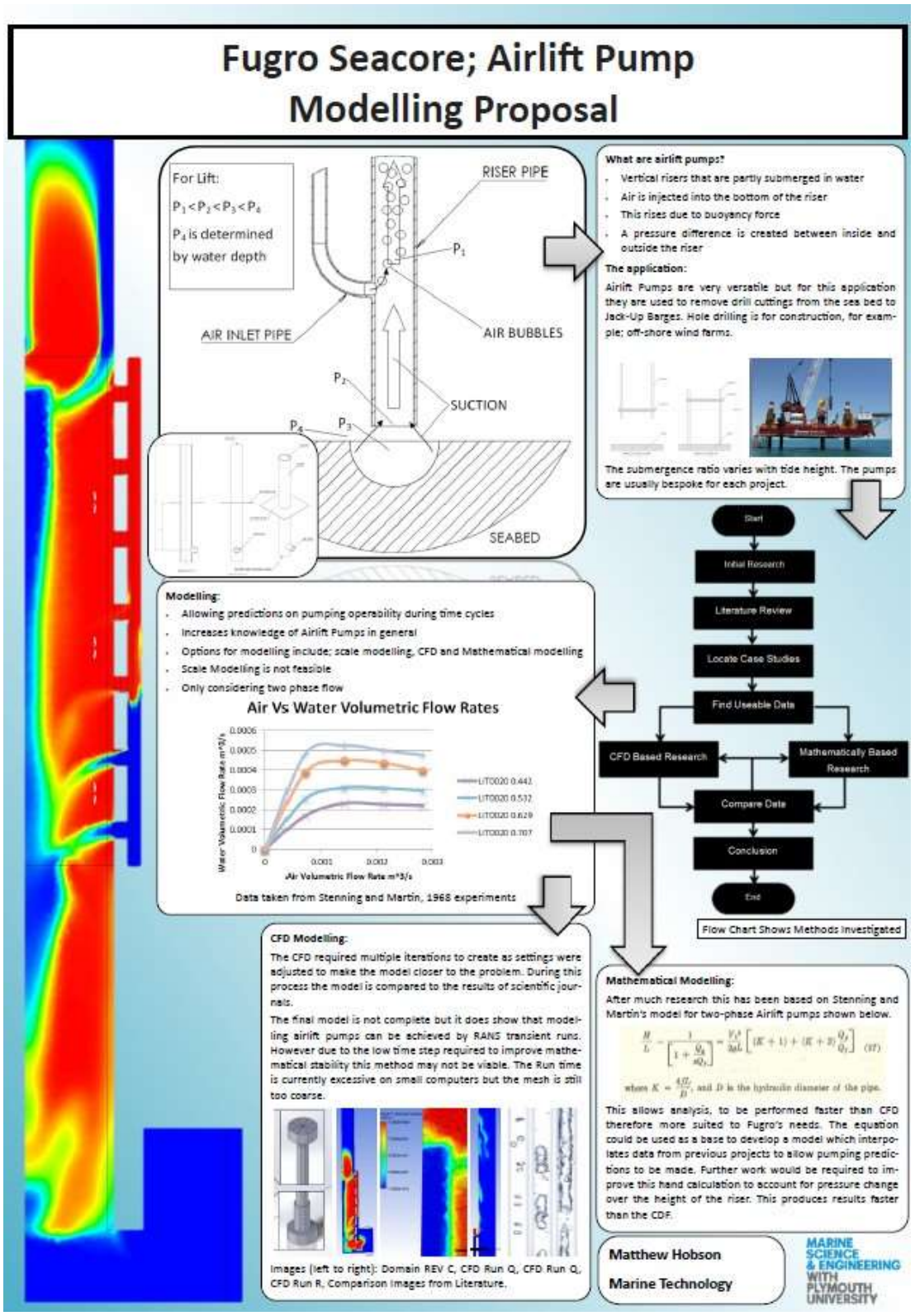

Figure 1 – The Project Poster (originally printed in A1)

Water Levels over Tide Cycles

This document proved that it will be easy for Fugro to predict tide cycles as locations of work. This is crucial for Airlift pumping prediction as it causes the submergence ratio of the Air lift pump to change.

The relationship of water depth to tide height can be generally given by the 12ths rule whereby during the six hours between high a low tide, the tides height will decrease by 1/12 during the first hour; 2/12 in the second hour, 3/12 in the third hour, 3/12 in the fourth hour, 2/12 in the fifth hour and 1/12 in the sixth hour (Towle & Fishwick, 2015). This information is plotted for a 24 hour time cycle in Graph 1, which uses information of high and low water heights taken from Figure 1. The 12ths rule is appropriate for Jersey harbour however it may require adjustment if working in large estuaries or areas such as the Isle of Wight where different models should be adopted due to the shape of the coastline (Towle & Fishwick, 2015). The twelfths rule is the most efficient way of estimating tide heights at different times over a tide cycle and is understood by any mariner, therefore it is the chosen method of estimating for the level of accuracy needed when predicting Airlift operability which is only required to the nearest hour.

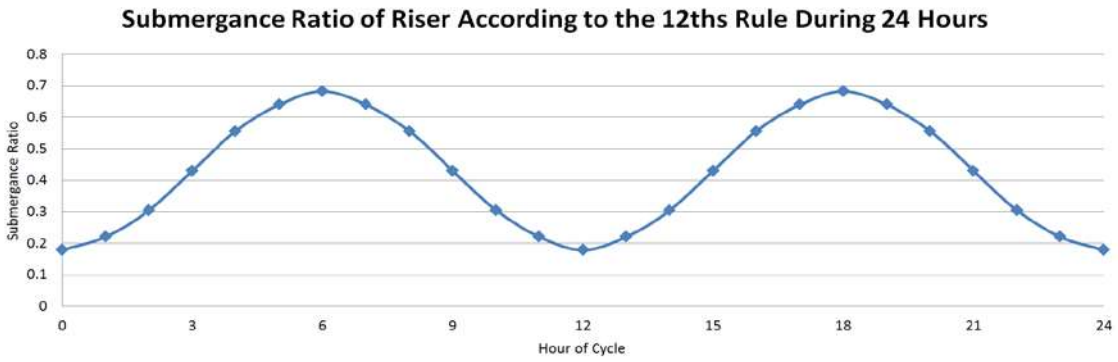

Graph 1; Submergence Ratio Vs Tide Heights calculated using data from (Hackwell, 2015) and (Towle & Fishwick, 2015).

The information given by (Towle & Fishwick, 2015) show that the submergence ratio will be known during the planning stage of any project. This means that it is a known input for any model.

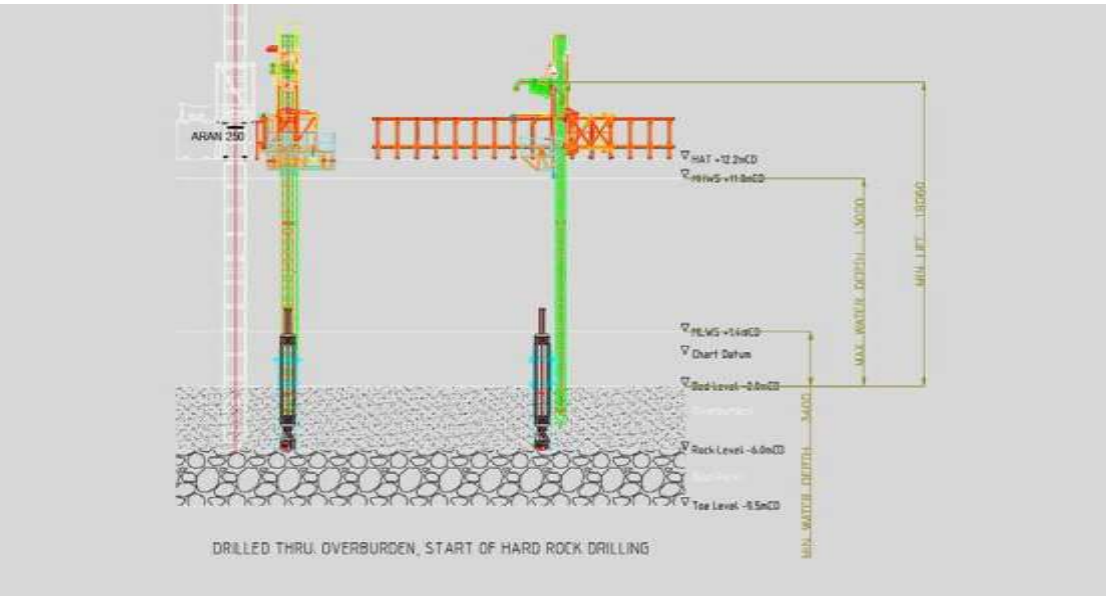

"Figure 1; A Diagram of Fugro's Jersey Project Setup from (Hackwell, 2015)"